Global Forest Monitoring from Earth Observation

Earth Observation of Global Changes

Series Editor
Chuvieco Emilio

Global Forest Monitoring from Earth Observation
edited by Frédéric Achard and Matthew C. Hansen

Global Forest Monitoring from Earth Observation

Edited by

Frédéric Achard • Matthew C. Hansen

CRC Press
Taylor & Francis Group
Boca Raton London New York

CRC Press is an imprint of the
Taylor & Francis Group, an **informa** business

Joint Research Centre, Institute for Environment and Sustainability

CRC Press
Taylor & Francis Group
6000 Broken Sound Parkway NW, Suite 300
Boca Raton, FL 33487-2742

International Standard Book Number: 978-1-1380-7447-7 (Paperback)
International Standard Book Number: 978-1-4665-5201-2 (Hardback)

Library of Congress Cataloging-in-Publication Data

Global forest monitoring from earth observation / edited by Frederic Achard and Matthew C. Hansen.
p. cm.
Includes bibliographical references and index.
ISBN 978-1-4665-5201-2
1. Forests and forestry--Remote sensing. 2. Forest monitoring. I. Achard, Frédéric. II. Hansen, Matthew C.

SD387.R4G56 2012
333.75--dc23 2012018562

Visit the Taylor & Francis Web site at
http://www.taylorandfrancis.com

and the CRC Press Web site at
http://www.crcpress.com

Contents

Preface

Forest resources are crucial in the context of sustainable development and climate change mitigation. Dynamic information on the location and evolution of forest resources are needed to properly define, implement, and evaluate strategies related to multilateral environmental agreements such as the UN Framework Convention on Climate Change (UNFCCC) and the Convention on Biological Diversity. For the global change scientific community and the UNFCCC process, it is important to tackle the technical issues surrounding the ability to produce accurate and consistent estimates of greenhouse gas emissions and removals from forest area changes worldwide and at the country level.

The following compilation of chapters constitutes a review of why and how researchers currently use remotely sensed data to study forest cover extent and loss over large areas. Remotely sensed data are most valuable where other information, for example, forest inventory data, are not available, or for analyses of large areas for which such data cannot be easily acquired. The ability of a satellite sensor to synoptically measure the land surface from national to global scales provides researchers, governments, civil society, and private industry with an invaluable perspective on the spatial and temporal dynamics of forest cover changes. The reasons for quantifying forest extent and change rates are many. In addition to commercial exploitation and local livelihoods, forests provide key ecosystem services including climate regulation, carbon sequestration, watershed protection, and biodiversity conservation, to name a few. Many of our land use planning decisions are made without full understanding of the value of these services, or of the rate at which they are being lost in the pursuit of more immediate economic gains through direct forest exploitation. Our collection of papers begins with an introduction on the roles of forests in the provision of ecosystem services and the need for monitoring their change over time (Chapters 1 and 2).

We follow this introduction with an overview on the use of Earth observation datasets in support of forest monitoring (Chapters 3 through 5). General methodological differences, including wall-to-wall mapping and sampling approaches, as well as data availability, are discussed. For large-area monitoring applications, the need for systematically acquired low or no cost data cannot be overstated. To date, data policy has been the primary impediment to large-area monitoring, as national to global scale forest monitoring requires large volumes of consistently acquired and processed imagery. Without this, there is no prospect for tracking the changes to this key Earth system resource.

The main section of the book covers forest monitoring using optical data sets (Chapters 6 through 14). Optical datasets, such as Landsat, constitute the longest record of the Earth surface. Our experience of using them in mapping and monitoring forest cover is greater than that of other datasets due to the relatively rich record of optical imagery compared to actively acquired data sets such as radar imagery. The contributions to this section range from indicator mapping at coarse spatial resolution to sample-based assessments and wall-to-wall mapping at medium spatial resolution. The studies presented span scales, environments, and themes. For example, forest degradation, as opposed to stand-replacement disturbance, is analyzed in two chapters. Forest degradation is an important variable regarding biomass, emissions, and ecological integrity, as well as being a technically challenging theme to map. Chapters 6 through 14 also present a number of operational systems, from Brazil's PRODES and DETER products, to Australia's NCAS system. These chapters represent the maturity of methods as evidenced by their incorporation by governments into official environmental assessments. The fourth section covers the use of radar imagery in forest monitoring (Chapter 15). Radar data have a long history of experimental use and are presented here as a viable data source for global forest resource assessment.

We believe that this book is a point of departure for the future advancement of satellite-based monitoring of global forest resources. More and more observing systems are being launched, methods are quickly maturing, and the need for timely and accurate forest change information is increasing. If data policies are progressive, users of all kinds will soon have the opportunity to test and implement forest monitoring methods. Our collective understanding of forest change will improve dramatically. The information gained through these studies will be critical to informing policies that balance the various demands on our forest resources. The transparency provided by Earth observation data sets will, at a minimum, record how well we perform in this task.

We deeply thank Prof. Emilio Chuvieco from the University of Alcalá (Spain) who gave us the opportunity to publish this book and supported and encouraged us in its preparation. We also sincerely thank all the contributors who kindly agreed to take part in this publication and who together have produced a highly valuable book.

Frédéric Achard and Matthew C. Hansen

Editors

Dr. Frédéric Achard is a senior scientist at the Joint Research Centre (JRC), Ispra, Italy. He first worked in optical remote sensing at the Institute for the International Vegetation Map (CNRS/University) in Toulouse, France. Having joined the JRC in 1992, he started research over Southeast Asia in the framework of the TREES (TRopical Ecosystem Environment observations by Satellites) project. His current research interests include the development of Earth observation techniques for global and regional forest monitoring and the assessment of the implications of forest cover changes in the tropics and boreal Eurasia on the global carbon budget. Frédéric Achard received his PhD in tropical ecology and remote sensing from Toulouse University, Toulouse, France, in 1989. He has coauthored over 50 scientific peer-reviewed papers in leading scientific journals including *Nature*, *Science*, *International Journal of Remote Sensing*, *Forest Ecology and Management*, *Global Biogeochemical Cycles*, and *Remote Sensing of Environment*.

Dr. Matthew C. Hansen is a professor in the Department of Geographical Sciences at the University of Maryland, College Park, Maryland. He has a bachelor of electrical engineering degree from Auburn University, Auburn, Alabama. His graduate degrees include a master of engineering in civil engineering and a master of arts in geography from the University of North Carolina at Charlotte and a doctoral degree in geography from the University of Maryland, College Park, Maryland. His research specialization is in large-area land cover monitoring using multispectral, multitemporal, and multiresolution remotely sensed data sets. He is an associate member of the MODIS (Moderate Resolution Imaging Spectroradiometer) Land Science Team and a member of the GOFC-GOLD (Global Observations of Forest Cover and Land Dynamics) Implementation Working Group.

Taylor & Francis
Taylor & Francis Group
http://taylorandfrancis.com

Contributors

Frédéric Achard
Institute for Environment
and Sustainability
Joint Research Centre of
the European Commission
Ispra, Italy

Olivier Arino
Earth Observation Directorate
European Space Agency
Frascati, Italy

Sergey Bartalev
Space Research Institute
Russian Academy of Sciences
Moscow, Russian Federation

Alan Belward
Institute for Environment
and Sustainability
Joint Research Centre of
the European Commission
Ispra, Italy

René Beuchle
Institute for Environment
and Sustainability
Joint Research Centre of
the European Commission
Ispra, Italy

Peter Caccetta
Mathematics, Statistics
and Informatics
Commonwealth Scientific and
Industrial Research Organisation
Floreat, Western Australia,
Australia

Daniel Clewley
Institute of Geography and Earth
Sciences
Aberystwyth University
Aberystwyth, United Kingdom

Rémi D'Annunzio
Forestry Department
Food and Agriculture Organization
of the United Nations
Rome, Italy

Ruth DeFries
Department of Ecology, Evolution
and Environmental Biology
Columbia University
New York, New York

Valdete Duarte
Remote Sensing Division
Brazilian Institute for Space
Research
São Paulo, Brazil

Victor Efremov
Space Research Institute
Russian Academy of Sciences
Moscow, Russian Federation

Vyacheslav Egorov
Space Research Institute
Russian Academy of Sciences
Moscow, Russian Federation

Evgeny Flitman
Space Research Institute
Russian Academy of Sciences
Moscow, Russian Federation

Antonio Roberto Formaggio
Remote Sensing Division
Brazilian Institute for Space Research
São Paulo, Brazil

Suzanne Furby
Mathematics, Statistics
and Informatics
Commonwealth Scientific
and Industrial Research
Organisation
Floreat, Western Australia, Australia

Matthew C. Hansen
Department of Geographical
Sciences
University of Maryland
College Park, Maryland

Sean P. Healey
Rocky Mountain Research Station
U.S. Forest Service
Ogden, Utah

Dirk Hoekman
Department of Environmental
Sciences, Earth System Science
and Climate Change Group
Wageningen University
Wageningen, The Netherlands

Richard A. Houghton
Woods Hole Research Center
Falmouth, Massachusetts

Josef Kellndorfer
Woods Hole Research Center
Falmouth, Massachusetts

Pieter Kempeneers
Earth Observation Department
Flemish Institute for Technological
Research
Mol, Belgium

Lars Laestadius
People and Ecosystems
Department
World Resources Institute
Washington, DC

Erik Lindquist
Forestry Department
Food and Agriculture Organization
of the United Nations
Rome, Italy

Evgeny Loupian
Space Research Institute
Russian Academy of Sciences
Moscow, Russian Federation

Thomas R. Loveland
Earth Resources Observation
and Science Center
U.S. Geological Survey
Sioux Falls, South Dakota

Richard Lucas
Institute of Geography
and Earth Sciences
Aberystwyth University
Aberystwyth, United Kingdom

Jeffrey G. Masek
NASA Goddard Space Flight Center
Greenbelt, Maryland

Daniel McInerney
Institute for Environment
and Sustainability
Joint Research Centre of the
European Commission
Ispra, Italy

Humberto Navarro de Mesquita, Jr.
National Forest Registry
Brazilian Forest Service
Brasilia, Brazil

Anssi Pekkarinen
Forestry Department
United Nations Food and Agriculture Organization
Rome, Italy

Peter Potapov
Department of Geographical Sciences
University of Maryland
College Park, Maryland

Gary Richards
Department of Climate Change and Energy Efficiency
Canberra, Australia
and
Fenner School of Environment and Society
Australian National University
Canberra, Australia

Ake Rosenqvist
solo Earth Observation
Tokyo, Japan

Bernardo Friedrich Theodor Rudorff
Remote Sensing Division
Brazilian Institute for Space Research
São Paulo, Brazil

Jesús San-Miguel-Ayanz
Institute for Environment and Sustainability
Joint Research Centre of the European Commission
Ispra, Italy

João Roberto dos Santos
Remote Sensing Division
Brazilian Institute for Space Research
São Paulo, Brazil

Fernando Sedano
Institute for Environment and Sustainability
Joint Research Centre of the European Commission
Ispra, Italy

Lucia Seebach
Department of Forest and Landscape
University of Copenhagen
Copenhagen, Denmark

Yosio Edemir Shimabukuro
Remote Sensing Division
Brazilian Institute for Space Research
São Paulo, Brazil

Masanobu Shimada
Earth Observation Research Center
Japan Aerospace Exploration Agency
Tokyo, Japan

Carlos Souza, Jr.
Amazon Institute of People and the Environment
Belém, Pará, Brazil

Stephen V. Stehman
College of Environmental Science and Forestry
State University of New York
Syracuse, New York

Hans-Jürgen Stibig
Institute for Environment and Sustainability
Joint Research Centre of the European Commission
Ispra, Italy

Peter Strobl
Institute for Environment and Sustainability
Joint Research Centre of the European Commission
Ispra, Italy

Fedor Stytsenko
Space Research Institute
Russian Academy of Sciences
Moscow, Russian Federation

Svetlana Turubanova
Department of Geographical Sciences
University of Maryland
College Park, Maryland

Wayne Walker
Woods Hole Research Center
Falmouth, Massachusetts

Jeremy Wallace
Mathematics, Statistics and Informatics
Commonwealth Scientific and Industrial Research Organisation
Floreat, Western Australia, Australia

Robert Waterworth
Department of Climate Change and Energy Efficiency
Canberra, Australia

Xiaoliang Wu
Mathematics, Statistics and Informatics
Commonwealth Scientific and Industrial Research Organisation
Floreat, Western Australia, Australia

Alexey Yaroshenko
Greenpeace Russia
Moscow, Russian Federation

Ilona Zhuravleva
Greenpeace Russia
Moscow, Russian Federation

12

Monitoring U.S. Forest Dynamics with Landsat

Jeffrey G. Masek
NASA Goddard Space Flight Center

Sean P. Healey
U.S. Forest Service

CONTENTS

12.1 Introduction: U.S. Forest Dynamics in the Global Context

Forest dynamics in the United States differ substantially from those in the developing world and thus present unique monitoring requirements. While deforestation and conversion to semipermanent agriculture dominate tropical forest dynamics, the area of forest land in the United States has remained fairly constant for the last 50–60 years (Birdsey and Lewis 2003). Although the United States experienced rapid deforestation during the eighteenth and nineteenth centuries, much of the eastern clearing regrew during the twentieth century as marginal agricultural land was abandoned.

Recent inventory reports indicate very small rates of net forest cover change in recent decades, with the area of U.S. forests increasing by slightly more than one-tenth of 1% per year since 1987 (Smith et al. 2009).

Rather than land use conversion, forest dynamics in the United States are dominated by harvest, fire, and other temporary disturbance processes. These processes do not change the net area of forest land use, but dramatically affect the forest age structure, landscape ecology, carbon balance, and habitat suitability. It is thought that about 1.4% of forest land area is affected by harvest each year in the United States, and another 0.4% is affected by fire (Smith et al. 2009; U.S. EPA 2011). However, these disturbance rates are not static. Changes in forest management as well as recent climate change may be affecting contemporary disturbance rates relative to historic norms (e.g., van Mantgem et al. 2009).

The United States relies on its national forest inventory for domestic and international reporting of forest change. The U.S. Forest Inventory and Analysis (FIA) program collects data on a set of over 300,000 plots across the United States, with one plot per every ~2,430 ha. A range of attributes are collected in addition to stand volume, including stand age, species composition, and management practice. The key aspect of this design-based inventory is that the sampling error associated with any variable is well constrained, and thus robust estimates across broad areas can be made with known sampling uncertainty. Plots are remeasured on a 5- to 10-year cycle, depending on the state. Like other nations, the United States reports national forest carbon dynamics as part of the United Nations Framework Convention on Climate Change (UNFCCC). In this case, inventory data from the FIA and other agencies are collated and reported by the U.S. Environmental Protection Agency (EPA).

While the FIA is well suited for estimating national forest statistics, it is not designed to accurately capture local dynamics due to disturbance and other rare events. For example, while a difference between a 1% per year and 2% per year disturbance rate is truly significant from an ecological point of view, a very large number of random samples is needed to distinguish those two rates with any level of precision. Given the FIA plot spacing, this implies that disturbance rates cannot be accurately characterized below the scale of 100s of kilometers.

The desire for consistent, geospatial information on forest disturbance and conversion has invigorated the application of Landsat-type remote sensing technology for forest monitoring in the United States. This work builds on a significant legacy that dates back to the launch of Landsat-1 in 1972 (Cohen and Goward 2004). Early efforts at basic land cover mapping identified forests as a unique spectral region (the so-called badge of trees in red-near-IR space) that enabled reliable single-image mapping of forest cover. Studies during the 1980s and 1990s established the opportunity to use multidate Landsat imagery to characterize forest conversion, harvest, burned area, and insect damage. Recent increases in computing power, coupled with the gradual opening of the Landsat archive for free distribution, have resulted in researchers undertaking increasingly ambitious programs in large-area forest dynamics monitoring. Here we describe several of these efforts, focusing on national-scale work in the United States.

12.2 Overall Forest Disturbance: LEDAPS and NAFD Projects

The North American Carbon Program (NACP) is an ongoing interagency effort within the United States to constrain the North American carbon budget, improve process understanding, and forecast future scenarios. The NACP Science Strategy recognized at the outset that ecosystem disturbance was a critical but poorly known parameter required for more accurate assessments of ecosystem carbon flux. Accordingly, two Landsat-based projects were organized during 2004–2005 in order to meet NACP modeling needs (Goward et al. 2008).

The LEDAPS (Landsat Ecosystem Disturbance Adaptive Processing System) project was based on traditional two-date change detection, but across very broad spatial scales (Masek et al. 2008). The main objective was to map stand-clearing disturbance (primarily fire and clearcut harvest) across all forested land in the conterminous United States and Canada. At the start of the project, the Landsat archive was not yet free. Instead, the project chose to use the Global Land Survey (GLS) preprocessed Landsat data sets (Tucker et al. 2004). The GLS data sets consist of cloud-free imagery for epochs centered on 1975, 1990, 2000, 2005, and 2010. For the LEDAPS project, the focus was on estimating forest disturbance between 1990 and 2000.

The LEDAPS processing approach focused on establishing accurate surface reflectance values from each image, and then using those data to perform two-date change detection using a tasseled cap disturbance index. Considerable work went into establishing a sensor calibration and atmospheric correction approach suitable for use with the GLS data sets, including revising the Landsat-5 calibration look-up table based on invariant desert targets and adjusting the calibration of the older GLS data sets to reflect the new table. The development of a stand-alone atmospheric correction code for Landsat was a significant side benefit of the project.

Beyond sensor calibration, a number of other challenges were encountered during the disturbance mapping. First, the 10-year (1990–2000) change-detection span caused stands disturbed during the early part of the epoch to exhibit significant regrowth, resulting in high omission errors of 40%–50%. This issue has previously been documented (Jin and Sader 2005) and suggests that change detection on closer to annual timesteps is more appropriate for most forest monitoring applications. Statistical summaries reported in Masek et al. (2008) compensated for this issue by adjusting rates by the difference between omission and commission errors. Second, many of the GLS images from the 1990 and 2000 data sets were acquired during senescent parts of the growing season, confusing the change-detection approach. These images were replaced with new imagery purchased from U.S. Geological Survey (USGS).

The results of the continental mapping indicated that 2.3 Mha/year of U.S. forest land was affected by stand-clearing disturbance during the 1990s, representing a fractional disturbance rate of 0.9% per year, or an equivalent "turnover" period of 110 years. The highest disturbance rates were found in areas with significant harvest activity, including the southeastern United States, Maine/Quebec, and the Pacific Northwest. Rates in the mid-Atlantic and New England were lower, reflecting both less overall harvest activity and greater prevalence of partial harvest, which could not be reliably detected using the LEDAPS measurement period.

While LEDAPS focused on wall-to-wall assessment of disturbance at a coarse temporal timestep, the North American Forest Dynamics (NAFD) project took an alternate path: characterizing disturbance using a sparse geographic sample of Landsat imagery at annual temporal resolution (Goward et al. 2008). The NAFD originally began with a sample of 23 Landsat frames across the United States and later expanded to a set of 50 frames. For each frame, a set of biennial (later annual) Landsat imagery was assembled, and time-series analysis was used to map forest disturbance.

The NAFD geographic sample was designed to support robust characterization of national disturbance rates (eastern and western United States as separate estimates) based on an unequal probability sampling design. This sampling design was based on selecting across strata for U.S. forest types (Ruefenacht et al. 2008) while also accommodating the inclusion of fixed sites from earlier phases of the work. The decision to increase the number of samples from 23 to 50 reflected the desire to reduce the national sampling error to less than 10% (Figure 12.1).

Aligned with several other recent studies (Kennedy et al. 2007), the NAFD disturbance-mapping effort relied on detecting anomalies in per-pixel spectral time series. The specific algorithm, the vegetation change tracker (VCT; Huang et al. 2010), used a Z-score procedure to normalize each image in the time series by dividing by the standard deviation of reflectance values for a set of undisturbed forest pixels. Anomalies were then mapped based on significant, long-lasting excursions from the time series (Huang et al. 2010). Both the year of disturbance and the spectral magnitude were included in the final products (Figure 12.2). It should be noted that the annual timestep used in the algorithm allows partial disturbances (such as thinning, partial harvest, and mortality from storms and insects) to be tracked.

Overall, the sampling results indicate about 1.1% of forest area disturbed each year in the United States during the 1985–2005 period. Although

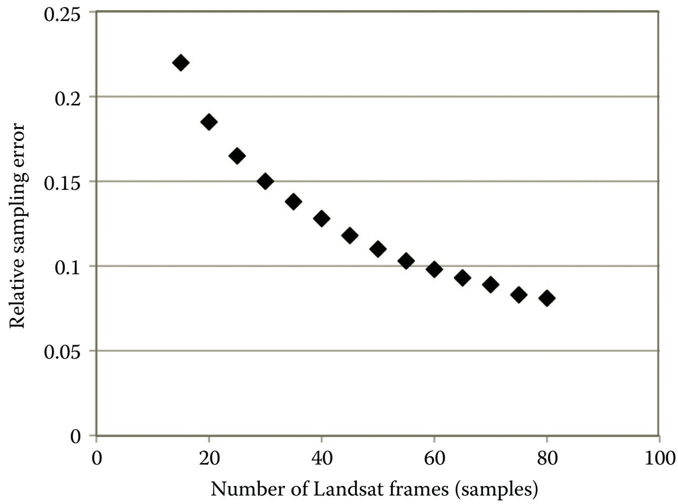

FIGURE 12.1
Relative error of U.S. national disturbance rate estimates as a function of the number of Landsat frames (path/row locations) used in the geographic sample, estimated from initial drafts of sample-level disturbance rate for all years from 1985 to 2005. Relative error is the proportional difference between the estimated value from the sample and the unknown true value, subject to a 90% confidence interval. (Analysis courtesy of Robert Kennedy, Oregon State University, Corvallis, OR.)

disturbance rates in the western United States are dominated by fire and insect damage, while rates in the east are dominated by harvest, overall disturbance rates were not significantly different between the west and east. However, there were significant year-to-year differences. For example, disturbance rates in the western United States increased to 1.5% per year during the early 2000s as a result of extremely active fire years. There were also significant geographic differences in disturbance rate within individual forest type strata.

The fact that disturbance rates vary significantly in both space and time raises doubts that sampling approaches can adequately characterize the disturbance regime at continental scales. The assumption behind the NAFD sampling approach was that disturbance rate was fundamentally a function of forest type (or at least that forest type could act as a proxy for the controlling factors). This assumption has not been borne out by the scene-by-scene results. As a result, the latest phase of the NAFD project has abandoned the geographic sampling scheme and switched to an ambitious "wall-to-wall" characterization of annual disturbance rate for the entire conterminous United States. This effort will require processing in excess of 20,000 Landsat images and is taking advantage of

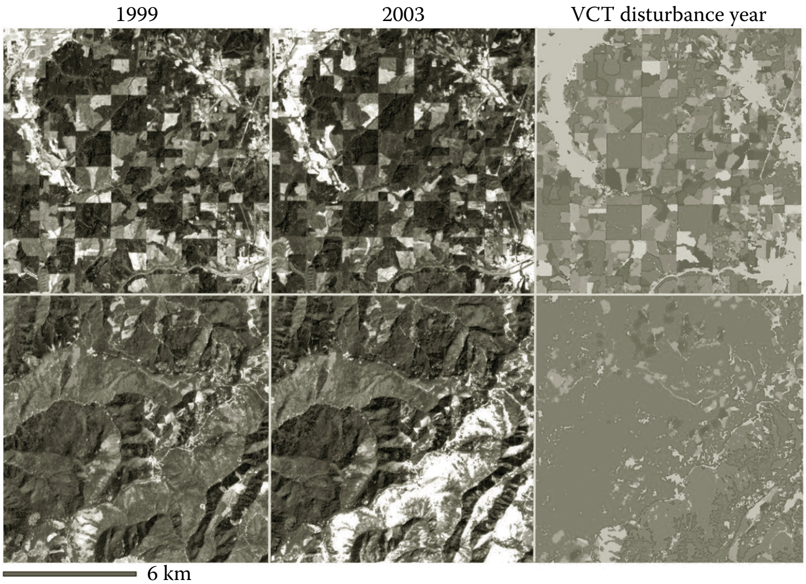

FIGURE 12.2
(See color insert.) Examples of NAFD disturbance mapping from southern Oregon (Landsat path 46, row 30). Top row: RGB imagery (bands 7, 5, 3) and VCT disturbance maps for an area of active harvest; bottom row: RGB imagery and disturbance map for the northern edge of the 2002 Biscuit Fire. The VCT maps shows permanent forest (green), permanent nonforest (gray), and the year of mapped disturbance from 1985 to 2009 (other colors).

the NASA Earth Exchange (NEX) parallel computing environment at the NASA Ames Research Center.

12.3 Operational Fire Monitoring: MTBS and LANDFIRE

Although wildfire is a primary disturbance agent within the United States, the area affected by forest fire has not been well characterized. The National Interagency Fire Center (NIFC) maintains a database of major wildfires, but does not consistently discriminate between forest fires and other wildfires (e.g., brushfire or grassfire). Furthermore, the area recorded is based on an external perimeter of each large fire, rather than the actual area affected by burning. Two operational projects, Monitoring Trends in Burn Severity (MTBS) and LANDFIRE, are using Landsat remote sensing to improve burned area and fire risk monitoring.

A collaboration between the USGS and the U.S. Forest Service (USFS), the MTBS project is seeking to supplement the NIFC database with accurate information on U.S. fire area and burn severity (Eidenshink et al. 2007). The primary goal of MTBS is to provide sufficient information to quantify interannual variability in U.S. burned area and to understand the extent to which forest management and environmental factors may be influencing longer term trends in fire.

MTBS has acquired preburn and postburn (1 year after fire) Landsat imagery for all major wildfires within the United States since 1984, as identified from government databases (Eidenshink et al. 2007). Fires larger than 1,000 acres in the western United States and larger than 500 acres in the eastern United States are considered in the project. The normalized burn ratio (NBR) spectral index is calculated for the image pair bracketing a major fire, and a difference (dNBR) image is generated by subtracting the pre- and postfire NBR values. The NBR metric takes advantage of the fact that recent fires leave considerable char, ash, and mineral soil, which tend to be relatively bright in the shortwave infrared compared to the near-infrared. While the NBR metric has been questioned as a suitable proxy for overall fire severity in Boreal ecosystems (Hoy et al. 2008), it has also been shown to be highly correlated with canopy damage (Hoy et al. 2008) and overall fire impact in temperate ecosystems (Cocke et al. 2005). MTBS data are available online (http://www.mtbs.gov) in a variety of formats, including geospatial products and statistical summaries of annual burned area by region and ecosystem.

LANDFIRE is a multipartner project producing 30 m Landsat-based maps of vegetation, fuel, fire regimes, and ecological departure from historical conditions across the United States (Rollins 2009). Leadership is shared by the wildland fire management programs of the USDA Forest Service and the U.S. Department of the Interior. LANDFIRE's maps are widely used for both fire management and ecological modeling. Circa-2000 imagery was used to produce LANDFIRE's original maps, and a combination of approaches is used to track subsequent disturbances so that maps may be kept up to date (Vogelmann et al. 2011).

The initial updating mechanism involved intersecting LANDFIRE maps with the fire events mapped by the MTBS project (described above). This approach has recently been augmented with management activities (conducted mostly on federal lands), which have been recorded in a spatial database. Because a more automated process was needed for incorporating the effects of disturbance events, LANDFIRE has recently done extensive work with the VCT algorithm described earlier under the activities of the NAFD project. An estimated 30,000 Landsat images will ultimately be used to map disturbance extent and magnitude across the conterminous United States (Vogelmann et al. 2011).

Because the cause, or type, of a disturbance plays an important role in its effect upon fuel conditions, cause attribution is underway for LANDFIRE's VCT maps. This process makes use of the MTBS data to some extent, but it also currently involves a good deal of manual classification. Current

LANDFIRE disturbance-mapping efforts focus on the Landsat TM era, but extension into the MSS era is a longer term goal, as is continued mapping into the future.

12.4 Forest Cover Conversion: Trends, NLCD, and C-CAP

While the emphasis of the preceding projects has been on characterizing forest disturbance rates, permanent conversion of forest cover remains an ongoing process within the United States. The trend during most of the twentieth century was toward increased forest cover via agricultural abandonment. However, increased urban and suburban growth during the last 50 years has altered this pattern in some areas. The projects discussed here have viewed forest change from the perspective of land cover conversion and have used Landsat-based change detection to separate gross forest change (including harvest and other disturbances) from the lower rates of long-term land cover and land use conversion.

The USGS Trends project began in the late-1990s using a random sample of Landsat subsets, stratified by EPA ecoregion, to characterize both regional and national trends in land cover (Loveland et al. 2002). Each Landsat subset was either 10,000 or 40,000 ha (e.g., 10 km × 10 km or 20 km × 20 km). For each subset, images were collected for the years 1973, 1980, 1986, 1992, and 2000 and manually classified into a series of land use classes, as well as two classes representing recent mechanical disturbance (harvest) and fire. As in the NAFD project, the sampling framework allowed sampling uncertainty to be quantified. The overall goals were to provide estimates of gross change with an uncertainty of <1% at an 85% confidence interval (Drummond and Loveland 2010).

The Trends data set has been used widely for studies of land use conversion (Drummond and Loveland 2010), ecosystem carbon (Liu et al. 2006), biodiversity, and surface energy balance (Barnes and Roy 2008). For the eastern United States, Drummond and Loveland (2010) assessed both gross and net forest cover change using the Trends data and concluded that eastern forests experienced 142,000 ha/year of net forest conversion during the 1973–2000 period due mostly to urbanization, surface mining, and reservoir construction. Gross forest change rates were 2.5 times higher and mostly reflected harvest activities.

The National Land Cover Database (NLCD) project, coordinated by the USGS EROS Data Center, has produced wall-to-wall U.S. maps of land cover for 1992, 2001, and 2006. While NLCD image selection criteria, classification methods, and target classes have evolved over the course of the project, significant efforts have been made to ensure interpretable maps of change among different land covers (Xian et al. 2009; Fry et al. 2011). Changes between the 1991 and 2001 products were identified through a "retrofitting" process, which involved standardization of classification schemes, and a sequence of decision tree–based operations that first identified and then labeled land cover transitions. Differences in Landsat ratio-based indices were primary predictors for this process.

Likewise, (different) Landsat-based indices were used in the 2001–2006 change identification process, which used complex heuristic-based threshold rules to identify changed pixels and to indicate whether changed pixels were losing or gaining biomass. This change-detection process, multi-index integrated change analysis (MIICA; Fry et al. 2011), produced change maps that were intersected with the land cover product from 2001 (considered to be the base year) in nondeveloped areas to generate the 2006 cover product.

Mapping projects such as the NLCD's are an important complement to inventory estimates of forest change. In the United States, the FIA provides ground-acquired estimates of land use not available from automated satellite processes, and it provides a design-based error structure for its estimates of net change of forest area. However, the FIA does not measure gross transitions to and from other cover types. NLCD can specify that its estimate of a net loss of 16,720 km^2 of evergreen forest cover, for example, is the result of a 36,000 km^2 gross loss and a 19,000 km^2 gross gain (Fry et al. 2011). As discussed earlier, maps also provide a picture of change at much more localized scales than is achievable with a simple random sample.

The NOAA's Coastal Change Analysis Program (C-CAP) maintains a nationally standardized database of landcover and landcover change in coastal regions of the country (Dobson et al. 1995). Thematic classes, including those for forests, are consistent with those used in the NLCD (described earlier), and C-CAP is actually the source of the NLCD data in coastal zones. Landsat has been the basis for classification and change detection for C-CAP national maps using imagery from 1996, 2001, 2006, and 2011 (in progress), as well as high-priority local analyses going back to the mid-1980s.

The 2001 cover map, produced from three dates of imagery collected by the MRLC (multiresolution land characteristics consortium), is considered the baseline product, and only those areas determined to have changed are reclassified in subsequent products (J. McCombs, NOAA, personal communication). For changes between 2001 and 2006, CCA (crosscorrelation analysis) was used to detect change using imagery from the two dates. Landcover transitions were estimated with classification and regression trees (CARTs). Change detection between 2006 and 2011 will be consistent with the multithreshold change vector analysis used by NLCD (Xian et al. 2009). Spatial data and customized summaries of CCAP maps are freely available from the CCAP Web site.*

* http://www.csc.noaa.gov/digitalcoast/data/ccapregional/index.html

12.5 Synthesis of U.S. Forest Dynamics

Given that several studies have used satellite data to quantify forest disturbance rates in the United States, how do these estimates compare with each other, and with inventory-based rates? Satellite-based estimates of disturbance rates are available in Masek et al. (2008), and via the MTBS data products (available online). In addition, Hansen et al. (2010) presented MODIS-based measures of gross forest loss that includes both disturbance and deforestation. Figure 12.3 shows a comparison among these estimates. We also show inventory-based estimates of harvest, fire, and insect damage from Smith et al. (2009) and U.S. EPA (2011) annualized for the 2000–2008 period. Finally, we also derived an annualized rate of "stand-clearing" disturbance from the FIA by taking the area of U.S. forests less than 20 years of age, and dividing by 20, under the assumption that a stand-clearing event should reset the measured stand age on the FIA plot.

The range of estimates shows an expected trend, with shorter remeasurement periods (e.g., the annual NAFD) and finer resolution (e.g., Landsat vs. MODIS),

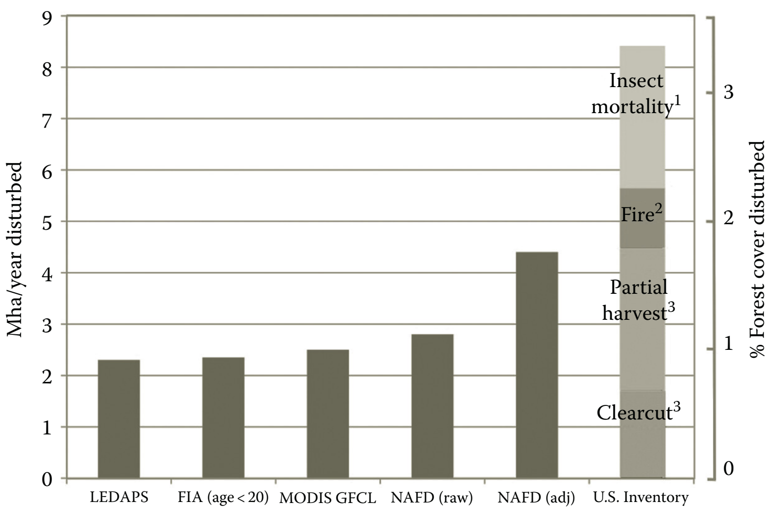

1. USDA Forest Service (2010) for USA—includes areas of mortality only, excluding defoliation without mortality.
2. U.S. EPA (2010)—includes Alaska fires.
3. Smith et al. (2009).

FIGURE 12.3
(See color insert.) Comparison of disturbance rates among satellite-based and inventory-based studies. LEDAPS (Masek et al. 2008) and NAFD (Kennedy et al. in preparation) are based on Landsat change detection. NAFD (adj) reflects compensation for net omission errors based on visual validation. MODIS GFCL is based on MODIS gross forest cover loss (GFCL) (Hansen et al. 2010). The FIA (age < 20) is based on equating the area of young forestland from the FIA with an annualized turnover rate. The percent forest cover values are based on the area of forest land in the "lower 48" conterminous United States (~250 Mha).

leading to more disturbances mapped and higher overall rates (Figure 12.3). The LEDAPS result of 0.9% per year corresponds closely to the FIA-derived stand-clearing rate (0.9% per year) and the gross loss derived from MODIS (1.0% per year). The ability of the NAFD annual data to capture some thinning and partial harvest likely explains the somewhat higher rates (1.1% per year). Further adjusting the NAFD rates for the net omission error of the products would increase these rates further, to about 1.5% per year.

All of these rates are significantly lower than what can be derived from inventory estimates alone (Smith et al. 2009; U.S. EPA 2010). This may reflect the difficulty in measuring minor disturbances using remote sensing, including selective harvest that does not significantly alter the forest canopy. Field- and satellite-based disturbance estimates may also differ in what they label "disturbance." The FIA's definition of disturbance includes "mortality and/or damage to 25 percent of all trees in a stand or 50 percent of an individual species' count" (FIA 2011). In addition to the canopy mortality targeted through remote sensing, this characterization certainly includes large areas affected by insects or storms, where sublethal damage may affect only a small fraction of the trees. Thus, discrepancies in Figure 12.3 may be due to both varying sensitivity and inconsistent definitions among data sources.

12.6 Looking Forward

The opening of the Landsat archive and advances in computing technology have paved the way for broader and more innovative applications of Landsat data for forest monitoring. These innovations include mapping at wider geographic scales (e.g., wall-to-wall national monitoring), the use of dense time series to better characterize intra- and interannual variability, and a greater sophistication in leveraging multiple data sources to attribute the origin of forest change as well as ecosystem consequences. Given that the Landsat archive is most complete within the United States, it is natural that many of these techniques are being pioneered for U.S. applications. However, given the increased global data collections implemented for Landsat-7 and the upcoming LDCM (Landsat Data Continuity Mission), these approaches could be applied to global monitoring as well.

12.6.1 Operational Monitoring of Forest Dynamics: LCMS

The Landscape Change Monitoring System (LCMS) is under development by a consortium of scientists, agencies, and projects engaged in remotely sensed change detection in the United States. Coordinated by the Forest Service and Department of Interior/USGS, LCMS is intended to be a hub around which existing national change products such as those from MTBS and NLCD may be integrated and extended. The ideal change monitoring system would provide up-to-date and consistent information about the location, magnitude, and nature of vegetation changes on all land cover types across the country. The research- and agency-based monitoring efforts described in this chapter address different aspects of this ideal system, and several steps are being taken under LCMS to promote both integration of existing products and cooperation on the development of new products.

First, LCMS is conducting an independent needs assessment of the land management community. Acquired information about the type, precision, and frequency of needed land change information will guide development of new monitoring strategies. Many of the needed answers are likely to come from the combination of current resources. For instance, LANDFIRE is anticipating a more meaningful update of their fuel maps as fire records from the MTBS are augmented with more general all-disturbance mapping achieved through the VCT (Vogelmann et al. 2011). Similar benefits of product integration likely extend into processes such as carbon accounting, where disturbance emissions are strongly influenced by event type and magnitude.

Any new products developed by the LCMS to meet identified needs will likely depend heavily upon the Landsat archive and will draw upon the experience of participating partners. Like the MTBS project, the LCMS will follow a collaborative multiagency business model, with an emphasis upon meeting operational monitoring needs by producing consistently updated and validated products. The LCMS is expected to be deployed during 2013.

12.6.2 Hypertemporal and Near-Real-Time Change Detection

The use of dense image time series has pushed the "epoch length" (i.e., the time between images used for monitoring change) to shorter and shorter periods. Not surprisingly, the range of forest dynamics that can be assessed has expanded as well. While semidecadal time series are useful for monitoring net land cover change and stand-clearing disturbance (Jin and Sader 2002; Drummond and Loveland 2010; Masek et al. 2008), more subtle disturbances require annual image acquisition. Thus the algorithms proposed by Kennedy et al. (2007) and Huang et al. (2010) are capable of detecting significant thinning, partial harvest, and selective mortality from insects and disease. However, even these algorithms may not record subtle and short-lived degradation of the forest canopy due to insect defoliation, storm damage, and selective cutting.

A variety of approaches are being prototyped to obtain seasonal or even submonthly information from Landsat. The WELD (Web-Enabled Landsat Dataset) project at the University of South Dakota is using MODIS-style compositing to generate monthly and seasonal gridded composites of Landsat-7 data. Zhu and Woodcock (in press) have proposed an approach to mapping forest disturbance by fitting per-pixel phenological curves using every available Landsat observation. These methods not only obtain greater sensitivity to short-term canopy changes, but by explicitly considering changes relative to observed phenology they minimize errors due to mismatches between annual image dates.

12.6.3 Integration of Landsat with Active RS for Biomass Change

Landsat data have proven robust for estimating the area affected by forest change processes. However, Landsat data have not proven as useful for forest volume or biomass estimation, except in conditions of sparse tree cover where volume can be directly related to canopy cover (Powell et al. 2010). There are, however, a variety of ways in which change area from Landsat can be combined with active remote sensing in order to better quantify "three-dimensional" changes in forest structure and biomass. Direct fusion between Light Detection and Ranging (LIDAR) and Landsat has been proposed to improve retrieval of biomass. Landsat imagery has also been proposed as a way to spatially interpolate LIDAR "samples" across the landscape using krigging techniques as well as a way to group LIDAR measurements based upon patterns of forest structure and disturbance. More recently, disturbance and age information derived from Landsat have been combined with LIDAR data to estimate postdisturbance carbon accumulation rates and to improve spatial interpolation of height (Li et al. 2011). In principle, similar work could be carried out using one-time biomass retrievals from radar (including interferometric SAR) combined with historical disturbance data from Landsat.

12.6.4 Ecological Impacts of Climate Change and Recovery Trajectories

The projects discussed here have focused mostly on quantifying the fraction of U.S. forest land disturbed and the fraction that reverts back to forest after disturbance. The spectral information of Landsat time-series data also offers important information on the *rate* at which ecosystems recover from disturbance. In one example, Schroeder et al. (2007) related postharvest Landsat spectral trajectories in the Pacific Northwest to increases in canopy cover deduced from air photos. The current phase of the NAFD project is extending this work by assessing rates of forest recovery for all recently disturbed patches in the United States.

One application for such approaches is to understand how ecosystem recovery may be responding to climate warming. A number of studies have suggested increased rates of forest decline in the southwestern United States due to prolonged drought (Williams et al. 2010), and van Mantgem et al. (2009) found evidence for increased rates of tree mortality throughout the western United States. Disturbance events (fire, insect outbreaks, and disease) may be accelerated in climate-stressed forests, and successional pathways may be altered or slowed. Ultimately the 40+ year Landsat record will prove valuable for understanding the long-term shifts in forest composition and mortality associated with climate warming in the United States.

12.7 Conclusions

The application of Landsat remote sensing to the monitoring of U.S. forests has accelerated during the last decade. This trend reflects both the development of new algorithmic and computational approaches for dealing with large volumes of data and the opening of the Landsat archive for free distribution by the USGS. The projects discussed here represent large-scale mapping efforts that have sought to characterize U.S. forest dynamics during the Landsat era, including disturbance, recovery, and conversion.

Although the U.S. forest inventory will continue to provide our most robust national estimates of forest attributes, remote sensing is increasingly being called on to perform operational monitoring of forest and land cover change. The appropriate integration of geospatial information from remote sensing with forest attribute available from the FIA remains one of the significant challenges for the future. The *k*-nearest neighbor approach of assigning suites of FIA attribute data based on spectral properties has found acceptance within the USFS as it allows the statistical variance of the FIA-reported attributes to be "imported" to the geospatial products (McRoberts et al. 2002). Alternative approaches have sought instead to use statistical models to predict attributes from Landsat spectral data using the FIA attributes as training data (e.g., Powell et al. 2010) or to use Landsat-derived harvest maps to spatially distribute the FIA-recorded harvest volumes (Healey et al. 2009). Ultimately the extent to which remote sensing can support operational needs depends on the trade-off between measurement error and sampling error. Landsat remote sensing can record wall-to-wall dynamics, and thus has no sampling error, but may exhibit significant errors of omission and commission (measurement errors) depending on the attribute of interest.

The launch of LDCM in early 2013 will continue the Landsat legacy while providing a greater density of global acquisitions compared to Landsat-7. In addition, the ESA Sentinel-2 satellites will be launched during 2013–2014. Like Landsat, the Sentinel program has committed to open access for its archive. Taken together, the LDCM and Sentinel missions will provide an extremely rich source of global observations for the next decade. It is anticipated that many of the advances in the use of Landsat data described here, including time-series methods, will soon find global use.

About the Contributors

Jeffrey G. Masek is a research scientist in the Biospheric Sciences Laboratory at the NASA Goddard Space Flight Center. His research interests include mapping landcover change in temperate environments, application of advanced computing to remote sensing, and satellite remote sensing techniques. Dr. Masek currently serves as the Landsat project scientist at NASA. He received a BA in geology from Haverford College (1989) and a PhD in geological sciences from Cornell University (1994).

Sean P. Healey is a research ecologist who works for the FIA program at the U.S. Forest Service's Rocky Mountain Research Station. His interests include linking Landsat data to inventory records for the purpose of tracking forest carbon storage over time.

References

Barnes, C.A. and Roy, D.P., Radiative forcing over the conterminous United States due to contemporary land cover land use albedo change. *Geophysical Research Letters*, 35, L09706, 2008.

Birdsey, R.A. and Lewis, G.M., Current and historical trends in use, management, and disturbance of U.S. forestlands. in *The Potential of U.S. Forest Soils to Sequester Carbon and Mitigate the Greenhouse Effect*, edited by J.M. Kimble et al., pp. 15–33, CRC Press, New York, 2003.

Cocke, A.E. et al., Comparison of burn severity assessments using differenced normalized burn ratio and ground data. *International Journal of Wildland Fire,* 14, 189–198, 2005.

Cohen, W.B. and Goward, S.N., Landsat's role in ecological applications of remote sensing. *BioScience*, 54(6), 535–545, 2004.

Dobson, J.E. et al., *NOAA Coastal Change Analysis Program: Guidance for Regional Implementation*, Version 1.0.NOAA Technical Report NMFS 123, Scientific Publications Office, National Marine Fisheries Service, NOAA, Seattle, WA, 92 p., 1995.

Drummond, M.A. and Loveland, T.R., Land-use pressure and a transition to forest-cover loss in the eastern United States. *BioScience*, 60(4), 286–298, 2010.

Eidenshink, J. et al., A project for monitoring trends in burn severity. *Fire Ecology*, 3, 3–21, 2007.

FIA (Forest Inventory and Analysis Program of the U.S. Forest Service). *Interior West Forest Inventory & Analysis P2 Field Procedures, V5.00*. USDA Forest Service Rocky Mountain Research Station. Ft. Collins, CO., 409 pp., 2011.

Fry, J. et al., Completion of the National Land Cover Database for the conterminous United States. *Photogrammetric Engineering and Remote Sensing*, 77, 858–864, 2011.

Goward, S.N. et al., Forest disturbance and North American carbon flux. *American Geophysical Union EOS Transactions*, 89, 105–116, 2008.

Hansen, M.C. et al., Quantification of global gross forest cover loss. *Proceedings of the National Academy of Sciences*, 107, 8650–8655, 2010.

Healey, S.P. et al., Changes in timber haul emissions in the context of shifting forest management and infrastructure. *Carbon Balance and Management*, 4, 9, 2009.

Hoy, E.E. et al., Evaluating the potential of Landsat TM/ETM+ imagery for assessing fire severity in Alaskan black spruce forests. *International Journal of Wildland Fire,* 17, 500–514, 2008.

Huang, C.Q. et al., An automated approach for reconstructing recent forest disturbance history using dense Landsat time series stacks. *Remote Sensing of Environment*, 114, 183–198, 2010.

Jin, S. and Sader, S.A., Comparison of time-series tasseled cap wetness and the normalized difference moisture index in detecting forest disturbances. *Remote Sensing of Environment*, 94, 364–372, 2005.

Kennedy, R.E. et al., Trajectory-based change detection for automated characterization of forest disturbance dynamics. *Remote Sensing of Environment*, 110, 370–386, 2007.

Li, A. et al., Modeling the height of young forests regenerating from recent disturbances in Mississippi using Landsat and Icesat data. *Remote Sensing of Environment*, 115, 1837–1849, 2011.

Liu, J. et al., Temporal evolution of carbon budgets of the Appalachian forests in the U.S. from 1972 to 2000. *Forest Ecology and Management*, 222, 191–201, 2006.

Loveland, T.R. et al., A strategy for estimating the rates of recent United States Land Cover changes. *Photogrammetric Engineering and Remote Sensing*, 68, 1091–1099, 2002.

Masek, J.G. et al., North American forest disturbance mapped from a decadal Landsat record: Methodology and initial results. *Remote Sensing of Environment*, 112, 2914–2926, 2008.

McRoberts, R.E. et al., Stratified estimation of forest area using satellite imagery, inventory data, and the k-nearest neighbors technique. *Remote Sensing of Environment*, 82, 457–468, 2002.

Powell, S.L. et al., Quantification of live above-ground forest biomass dynamics with Landsat time-series and field inventory data: a comparison of empirical modeling approaches. *Remote Sensing of Environment*, 114, 1053–1068, 2010.

Rollins, MG., LANDFIRE: A nationally consistent vegetation, wildland fire, and fuel assessment. *International Journal of Wildland Fire*, 18, 235–249, 2009.

Ruefenacht, B. et al., Conterminous U.S. and Alaska forest type mapping using forest inventory and analysis data. *Photogrammetric Engineering and Remote Sensing*, 74, 1379–1388, 2008.

Schroeder, T.A. et al., Patterns of forest regrowth following clearcutting in western Oregon as determined from a Landsat time-series. *Forest Ecology and Management*, 243, 259–273, 2007.

Smith, W.B. et al., *Forest Resources of the United States, 2007*, General Technical Report WO-78, Forest Service, U.S. Department of Agriculture, Washington, DC, 336 pp., 2009.

Tucker, C.J. et al., NASA's global orthorectified Landsat data set. *Photogrammetric Engineering and Remote Sensing*, 70, 313–322, 2004.

U.S. Environmental Protection Agency. *Inventory of U.S. Greenhouse Gas Emissions and Sinks: 1990–2009* (EPA 430-R-11-005). US EPA, Washington, DC, 2011.

van Mantgem, P.J. et al., Widespread increase of tree mortality rates in the western United States. *Science,* 323, 521–524, 2009.

Vogelmann, J.E. et al., Monitoring landscape change for LANDFIRE using multi-temporal satellite imagery and ancillary data. *IEEE Journal of Selected Topics in Applied Earth Observations and Remote Sensing*, 4, 252–264, 2011.

Williams, A.P. et al., Forest responses to increasing aridity and warmth in the southwestern United States. *Proceedings of the National Academy of Science*, 107, 21289–21294, 2010.

Xian, G. et al., Updating the 2001 National Land Cover Database classification to 2006 by using Landsat imagery change detection methods. *Remote Sensing of Environment*, 113, 1133–1147, 2009.

Zhu, Z. and Woodcock, C.E., Continuous monitoring of forest disturbance using all available Landsat imagery. *Remote Sensing of Environment* (in press).

13

Long-Term Monitoring of Australian Land Cover Change Using Landsat Data: Development, Implementation, and Operation

Peter Caccetta, Suzanne Furby, Jeremy Wallace, and Xiaoliang Wu
Commonwealth Scientific and Industrial Research Organisation

Gary Richards
Department of Climate Change and Energy Efficiency
and
Australian National University

Robert Waterworth
Department of Climate Change and Energy Efficiency

CONTENTS

13.1 Background

The need to monitor greenhouse gas (GHG) emissions accurately has become a task of major importance over the last decade. Emissions and removals of GHG in the land sector represent a large proportion of Australia's total GHG emissions. Following the signing of the Kyoto Protocol in 1997, Australia began developing a new system to account for emissions and removals from the land sector. The result, the National Carbon Accounting System (NCAS), is a fully integrated modeling system that utilizes data from a variety of sources to estimate emissions and removals for the purpose of reporting to the United Nations Framework Convention on Climate Change (UNFCCC 2001) and accounting under the Kyoto Protocol.

Under the Kyoto protocol, Australia was required to estimate emissions from land use and land use change in 1990 and from 2008 to 2012 (the first Kyoto Commitment period) while ensuring time-series consistency, limiting potential errors of omission and commission, allowing for annual updating at fine (subhectare) spatial resolution, and focusing on areas of change rather than total extent. The size of Australia (769 Mha) and the extent of its forests (110 Mha) required that robust and cost-effective methods that could be reliably operated into the foreseeable future be developed to estimate emissions and removals from the land sector. A key component of this system would be to track areas of land use change. As no such data existed in Australia that could meet all of these criteria, the NCAS needed to consider alternative options to traditional forest inventory and mapping.

The NCAS Land Cover Change Program (NCAS-LCCP) was developed by the Australian government in collaboration with the Commonwealth Scientific and Industrial Research Organisation (CSIRO) and other partners to meet the exacting requirements of the Kyoto Protocol. The NCAS-LCCP delivers the framework for fine-scale continental mapping and monitoring of the extent and change in perennial vegetation using Landsat satellite imagery, allowing for an effective estimation of the GHG emissions from land use and land use change (Brack et al. 2006; Caccetta et al. 2010). The program has been successively developed (see, for example, Furby 2002; Caccetta et al. 2003, 2007; Furby et al. 2008) over a number of years and currently uses over 7,000 Landsat MSS, TM, and ETM+ images at a resolution of 25 m for 18 time periods from 1972 to the present time (2011) and continues on an annual update cycle, making it one of the largest and most intensive land cover monitoring programs of its kind in the world.

While the remote sensing program was designed specifically for the purposes of GHG accounting, it has many additional benefits for bodies interested in monitoring land use change generally. The resultant products represent one of the few nationally consistent time-series data for the land sector.

Moving remote sensing from the realm of a technical research program to fully operational systems with ongoing update cycles was a considerable undertaking. Issues of scientific expertise, technical capacity, ongoing data supply and analysis, and accessing and processing large archives of data all needed to be considered. While many of these issues, in particular, those related to storage and compute capacity, have largely been removed through technological advancements, the operation of such a system still requires ongoing planning and management. The operational procedures adhere to a strict processing guideline: the output from each processing stage is checked against specific accuracy and consistency standards through a rigorous quality assurance process. Given the above operating environment, accuracy, interpretability (for outsourcing and QA), computational efficiency, the ability to incorporate "better" algorithms, and reliability when applied through space and time are important aspects for consideration during methodology development.

13.2 Materials and Methods

13.2.1 Method Selection

Although no national-scale remote sensing program for land use change existed at the start of the NCAS program, several operational broad-scale monitoring programs [for example, Land Monitor (Caccetta et al. 2000; Land Monitor 2008) and SLATS (Goulevitch et al. 1999)] did exist at the subnational scale. These had been implemented to serve the natural resource management needs of subnational agencies rather than for the specific purposes of tracking land use change for carbon accounting. To assess the suitability of the differing methods, a series of workshops and pilot projects were conducted from which the national Landsat-based forest monitoring program was established. The end product was not the whole-scale adoption of a single method but rather a selection of the best aspects of several different systems.

The approach adopted is based on:

- Long-term sequences of orthorectified and calibrated Landsat MSS, TM, ETM+ satellite data
- Discriminant analysis techniques to (spectrally) separate classes of interest

- Supervised and automated approaches to specify/estimate classifier parameters
- Spatial/temporal models to reduce errors

As the task included the analysis and processing of thousands of historical Landsat scenes, as well as the requirement that the information be updated annually during reporting periods, operational components of the methodology were vital to the success of the system. To do this required:

- Detailed specification of the application of the methods in operations manuals (Furby 2002)
- Training and subsequent processing of the data by third parties with documented quality assurance checks
- Independent review of the outputs by an independent third party to provide insight into the characteristics of errors (Jones et al. 2004) for use in method refinement through a continuous improvement exercise

13.2.2 Landsat Data

The initial step for the program was to develop specifications for the selection of Landsat scenes. Landsat has a return time of 16 days, resulting in around 22 images available per year for any specific area. To develop the annual maps of forest extent required by the system required selection of the optimal image. The selections were based on both preferred time sequence according to factors including reporting requirements, seasonality, greenness, sun angle, and other artifacts such as cloud, fire, and smoke. As the purpose of the program is to determine changes in forest cover, images that maximize the separation between tree and other cover (i.e., usually drier conditions) are generally selected.

13.2.3 Landsat Data Geometric Rectification

Accurate orthorectification of the Landsat data is vital to ensure that any change is due to real changes on the ground rather than edge effects due to image misalignment. In the NCAS-LCCP, this was achieved using a rigorous earth orbital model (PCI OrthoEngine software; Toutin 1994; Cheng and Toutin 1995), with a specification requiring subpixel accuracy. The first step was to establish a common orthorectified base mosaic of Landsat data. Once the orthorectified base was established, ground control points (GCPs) were automatically matched using a crosscorrelation technique and the temporal sequences of images orthorectified to the common base. This approach improves efficiency and accuracy of the results. For quality assurance, visual inspection and numerical summaries based on crosscorrelation feature matching are used to assess the accuracy of orthorectification of the time-series images.

13.2.4 Image Calibration/Normalization

Radiometrically calibrated images allow for comparisons between image scenes and the possibility of better extrapolation of a chosen classifier. We convert raw digital counts to be consistent with a chosen reference image.

The five main steps in the calibration and normalization (see Figure 13.1) of the Landsat data are:

- Top-of-atmosphere (TOA) reflectance calibration (as described by Vermote et al. (1997), which is to correct the reflectance differences caused by the solar distance and angle.
- Bidirectional reflectance distribution function (BRDF) calibration, described by Wu et al. (2001).
- Empirical correction for atmospheric and other affine effects via the use of invariant targets (Furby and Campbell 2001).
- Terrain illumination correction (Wu et al. 2004), which is based on the C-correction (Teillet et al. 1982). This step is required where there are significant terrain illumination effects, resulting in bright and dark sides of hills and mountains.

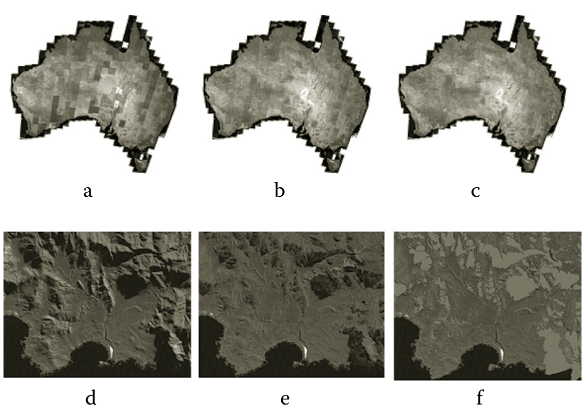

FIGURE 13.1
(See color insert.) Image calibration (top) and normalization (bottom). Calibration: Landsat mosaic of Australia showing (a) uncalibrated, (b) TOA correction, and (c) TOA + BRDF correction. Normalization (From Wu et. al., 2004.): (d) uncorrected, (e) terrain illumination correction, and (f) estimated occlusion mask overlaid and shown in gray. (From Wu, X., et al., An approach for terrain illumination correction. Australasian Remote Sensing and Photogrammetry Conference, Fremantle, Western Australia, 2004.)

- Occlusion detection (Wu et al. 2004) to identify terrain not observed due to the combination of terrain and the viewing geometry. This step identifies true shadow, which is labeled as missing data.

A relatively high-resolution digital elevation model (typically better than the 90 m SRTM) is required to achieve adequate occlusion detection and removal of terrain illumination effects.

13.2.5 Landsat-Derived Texture Measures

There are many natural and seminatural areas that have significant extents of heterogeneous perennial woody vegetation that do not meet the structural definition of forests or are at the lower limit of the definition of forests that is difficult to interpret and draw a line on a map so to speak. Here we refer to perennial woody vegetation having less than 20% canopy cover as sparse.

Seasonal weather changes and management effects may change the characteristics of these regions, and this in conjunction with the limited ability of remote sensing technology to distinguish this 20% canopy cover limit typically results in seasonal transitions between forests and sparse.

Based on observations that some sparse regions had a textured appearance, measures of texture were demonstrated to have useful information for distinguishing between forest, sparse, and nonforest classes and have been trialled at subnational scale (Caccetta and Furby 2004), progressively being incorporated into the work described here (Furby et al. 2007), where the Landsat image bands are augmented with texture measures in the analysis. The "texture" measures are derived using an overcomplete wavelet decomposition (Unser 1995), with Haar basis functions applied to forest/nonforest linear discriminant functions of the original Landsat bands. These measures are smoothed using an adaptive filter. This results in an n-band "texture image," where each band is a texture estimated at a coarser scale. The textures range from fine-scale textures in band 1 through coarse-scale textures in band n. In the following, bands are indexed as $h_0 \ldots h_n$ where h_0 is the finest scale texture and h_n the coarsest.

13.2.6 Comments

Some 7,000 Landsat MSS, TM, and ETM+ images over the past 39 years (from 1972 until the present) have been coregistered to a common orthorectified base mosaic using the above methods. The process is ongoing with an annual updating process. The program also periodically evaluates the potential for data from other sensors such as IRS, SPOT, and CBERS (Furby and Wu 2007, 2009; Wu et al. 2009) as possible candidates for operational use should data from the Landsat series no longer be available. To ensure access to those wishing to use data processed to this national standard, the data are then provided back to the Australian government agency responsible for remote sensing. These data are then made available for the cost of data transfer.

13.2.7 Forest Extent and Change Analysis

13.2.7.1 Geographic Stratification

Consistent with the experience of subnational programs, a stratified approach was adopted, allowing the local optimization of classifier parameters across the many different land cover–soil associations (Commonwealth of Australia 2005, 2009) that exist in such a large area. The stratification was adaptively derived, starting from boundaries based on (Landsat) spectral and other (such as topographic) consistency properties of strata during analysis. In all, about 400 strata were defined, as depicted in Figure 13.2.

13.2.7.2 Training and Validation Data

The process of classification requires that a quantitative assessment of the information in the available data is performed; the class labels, after having assessed the information in the data, are defined; a choice of model is made; and the accuracy of the results validated. Sample locations of known land cover are used to derive the classifier parameters or to train the classifier, and we refer to such data as training data. Similar sites independent of the training data are used to assess the accuracy of the results, and we refer to these data as validation data. The primary sources of training and validation data that have been used for the project include: about 800 historical aerial photographs whose locations are distributed across the continent;

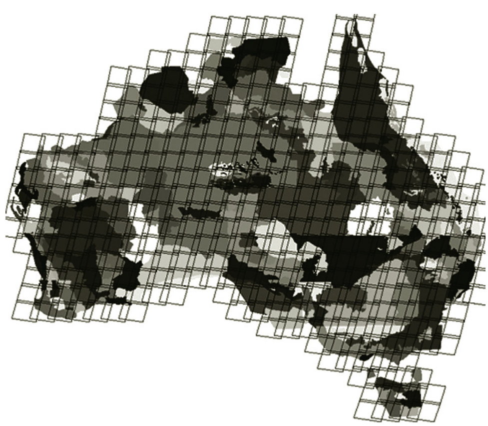

FIGURE 13.2
Stratification zones with Landsat scene boundaries overlaid used in analysis and subsequent processing. Within each zone, training data are used to estimate the parameters of the multitemporal classifier.

FIGURE 13.3
(See color insert.) (Left) Graphical depiction of the location of high-resolution IKONOS data used in the derivation of classifier training information. (Right) Typically, samples are required by intersection of zone and image, though well-calibrated data can reduce this requirement by allowing extrapolation across scene boundaries in many cases.

about 1,000 IKONOS images distributed across the continent (locations as depicted in Figure 13.3); and secondary less formal and generally available information such as regional expert knowledge, plantation location, and type information as provided by ground-based surveys and inventory information where it exists.

13.2.7.3 Multitemporal Model Used for Classification

Here we follow the approach described by Caccetta (1997) and Kiiveri and Caccetta (1998) for combining the multitemporal land cover information provided by the Landsat observations to form multitemporal classifications of land cover. The approach uses a probabilistic framework for combining data, with the view to classifying the data. Useful properties of the approach include:

- Propagation of uncertainties in inputs and calculation of uncertainties in outputs
- Production of hard and soft maps
- Handling of missing data by using all available information to make predictions
- Existence of well-developed statistical tools for parameter estimation

We note these characteristics are useful in practice as operational monitoring programs face issues such as availability of cloud-free imagery, variable (historic) atmospheric conditions, and changing sensor characteristics resulting in time-series data that vary in quality, completeness, and spectral discrimination.

13.2.8 Accuracy Assessment

The accuracy of the final forest presence/absence classification was independently validated, with initial results recorded by Lowell et al. (2003) and a subsequent update by Jones et al. (2004). Results from the latter are summarized below (see Section 13.3.3). Validation involved the comparison of classifications against "truth" obtained from aerial photo interpretation. The classes "forest," "nonforest," "regrowth," and "deforestation" were considered. As noted by Lowell et al. (2003) and Jones et al. (2004), the sampling strategy was constrained by the availability of (historical) aerial photography and was further constrained by the variable quality and scale of the photography. Routine collection of aerial photography resides with the states within Australia, with the collection being tailored by the states to individual state needs. This results in variable geographic, temporal, and spatial resolution when considering a national program.

Due to the variable availability and quality of aerial photography, Lowell et al. (2003) and Jones et al. (2004) adopted an approach that required the analyst to attach a degree of confidence to the cover class interpretations. Results were thus summarized as a "fuzzy" confusion matrix.

13.2.9 Attribution

Land cover change does not directly relate to land use change, in particular for deforestation and reforestation. Forest cover can change for a variety of reasons including clearing or establishment of trees, fire, pest attack, and drought. Further, there is a degree of error in any remote sensing analysis that need to be removed wherever possible, especially to remove false change due to the random errors in forest extent between years.

Attribution is a largely manual process that relies on expert judgment and experience. However, it can be greatly assisted by other products that allow for rules-based methods to be applied. For example, tenure can be used in many cases to separate forest cover loss due to forest management (such as clear felling) from that due to clearing for agriculture (deforestation). Mapping of fire scars can be used to separate change in forest cover from fire from areas of deforestation or forest management. Other mapping products, such as areas of known plantation establishment, allow for separation of areas of natural regrowth from human-induced reforestation.

The process of attribution is directly related to the policy, reporting, and accounting requirements. While the remote sensing sets the base for the system, it is the attribution that ensures that the final outputs of the system are policy relevant.

13.3 Results and Discussion

The key outputs from the system are raw and policy-relevant time-series data of forest cover, forest cover change, forest cover trend, and plantations identified as being either hardwood or softwood. From these analyses, it is possible to effectively age areas of forest accurately from ages 1 to 38, with a further class of 38 years or older.

The dense and extended time-series data developed through the NCAS-LCCP allows for analysis that has not previously been available. Such data provide detailed insight into the key processes in the land sector that drive emissions and removals.

13.3.1 Comparison to Existing Manual Mapping Products

A variety of other mapping products exist in Australia that were developed for a number of purposes, including biodiversity, conservation, and watershed management (Commonwealth of Australia 2008, 2009). For the purposes of change analysis, such mapping products are unable to track the change in forest extent due to human-induced activities. For example, Commonwealth of Australia (2008) uses manual methods that are not time-series consistent. Although these mapping products are constrained for change analysis, they still play a vital role in the estimation of emissions and removals from forests. This is an excellent example of using data that are fit for purpose.

13.3.2 Relationship to Modeling and Natural Resource Management

The remote sensing program has produced a rich source of spatial information for use in the emissions modeling framework, allowing Australia to report accurately on emissions and removals from the land sectors (Figure 13.4) as well as being used to report on rates of forest conversion. As the program expands, new information is being derived and progressively incorporated into the framework. We briefly describe the progress of the land cover information derived to date.

The forest presence/absence information has been derived for each of the Landsat epochs in the time series. Based on spatial and temporal rules, areas most likely to be plantations are identified and classified as being either hardwood or softwood (Chia et al. 2006).

Spectral indices providing an ordination from forest to nonforest have been derived for each Landsat TM epoch for 1989 onward. The perennial vegetation cover trend information provides subtle information on historic changes within forest (and ultimately sparse) areas and offers a surveillance tool for forest managers (Wallace et al. 2006). See Lehmann et al. (2011) for details. These indices are used with an "ever forest" mask, which is derived

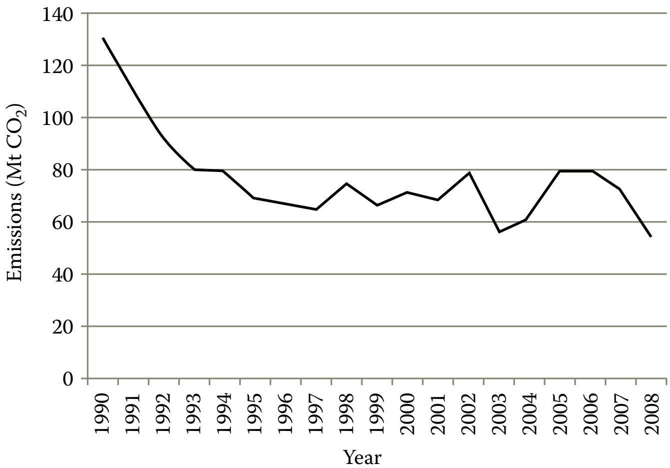

FIGURE 13.4
Emissions from forest land converted to cropland and grassland in Australia, 1990–2008. (From Australia National Inventory Report 2008.)

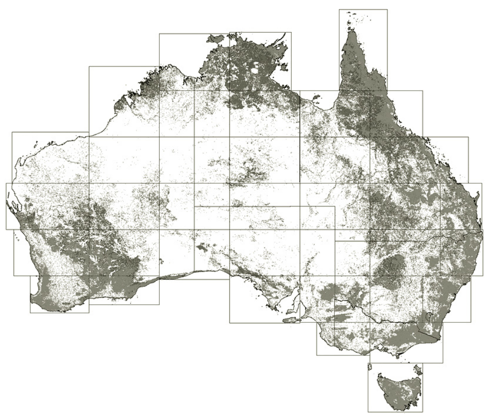

FIGURE 13.5
(See color insert.) Map of Australia showing NCAS forest extent (green) and sparse extent (red).

from the union of any area identified as forests at any point in the forest presence/absence time series. Together they provide temporal information on the trajectory of a pixel.

Sparse cover presence/absence classification (see Figure 13.5), which relies on image-derived spatial texture measures for discrimination, has been derived from the Landsat TM epochs in the time series 1989 onward (Furby et al. 2007). At the time of writing, the sparse cover information was being prepared and was not temporally complete. Upon completion, the trend information will also be derived for this class similar as for the forest class.

The land cover change information currently used for emissions modeling is the forest change (derived from the time-series presence/absence classifications) and the plantation type classification (Furby et al. 2008).

13.3.3 Accuracy Assessment

The overall forest presence/absence accuracy statement, as summarized by Jones et al. (2004), p. 8 of the report, is:

- Nationwide, the NCAS definite error rate was ~3%.
- Combined NCAS definite and probable error rate was ~12%.
- Nationwide, the forest definite error rate was ~2%.
- Nationwide, the nonforest definite error rate was ~4%.
- Nationwide, the forest combined definite and probable error rate was ~6%.
- Nationwide, the nonforest combined definite and probable error rate was ~15%.
- The amount of forest is likely to be underestimated continent wide, but the exact amount is difficult to determine because the CIVP sampling scheme was not a stratified or random sample.
- Regrowth and deforestation have considerably higher levels of errors associated with them, but are much rarer classes (only occurring ~2% and 1% of the time, respectively).

For the sparse covers, plantation, and trend information, validation is yet to be performed and will be in the scope of future works.

Acknowledgments

The authors thank all those who have also contributed to the larger NCAS system. This includes the number of contractors, scientists, and public servants involved in all stages of the NCAS development. In particular, the authors acknowledge the foresight of those who supported and promoted such a system in the late 1990s, including Gwen Andrews, Howard Bamsey, and Ian Carruthers, and for early scientific guidance from Dr Norm Campbell. The role of such dedicated public servants in ensuring that a vision reaches reality was a key factor in such success.

About the Contributors

Peter Caccetta received his PhD in computing science from the Curtin University of Technology, Perth, Australia. He is currently an adjunct professor with the Curtin University of Technology. He joined the Division of Mathematics, Informatics and Statistics, CSIRO, Wembley, Australia, in 1991, and worked on the development of broad-scale land cover mapping and monitoring technologies. Since 1999, he has been the principal scientist and leader of the Mapping and Monitoring Group, CSIRO. His current research interests include the application of remote sensing technologies for monitoring for natural resource management, including satellite and high-resolution monitoring obtained from aerial photography of urban and periurban environments.

Suzanne Furby is a member of the Mapping and Monitoring Research Group in the CSIRO Division of Mathematics, Informatics and Statistics, Perth, Australia. She has developed image calibration methodology and has been a key member of the team that developed methods for deriving quantitative information on land cover and condition change from remotely sensed and other spatial data, including the mapping and monitoring of dryland salinity and trends in perennial vegetation cover. She coordinated the remote sensing program to monitor land use changes across the continent. Results from this program data are used in the Australian National Carbon Accounting System (NCAS).

Xiaoliang Wu received his PhD in photogrammetry and remote sensing from the Wuhan Technical University of Surveying and Mapping, Wuhan, China, in 1993. In 1996, he joined the CSIRO, Perth, Australia, as a research scientist, where he contributed to the development and delivery of a satellite-based monitoring system—Australian NCAS. He is currently a principal research scientist with the CSIRO Division of Mathematics, Informatics and Statistics, developing an airborne-based monitoring system called "urban monitor."

Jeremy Wallace is a member of the CSIRO's Division of Mathematics for Mapping and Monitoring Group, based in Perth, Western Australia. This group has focused on the operational development of monitoring systems for land and vegetation using remote sensing. He has worked on Australia's National Carbon Accounting System Land Cover Change Program (NCAS-LCCP) since its inception and more recently in the training and implementation of remote sensing monitoring in Indonesia. He also has interests in the applications of remote sensing and related data for ecological and natural resource management applications.

Robert Waterworth has a PhD from the Fenner School of Resources, Environment and Society, Australian National University, Canberra, Australia. He is currently the director and senior research scientist of the International Forest Monitoring Section. Previous to this, Waterworth was a senior research scientist with Australia's NCAS and was responsible for the development of models and inventory systems. Prior to this, he worked in forest inventory systems and developed field measurement procedures for carbon accounting. His main area of expertise is system framework design, specifically implementing technical systems that meet policy and reporting requirements, forest growth modeling, and carbon accounting.

Gary Richards has a PhD in forestry and is an adjunct professor at the Fenner School of Resources, Environment and Society, Australian National University, Canberra, Australia. Richards is also cochair of the Clinton Climate Initiative, Carbon Measurement Collaborative, is an active participant on the work of the Intergovernmental Panel on Climate Change, is a national colead for the intergovernmental Group on Earth Observations (GEO) Forest Carbon Tracking Task, and convenes the GEO Global Forest Observations Initiative.

He is currently assistant secretary for the Energy Branch of the Department of Climate Change and Energy Efficiency. Richards was formerly principal advisor (International Forest Monitoring) for the Australian Government Department of Climate Change and Energy Efficiency. Richards was responsible for establishing Australia's NCAS that pioneered the combination of remotely sensed data, ground data, and carbon cycle models as the basis for national emissions reporting from land sectors.

References

Brack, C. Richards, G., and Waterworth, R., Integrated and comprehensive estimation of greenhouse gas emissions from land systems. *Sustainability Science*, 1, 91, 2006.

Caccetta, P.A., Allen, A., and Watson, I., The Land monitor project. The 10th Australasian Remote Sensing and Photogrammetry Conference, Adelaide, Australia, August 21–25, Remote Sensing and Photogrammetry Association of Australasia Ltd., Australia, 2000.

Caccetta, P.A. Remote sensing, GIS and Bayesian knowledge-based methods for monitoring land condition. PhD thesis, School of Computing, Curtin University of Technology, 1997.

Caccetta, P.A., et al., Notes on mapping and monitoring forest change in Australia using remote sensing and other data. Proceedings 30th ISRSE Honolulu, Hawaii, November 10–14, 2003.

Caccetta, P.A. and Furby, S.L., Monitoring sparse perennial vegetation cover. Proceedings 12th Australasian Remote Sensing and Photogrammetry Conference, Fremantle, Western Australia, October, 18–22, 2004.

Caccetta, P., et al., Continental monitoring: 34 years of land cover change using Landsat imagery. International Symposium on Remote Sensing of Environment, San José, Costa Rica, 2007.

Caccetta, P., et al., Monitoring Australian continental land cover changes using Landsat Imagery as a component of assessing the role of vegetation dynamics on Terrestrial Carbon Cycling. ESA Living Planet Symposium, Bergen Norway, June 28–July 2, 2010.

Cheng, P. and Toutin, Th. High accuracy data fusion of satellite and airphoto images. *Proceedings of ACSM/ASPRS Annual Convention*, Charlotte, North Carolina, American Congress on Surveying and Mapping (ACSM) and American Society for Photogrammetry and Remote Sensing (ASPRS), Bethesda, Maryland, Vol. 2, 453–464, 1995.

Chia, J., et al., Derivation of a perennial vegetation density map for the Australian continent. Australasian Remote Sensing and Photogrammetry Conference, Canberra, ACT, Australia, 2006.

Commonwealth of Australia, Assessment of Australia's terrestrial biodiversity 2008. (Available online at http://www.environment.gov.au/biodiversity/publications/terrestrial-assessment/index.html. Last accessed 11 October 2011), 2009.

Commonwealth of Australia, Interim biogeographical regions of Australia. (Available online at http://www.environment.gov.au/parks/nrs/science/pubs/regions.pdf. Last accessed 11 October 2011), 2005.

Commonwealth of Australia, Australia's State of the Forests Report: Five-yearly report 2008. (Available online at http://adl.brs.gov.au/forestsaustralia/_pubs/sofr2008reduced.pdf. Last accessed 11 October, 2011), 2008.

Furby, S. and Campbell, N., Calibrating images from different dates to 'like-value' digital counts. *Remote Sensing of Environment*, 77, 186, 2001.

Furby, S.L., Land cover change: Specification for remote sensing analysis. National Carbon Accounting System technical report no. 9, Australian Greenhouse Office, Canberra, 2002.

Furby, S.L, Wallace, J.F., and Caccetta, P.A., Monitoring Sparse Perennial Vegetation Cover over Australia using Sequences of Landsat Imagery. 6th International Conference on Environmental Informatics, Bangkok, Thailand, November 2007.

Furby, S., et al., Continental scale land cover change monitoring in Australia using Landsat imagery. International Earth Conference: Studying, Modeling and Sense Making of Planet Earth, Mytilene, Lesvos, Greece, 2008.

Furby, S. and Wu, X., Evaluation of IRS P6 LISS-III and AWiFS image data for forest cover mapping. CSIRO Mathematical and Information Sciences CMIS Technical Report 06/199, 2007.

Furby, S.L. and Wu, X., Evaluation of alternative sensors for a Landsat-based monitoring program. *Innovations in Remote Sensing and Photogrammetry*, 75, 2009.

Goulevitch, B.M., Danaher, T.J., and Walls J.W., The statewide landcover and trees study (SLATS)-monitoring land cover change and greenhouse gas emissions in Queensland. Proceedings of IEEE International Geoscience and Remote Sensing Symposium, Hamburg, June 1999.

Jones, S., et al., Update on the NCAS continuous improvement and verification methodology. NCAS Technical Report No. 46, 2004.

Kiiveri, H.T. and Caccetta, P.A., Image fusion with conditional probability networks for monitoring salinisation of farmland. *Digital Signal Processing*, 8(4), 225–230, 1998.

Kiiveri, H.T., et al., Environmental monitoring using a time series of satellite images and other spatial data sets. In *Nonlinear Estimation and Classification* by D.D. Denison (Ed.), M.H. Hansen, C. Holmes, B. Mallick, B. Yu, Lecture Notes In Statistics, New York, Springer Verlag, 49, 2003.

Land Monitor, Land monitor: A project of the Western Australian salinity action plan. (Available at http://www.landmonitor.wa.gov.au, verified September 25, 2009). Western Australian Land Information Authority, Perth, WA, Australia, 2008.

Lehmann, E.A., et al., Forest cover trends from time series Landsat data for the Australian continent (submitted for publication), 2011.

Lowell, K., et al., (2003), Continuous Improvement of the national carbon accounting system land cover change mapping. National Carbon Accounting System technical report No. 39. 2003. (http://www.greenhouse.gov.au/ncas/reports/pubs/tr39final.pdf).

Teillet, P.M., Guindon, B., and Goodeonugh, D.G., On the slope-aspect correction of multispectral scanner data, *Canadian Journal of Remote Sensing*, 8(2):84–106, 1982.

Toutin, Th., Rigorous geometric processing of airborne and spaceborne data. Proceedings of EUROPTO Symposium on Image and Signal Processing for Remote Sensing, Rome, Italy, Vol SPIE 2315, 825–832, 1994.

UNFCCC, Report of the conference of the parties on its seventh session held in Marrakesh, Morocco – Addendum. Part 2: action taken by the conference of the parties, FCCC/CP/2001/13/Add.1, Bonn, Germany, 2001.

Unser, M., Multigrid adaptive image processing, In: *Proceedings of IEEE International Conference on Image Processing (ICIP)*, Vol. 1. Washington DC, USA, 49–52, 1995.

Vermote, E.F., et al., Second simulation of the satellite signal in the solar spectrum, 6S: an overview. *IEEE Transactions on Geoscience and Remote Sensing*, 35, 675, 1997.

Wallace, J.F., Behn, G., and Furby, S.L., Vegetation condition assessment and monitoring from sequences of satellite imagery. *Ecological Management and Restoration*, 7, 31, 2006.

Wu, X., et al., A BRDF-corrected Landsat 7 mosaic of the Australian continent. IEEE International Geoscience and Remote Sensing Symposium, Sydney, Australia, 3274, 2001.

Wu, X. Furby, S., and Wallace, J., An approach for terrain illumination correction. Australasian Remote Sensing and Photogrammetry Conference, Fremantle, Western Australia, 2004.

Wu, X. et al., Evaluation of CBERS image data: Geometric and radiometric aspects. In *Innovations in Remote Sensing and Photogrammetry,* Lecture Notes in Geoinformation and Cartography, Springer, Berlin Heidelberg, p. 91, 2009.

14

Assessment of Burned Forest Areas over the Russian Federation from MODIS and Landsat-TM/ETM+ Imagery

Sergey Bartalev, Vyacheslav Egorov, Victor Efremov, Evgeny Flitman, Evgeny Loupian, and Fedor Stytsenko
Russian Academy of Sciences

CONTENTS

14.1 Introduction

14.1.1 Background of Burned Area Mapping

Wildfires are one of the most important drivers of land cover changes in Russia. They affect annually millions of hectares of forests and other terrestrial ecosystems, such as tundra, grasslands, and peatlands (Korovin 1996). Earth observation allows characterizing the distribution and impact of wildfires from individual events up to the country level. Burned area mapping is a critical input for both fire management actions' planning and postfire impact assessment, including economic and environmental aspects.

There is a wide range of requirements for the delivery time and accuracy of burned area estimates in relation to the range of applications. Fire-fighting and suppression activities require information to be updated as frequently as possible and to be delivered to users as rapidly as possible. The fire-fighters require fire information to be updated very frequently, up to several times a day. However, they do not have stringent requirements for information accuracy. On another hand, the applications related to postfire impact assessment are highly dependent on the accuracy of burned area mapping, but do not have strong requirements for data delivery speed as postfire impact assessment data can be delivered a few weeks or even a few months after the fires. Postfire assessment is used in particular for forest inventories, forest management, biodiversity conservation, and carbon emissions reporting.

For more than two decades, earth observation techniques have demonstrated their capacities to provide various types of information related to vegetation fires, including active fire detection and monitoring, burned area mapping, and characterization. A number of methods have been developed for active fire detection based on the radiation temperature characteristics of fires. These methods are based on the use of a few main satellite remote sensing instruments: NOAA-AVHRR (Li et al. 2001), ERS-ATSR2 and Envisat-AATSR (Arino et al. 2005), as well as Terra-MODIS (Giglio et al. 2003). In spite of attempts made to assess the extent of burned area directly from the detection of active fire pixels, such approaches are not considered very robust and are reported with large ranges of uncertainties. Eva and Lambin (1998) did not find any significant correlation between estimates of active fire pixels (derived from NOAA-AVHRR sensor) and assessment of burned areas in Central Africa. By contrast, Loboda and Csiszar (2004) reported a very high correlation ($R^2 = 0.99$) between the number of active fire pixels (estimated from MODIS sensors) and burned areas (derived from Landsat-ETM+ imagery) in Russia, with only about 10% underestimation. The fundamental shortcomings of such approaches are due to the combination of a few factors (Giglio et al. 2006), mainly:

- Masking of active fires by clouds and smoke
- Limited temporal frequency of satellite observations
- Spatial and temporal heterogeneity of fires, related in particular to a large range of propagation speed, fuel contents, meteorological conditions, and temperature daily dynamics
- Coarse spatial resolution of the satellite sensors used for active fire detection

On the one hand, as some of these factors are stochastic in nature, a consistent assessment of burned area is difficult from these active fire detection approaches, and the accuracy of results may significantly vary between regions and time periods. On the other hand, such approaches are considered the most appropriate for fire-fighting activities for which data delivery time is the most critical factor.

A number of burned area mapping approaches are based on the detection of intra or interannual changes in land cover spectral properties using time series of coarse-resolution satellite imagery (500 m–1 km) mainly from NOAA-AVHRR (Sukhinin et al. 2005), SPOT-Vegetation (Grégoire et al. 2003), and Terra/Aqua-MODIS (Roy et al. 2008) instruments. These methods are usually based on surface reflectance measurements in the NIR or SWIR (near or short-wave infrared, respectively) spectral channels of these instruments. The NIR and SWIR channels are either used as direct inputs into change-detection algorithms or through spectral vegetation indexes (such as NDVI, SWVI, or NBI) with high discrimination power to separate burned areas from green vegetation. Other research studies (Fraser et al. 2000a,b; Bartalev et al. 2007) have demonstrated the efficiency of the combined use of both approaches, i.e., the combination of (1) active fire detection and (2) burned area assessment from changes in land cover spectral properties.

These latest approaches usually demonstrate higher accuracies for burned area estimates compared to methods based on active fire pixel detection only. Burned area products can also be produced on a regular basis, e.g., monthly (Zhang et al. 2003), decadal (Bartalev et al. 2007), or daily (Tansey et al. 2008) time frames. These products consist of multiannual time series of burned area data over large territories that are valuable inputs for the geosciences and for environmental assessments. However, they have very limited use for forest inventory and management applications because finer spatial resolution and higher accuracy are required by foresters. Moreover, so far such methods do not allow for rapid data delivery in an operational manner. The information is usually made available to users with a substantial delay.

There is also an extensive experience for burned area mapping from moderate spatial resolution (10 m–30 m) satellite optical imagery, such as Landsat-TM/ETM+ (Isaev et al. 2002). In spite of the existence of a number of methods, these methods have been mostly applied to episodic and local level assessments. Mapping of burned areas from moderate-resolution satellite imagery over large areas and at regular time intervals has been restricted mainly by data availability until recently. This restriction has been reduced drastically through the recent open data distribution policy and online access to the global multiannual Landsat-TM/ETM+ data archive (see Section II.2).

14.1.2 Forest Fire Monitoring Information System (FFMIS)

Mapping of burned area is one key feature of the FFMIS, developed by a consortium of institutes belonging to the Russian Academy of Sciences. The FFMIS constitutes an essential component of several environmental monitoring services, such as the VEGA service (Loupian et al. 2011), which is publicly available, and the forest monitoring information system (called in Russian *ISDM-Rosleshoz*) operated by the Russian Federal Forest Agency (Loupian et al. 2006; Bartalev et al. 2008). The FFMIS covers the full territory of Russia and provides information to a range of forestry services, from the local forestry districts up to the federal forest agency. The FFMIS focuses on daily information support for activities related to fire management and for environmental and economic impact assessment. Considering the size of the Russian territory and the users' requirements for information delivery speed and frequency, satellite remote sensing technology has been considered as the main source of data in the system. The FFMIS uses as main inputs the multiannual and daily updated archives of data acquired by the Terra-MODIS and the Landsat-TM/ETM+ instruments (since year 2000). The system considers three sources of input data for burned area assessment over Russia, as follows:

1. Locations of active fires detected using the MOD14 standard algorithm (Justice et al. 2006) and MODIS Level 1B data (Toller et al. 2006) collected via a network of satellite data-receiving stations distributed across Russia. As a backup data source, the Fire Information for Resource Management System (FIRMS) Web site is also used for the daily download of MOD14 products (http://firefly.geog.umd.edu/firms).
2. MODIS surface reflectance daily data including information on solar illumination and instrument viewing geometry (MOD09 standard products; http://lpdaac.usgs.gov/main.asp).
3. Landsat-TM/ETM+ data downloaded from USGS GLOVIS (http://glovis.usgs.gov). By the end of the year 2011, the FFMIS archive of Landsat-TM/ETM+ data contained more than 122,000 scenes over the Russian territory including about 23,000 scenes acquired during the year 2011 only.

A new approach for burned area assessment based on the integration of this large database has been developed by the Space Research Institute of the Russian Academy of Sciences. This new approach is aimed at benefiting from the complementarities of the different data sources and includes highly automatic satellite data processing. The system creates three different burned area products:

1. *AFBA product*: Burned area polygons at 1 km spatial resolution. This product is based on the spatiotemporal clustering of active fire pixels derived from MODIS data with the use of individual satellite passes.
2. *SRBA product*: Burned area at 250 m spatial resolution. This product is derived from MODIS data using land cover surface reflectance change combined with active fire detection.
3. *HRBA product*: Burned area at 30 m spatial resolution. This product is derived from Landsat-TM/ETM+ data.

The integrated burned area assessment approach produces continuous information during the fire season. All available satellite imagery from the three potential data sources are used for any date and fire event. In cases of more than one burned area product being available for a given fire event, the following priority ranking is used to select the potentially most accurate product: (1) HRBA, (2) SRBA, and (3) AFBA.

The AFBA product provides the most rapid assessment of burned areas. This product can then be complemented with one of both SRBA and HRBA products depending on their availability. The SRBA product is produced on a regular basis from daily MODIS data a few weeks after the AFBA product and is usually available before the HRBA product. However, when burned areas are too small to be retrieved from the SRBA product, only the HRBA product is used. In the following sections of this chapter, all three mentioned burned area products are described in more detail including the methods used to produce them and some results for Russia (national burned area estimates with accuracy assessment) are discussed.

14.2 Description of Three Burned Area Products

14.2.1 AFBA Product: Rapid Burned Area Mapping Based on Active Fire Detection from MODIS Sensor

The *AFBA* burned area product is generated from MODIS data. The raw MODIS data are acquired in the direct broadcast mode via a network of receiving stations located in Moscow, Pushkino (Moscow region), Khanty-Mansiysk, Novosibirsk, Krasnoyarsk, and Khabarovsk. The MODIS data are first preprocessed up to level 1B standard (MOD02 product) and are then used as inputs for the MOD14 active fire detection algorithm (Justice et al. 2006) in order to produce so-called hot spots. Each hot spot is characterized by a number of attributes: (1) geographical coordinates, (2) on-the-ground pixel size (including both pixel widths along and across the sensor scanning directions), and (3) brightness temperature derived from two MODIS spectral channels (with wavelength intervals centered at 4 μm and 11 μm). Then the hot spots detected from the acquired multitemporal MODIS imagery are used to generate burned area polygons and to monitor their temporal dynamics.

The FIRMS (http://firefly.geog.umd.edu) serves as an archive of hot spots detected with the MOD14 algorithm. All detected hot spots are automatically recorded into the FFMIS database with their attributes. The main role of the hot spot archive is to fill potential gaps resulting from accidental MODIS data-receiving stations' failures or data delivery delays.

The rapid burned area assessment includes the analysis of hot spot time series for the monitoring of fire temporal dynamics. An important step in this analysis includes the generation of active fire polygons from spatially scattered hot spot pixels. This polygon generation process is carried out for each new satellite image using available historical hot spot dynamics (i.e., hot spots detected on earlier imagery). The data-processing chain has been developed to provide both near-real-time burned area mapping and postfire season burned area assessment. The main steps of the near-real-time burned area mapping method are described hereafter in more detail.

Step 1: Retrieval of hot spot timing. The hot spots detected from MODIS imagery are first characterized with their satellite observation times. This timing information is incorporated into the FFMIS database in order to build a consistent data time series for further analysis. The hot spot observation time is assigned as the MODIS data-receiving time at the local receiving station or, in the case of FIRMS data, as the MODIS data granule time.

Step 2: Generation of hot spot polygons. The generation of polygons around individual hot spots is an intermediate step. This step uses the MODIS pixel dimensions along and across the sensor scanning directions. The MODIS pixel dimensions are approximated by using geographical directions (along parallels and meridians).

Step 3: Generation of active fire polygons. In order to generate active fire polygons for each satellite image, the corresponding hot spot polygons have to be merged considering a spatial proximity criteria. Two hot spot polygons are merged into one single fire event if their areas are overlapping or the distance between them is less than 0.3 km. For each MODIS image, an individual fire event polygon corresponds to a burned area estimate for the date of the satellite observation. By considering a full time series of such fire polygons, an exhaustive burned area assessment can be carried out.

Step 4: Generation of burned area polygons. This data-processing step is the most complex step. It consists in monitoring the fires dynamic and in aggregating all individual fire polygons detected at different dates into one single burned area polygon (corresponding to a single fire event). The FFMIS database includes full time series of all active fire polygons that have been detected from the beginning of the fire season. One essential step of the burned area polygon generation procedure is the decision to take for each newly generated fire polygon: either (i) to be aggregated to an existing registered fire event or (ii) to create a new fire event in the database. The fire polygon identification procedure aims to check if derived from of last satellite pass data active fire polygon overlapped with or close (distance is less than 1 km) to one of already existing burned area polygon. In case if outcome from such test was positive, the last active fire polygon is geometrically merged to one of existing burned area polygon, otherwise it is considered as new event to be recorded in the database. The algorithm for active fire polygon identification includes also the consideration of particular cases or outliers which can significantly impact the burned area mapping results. One main particular case relates to new active fire polygons which overlap with more than one previously detected burned area polygon. In such case we assume that at the date of the new active fire polygon, these burned area polygons get connected and have to be considered later on as a joint single event.

The hot spot pixels detected with 1 km spatial resolution MODIS data are used as input data for the generation of burned area polygons. These hot spot pixels are based on thresholds of radiation temperature within the sensor's field of view and can obviously include unburned area. Assuming that the burned area error reaches a maximum at the fire border and declines toward the center of the fire, we use a heuristic formula to correct directly the burned area estimates:

$$S_C = \begin{cases} \left(1 - \dfrac{k \times \Delta \times (1-\sigma)}{\sqrt{S_G}}\right) \times S_G \;\; \forall \; S_G > (k \times \Delta)^2 \\ \\ \sigma \times S_G \;\; \forall \; S_G \leq (k \times \Delta)^2 \end{cases} \tag{14.1}$$

where

S_G is the area of burned area polygons in km^2;
S_C is the corrected burned area in km^2;
$\Delta = 1.1$ is the nominal pixel size in km;
$\sigma = 0.25$ is the coefficient of correction;
$k = 4$ is a constant value.

Equation 14.1 assumes that a higher relative error corresponds to smaller areas (and vice versa) due to a larger proportion of boundary pixels. According to Equation 14.1, the correction procedure reduces the burned area estimates with a maximum factor of 4 for fires smaller than k^2 pixels. As fire size grows ($S_G \to \infty$), the correction coefficient decreases up to a value of 1, and thus for very large fires the correction does not change significantly the area estimates.

This burned area mapping method is implemented as an automatic processing chain within the FFMIS. Each new MODIS imagery is processed automatically when acquired in the system. The system provides burned area updates with a frequency of up to six times a day. The full data-processing cycle takes from 20–70 min depending on the number and area of active fires and on available computing resources. In case of the FIRMS being used as the source for hot spots, the data delivery extra time is at least 50 min and is usually about 2–3 hours after the satellite pass.

14.2.2 SBRA Product: Burned Area Mapping Based on Land Cover Change Detection from MODIS Sensor

This product is aimed at providing wall-to-wall assessments of burned areas during the fire season with higher accuracy and reliability than AFBA product. The method has been designed using existing approaches that combine two types of information derived from satellite imagery: surface reflectance changes and thermal anomalies (Fraser et al. 2000a,b; Bartalev et al. 2007). In such approaches, the thermal anomalies are used to separate fire-related land cover changes from other types of vegetation changes (due to other disturbance factors). The SBRA product includes a step of comparison to historical spectral dynamics. Historical multiannual satellite data time series are used to derive optimized land cover change-detection thresholds for any geographical location.

The *SRBA* burned area product is generated at 250 m spatial resolution based on the use of two MODIS data standard products, namely:

- The multiannual daily surface reflectance MOD09 data;
- The active fire (hot spots) MOD14 data for a single year.

The burned area mapping method includes several data-processing steps as follows:

- Detection of pixels contaminated by clouds and cloud shadows, sensor failures, and seasonal snow cover
- Building of multiannual time series of SWVI (short-wave vegetation index) daily composites from uncontaminated pixels
- Generation of the SWVI multiannual "reference" based on SWVI annual time series along a reference period
- Land cover change detection through detection of seasonal anomalies by comparison to SWVI reference
- Burned area mapping using a consistency criteria between detected land cover changes and active fires

The MODIS data preprocessing aims at detecting contaminated pixels and consists of following steps:

- Masking-out pixels with satellite observation and sun elimination angles above certain thresholds
- Detection of clouds, cloud shadows, and snow cover–related pixels
- Detection of residually contaminated pixels through statistical filtering of time-series data

The threshold criteria, such as view zenith angle $\theta > 40^0$ and sun zenith angle $\delta > 80^0$, are applied to mask-out pixels which are not suitable due to extreme geometrical observation and illumination conditions.

Clouds and snow-cover detection involves surface reflectance data as measured in the blue (459–479 nm) R_3 and SWIR (1,628–1,652 nm) R_6 MODIS channels, as well as normalized difference snow index (NDSI) (Hall et al. 1995), which is calculated using Formula 14.2:

$$\text{NDSI} = \frac{R_3 - R_6}{R_3 + R_6} \tag{14.2}$$

Assuming that any pixel can be assigned to one of four classes (clouds, semitransparent clouds, snow, and "clear surface"), the R_3-NDSI bidimensional space (Figure 14.1) can be subdivided as follows:

- «Snow» if $R_3 > 0.05$ and NDSI > 0.1
- «Clouds» if $R_3 > 0.05$ and $-0.2 <$ NDSI < 0.1 (14.3)
- «Semitransparent clouds» if $R_3 > 0.05$ and $-0.35 <$ NDSI < -0.2
- «Clear surface» in all other cases

Pixels that are located in surroundings of «clouds» and «semitransparent clouds» areas are also classified as «clouds» or «semitransparent clouds» if their R_3 value is equal or higher than 0.05.

Assuming a maximum clouds' height as $H = 12$ km and considering the measured sun and view zenith angles, we can reconstruct the potential

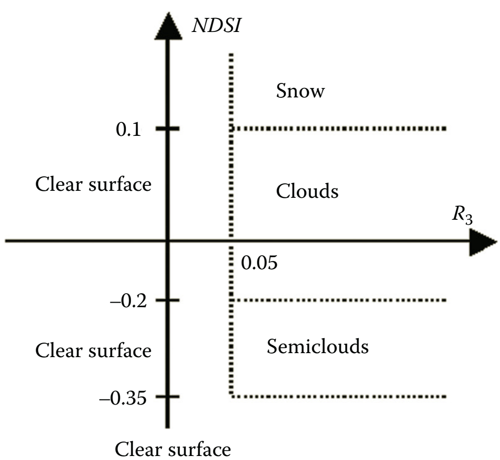

FIGURE 14.1
Discrimination of the classes of clouds, snow, and clear surface in the R_3-NDSI space.

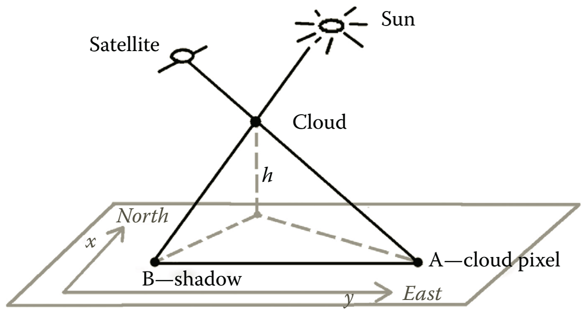

FIGURE 14.2
Geometrical modeling of the cloud-shadow position on the Earth surface (AB line).

cloud-shadow areas (Figure 14.2). If we consider an orthogonal coordinate system with origin *O* in a given cloud pixel with height *H* and axes *Ox* and *Oy* directed to geographical North and East, spatial shift of cloud shadow on the ground is estimated using Formula 14.4:

$$\begin{aligned} x &= H\left(\cos(\psi)\mathrm{tg}(\theta) - \cos(\beta)\mathrm{tg}(\delta)\right) \\ y &= H\left(\sin(\psi)\mathrm{tg}(\theta) - \sin(\beta)\mathrm{tg}(\delta)\right), \end{aligned} \tag{14.4}$$

where
ψ—view azimuth angle
θ—view zenith angle
β—sun azimuth angle
δ—sun zenith angle

In general the geometrically modeled cloud-shadow areas include also "clear surface" pixels, which are removed from contaminated pixels through an additional spatial analysis step. The MODIS NIR channel R_2 (841–876 nm) image profile is analyzed along the cloud-shadow line (Figure 14.3) to identify the correct shadow segments.

The next analysis step is aimed at removing further false shadow pixels due to possible misclassification as clouds or snow-covered area with relatively low NDSI. The shadow pixel is considered as false detection if during a monthly period it has never been classified as "clear surface" and the following expression is true for the potential cloud-shadow pixels:

$$R_1(\Theta^*, t) > M_{R_1}(\Theta^*, t) + \sigma_{R_1}(\Theta^*, t), \tag{14.5}$$

where
$M_{R_1}(\Theta^*, t)$ is the mean estimate of surface reflectance data in red (620–679 nm) channel centered at day t during a 31-day period

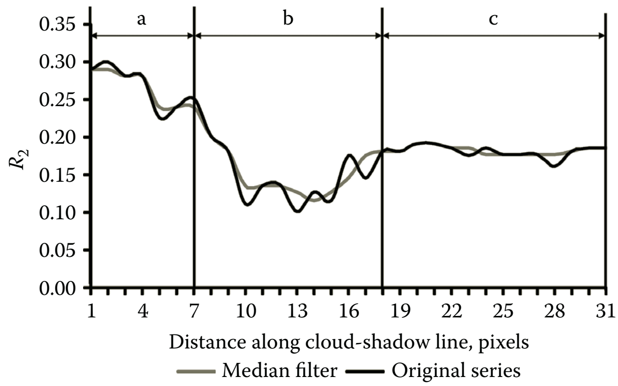

FIGURE 14.3
Example of spectral profile (MODIS NIR channel) with indication of sections corresponding to residual clouds (a), cloud shadows (b), and clear sky surface (c).

$\sigma_{R_1}(\Theta^*, t)$ is the standard deviation from mean
$R_1(\Theta^*, t)$ is the red surface reflectance data for given pixel with coordinates Θ^*

The additional statistical data filtering is aimed at reducing residual noise through the use of a monthly moving time window. The pixel with surface reflectance R_6 is considered as contaminated if the Expression 14.6 is true:

$$\left| R_6(\Theta^*, t) - M_{R_6}(\Theta^*, t) \right| \geq 2\sigma_{R_6}(\Theta^*, t) \tag{14.6}$$

From these preprocessing steps, the masks of different types of contaminated pixels are generated at 500 m spatial resolution.

Our main criteria to detect fires which are causing vegetation cover changes (i.e., which are burning the vegetation) is based on daily time series of the normalized SWVI (Fraser et al. 2000a)

$$\text{SWVI} = \frac{R_2 - R_6}{R_2 + R_6}, \tag{14.7}$$

SWSI is calculated using MODIS surface reflectance data (R_6) resampled from 500 to 250 m. The contaminated pixels (detected during preprocessing) are reconstructed based on a moving time-window polynomial algorithm to retrieve SWVI. The burned area mapping method uses the SWVI multiannual seasonal reference which is derived from MODIS time-series data acquired during previous years—so-called reference period. An experimental justification of the optimal reference period duration is given at the end of Section 14.2.2.

The assessment against the SWVI reference involves the estimation of mean $M^N_{\mathrm{SWVI}}(\Theta^*,t)$ and standard deviation $\sigma^N_{\mathrm{SWVI}}(\Theta^*,t)$ for every pixel with geographical coordinates Θ^* and image date t(DOY):

$$M^N_{\mathrm{SWVI}}(\Theta^*,t) = \sum_{y=1}^{Y}\sum_{t-\Delta t}^{t+\Delta t}\mathrm{SWVI}(\Theta^*,t,y) \tag{14.8}$$

$$\sigma^N_{\mathrm{SWVI}}(\Theta^*,t) = \frac{1}{N}\left(\sum_{y=1}^{Y}\sum_{t-\Delta t}^{t+\Delta t}(\mathrm{SWVI}(\Theta^*,t,y) - M^N_{\mathrm{SWVI}}(\Theta^*,t))^2\right)^{1/2} \tag{14.9}$$

$$\forall t(t=\overline{1,365}) \quad \text{and} \quad \forall y(y=\overline{1,Y})$$

where
 y is the year within the reference period with duration of Y years
 Δt is the moving time-window length parameter for the SWVI intrayear statistical assessment
 $N = Y(2\Delta t + 1)$ is the total number of measurements involved in the SWVI assessment for given pixel and DOY

The detection of pixels likely affected by fire is based on pixel-to-pixel and day-to-day differences between M^N_{SWVI} and the SWIR vegetation index time series for a given year SWVI^C. The detection of seasonal dynamic anomalies is based on following Formula 14.10:

$$\mathrm{SWVI}^C(\Theta^*,t) - M^N_{\mathrm{SWVI}}(\Theta^*,t) < -k\sigma^N_{\mathrm{SWVI}}(\Theta^*,t), \tag{14.10}$$

where k is an experimentally tuned constant that allows to define the range of the SWVI reference interannual dynamics. A pixel is considered as abnormal and likely affected by a fire causing a land cover change if its SWVI^C value is lower than reference SWVI seasonal values as presented in Figure 14.4. Such approach uses automatic thresholds $M^N_{\mathrm{SWVI}} - k\sigma^N_{\mathrm{SWVI}}$ which are calculated for any pixel location and date.

At this stage, the detected pixels include pixels affected by land cover changes caused by fire and by other disturbance factors such as, for example, flooding, insect outbreaks, and extreme weather conditions. They include also false changes due to particular atmospheric and angular conditions of observations and residual effects of interannual differences in phenological vegetation dynamics. A contextual spatial filtering is applied to remove such false detections. The mean $M^W_{\mathrm{SWVI}}(\Theta^*,t)$ and standard deviation $\sigma^W_{\mathrm{SWVI}}(\Theta^*,t)$ of SWVI^C are computed using an increasing window size W for each given date t from five or more pixels surrounding a potential change pixel, with

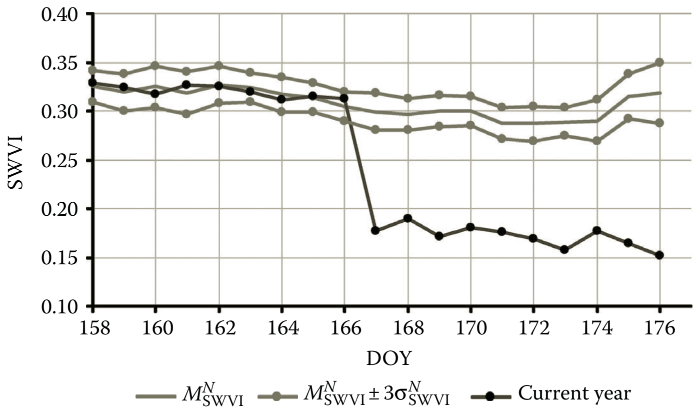

FIGURE 14.4
Example of fire detection from anomaly in the SWVI dynamics at pixel level. SWVI, short-wave vegetation index; DOY, day of the year.

geographical coordinates Θ^* excluding those pixels which have been detected at the previous stage. The pixel is considered as changed if its SWVI^C value is lower than $(M^W_{\mathrm{SWVI}} - \sigma^W_{\mathrm{SWVI}})$.

Finally, a clumping procedure is applied to group pixels detected as changed vegetation into spatially connected regions for each day. The resulting clumped areas are then compared to MODIS-derived active fire data to separate burned areas from areas that were subject to land cover changes resulting from other disturbances. The clumped area is considered as burned area if more than 1% of its total surface is spatially and temporally (within a 20-day time window) consistent with MODIS active fire data. This 1% area threshold has been determined empirically through visual tests and is aimed at elimination of false burned area detection such as crop harvesting.

This burned area mapping method requires setting values for a few main parameters. Two of them such as the reference period duration Y and the moving time-window length parameter Δt are aimed to determine the most appropriate SWVI reference parameters $M^N_{\mathrm{SWVI}}(\Theta^*, t)$ and $\sigma^N_{\mathrm{SWVI}}(\Theta^*, t)$. A third one, namely the scaling constant k, is used to define the reference range of SWVI for interannual variations. The most appropriate parameters' values have been estimated through a number of tests performed with MODIS data over the European part of Russia, which experienced an extreme fire season in 2010 due to exceptional heat wave and drought.

Figure 14.5 shows burned area as estimated by different combinations of reference period durations $Y(Y\ \ \overline{3,6})$ and time-window length parameter values ($\Delta t = 3$ and $\Delta t = 5$). Following these experiments, $Y = 5$ and $\Delta t = 3$ were considered as most appropriate parameters values. The shorter reference

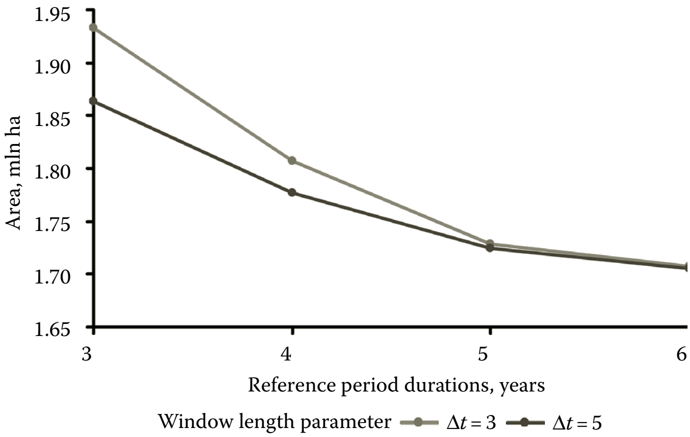

FIGURE 14.5
Burned area estimates for a MODIS tile (H20V03 granule) and for the year 2010 using different reference period durations and time-window lengths (SBRA product).

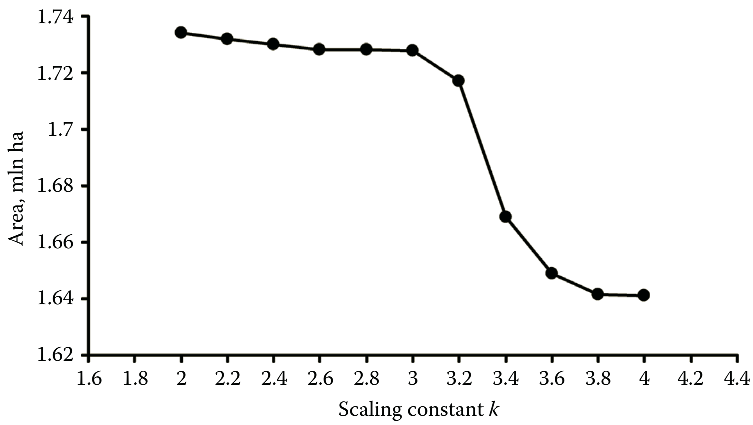

FIGURE 14.6
Burned area estimates with different scaling constant k values.

period ($Y < 5$) led to more false burned area pixels (controlled through visual interpretation), while an increase of the reference period to 6 years resulted in a negligible increase of burned area.

A number of burned area mapping tests have been also performed using different values of the scaling factor k. Figure 14.6 shows that when varying the scaling factor value between 2 and 3 it does not lead to significant changes in burned area estimates. The abrupt decline at $k = 3$ leads to the conclusion that this value can be considered as the most appropriate.

This method allows generating daily SRBA products over the entire Russian Federation in a routine manner within 20–30 days depending on the availability of uncontaminated satellite data.

14.2.3 HRBA Product: Burned Area Mapping from Landsat-TM/ETM+ Sensor

From the three burned area products of FFMIS, the HRBA is the product which takes most time to be delivered but which is potentially the most accurate at the level of individual fires. This product is derived from Landsat-TM/ETM images at 30 m spatial resolution. The main methodological difference with the two other burned area products stands is the involvement of human visual expertise for burned area control and delineation from Landsat-TM/ETM imagery. Another important characteristic of the HRBA product is that it cannot be used alone for an assessment at country level: the HRBA product can only complement the national estimates derived from AFBR and SRBA. This is due to the potential gaps in suitable quality Landsat-TM/ETM imagery over the country during the fire season (missing data). The national yearly completeness of the HRBA product may also significantly differ from year to year due to availability of human resources for assessment and interpretation of the imagery.

The HRBA approach has been developed from the FFMIS web-service interface which provides access to remote sensing data and products along with mapping tools (Figure 14.7). The web-service interface is based on the GEOSMIS system which includes generic GIS and dedicated vegetation analysis tools (Tolpin et al. 2011). The information available from the web interface includes imagery from both Landsat-TM/ETM+ and MODIS sensors as well as data on land cover, fires and meteorological conditions.

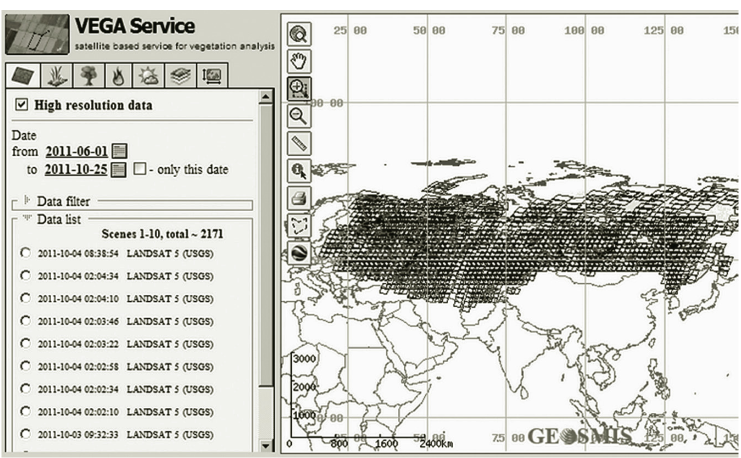

FIGURE 14.7
Display of the Web-service map interface with selected Landsat-TM frames.

In more details the web-service data analysis tools provide the following tools:

- Joint analysis of Landsat-TM/ETM+ and MODIS data, along with thematic maps and data
- Analysis of long-term time series of spectral vegetation indices to assess land cover changes and driving factors. The web-service allows to select an area of interest and to derive instantaneously a multiannual temporal profile of spatially averaged vegetation index
- Management of the database of burned areas (contours and characteristics)
- GIS analysis of satellite data and derived products

The web-service allows for an easy and quick access to all products derived from Landsat-TM/ETM+ and MODIS satellite data, which are automatically and continuously downloaded from the USGS data archive. Daily MODIS data are automatically processed. First, pixels contaminated by clouds and other noise are eliminated, and then weekly composite images are generated. These weekly composite images are used to produce normalized difference vegetation indices (NDVIs). Gaps in weekly time-series data are filled in though an interpolation procedure. Time-series data are then smoothed to reduce remaining noise due to cloud-contaminated pixels. The MODIS-derived NDVI time series are recorded into the database and used to create multiannual vegetation index profiles for each MODIS pixel. The Landsat-TM/ETM+ data are first preprocessed (radiometric and geometric correction), and then color composite images are made available trough the web interface. The MODIS data-derived land cover map of Russia for year 2010 at 250 m spatial resolution (Bartalev et al. 2011) is also made accessible through the web system. This map is the most up-to-date country-level map of forest type distribution.

The web-service allows mapping burned areas at 30 m resolution when an ABFA polygon exists in the FFMIS database and a corresponding appropriate postfire and cloud-free Landsat-TM/ETM+ image is available. The HRBA mapping procedure includes the following main steps:

- Selection of one MODIS-derived AFBA polygon and search of the best available Landsat-TM or ETM+ image
- Selection of the option: automatic or visual burned area delineation
- Visual evaluation of the automatic burned area delineation results and, in case of insufficient quality, replacement by visual burned area delineation

The automatic burned area delineation method is based on a multispectral image segmentation algorithm (Zlatopolskyy 1985) combined with automatic segment labeling and merging steps (Bartalev et al. 2009). The labeling

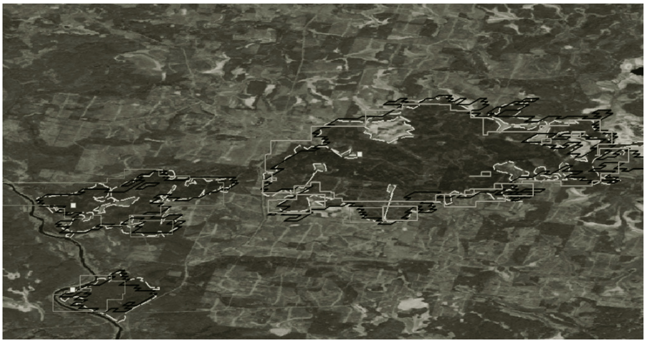

FIGURE 14.8
(See color insert.) Example of burned area polygons derived from the three methods: red polygon, AFBA product; black polygon, SRBA product; yellow polygon, HRBA product. The results are displayed in the Web-service user interface with the Landsat-TM scene used for the HRBA product as a background image.

and merging steps are based on distance criteria from corresponding AFBA and SRBA polygons along with the brightness histogram analysis of Landsat-TM/ETM+ image.

Figure 14.8 provides an example of burned area polygons derived from the three different methods available from the FFMIS web-service user interface.

14.3 Integrated Burned Area Assessment

The integrated burned area assessment approach consists in the combination of the three burned area products, *AFBA, SRBA* and *HRBA,* which are updated continuously during a fire season. This combination is aimed at producing best estimates of burned areas from all the products available in the FFMIS database. The fire events recorded from these three products are linked through an identification process which initiates from the MODIS hot spots–based polygons and related fire events in the AFBA database. The approach links these AFBA events to the fire events from the SRBA and HRBA databases. In case of a fire event existing only in the AFBA database (i.e., with no related event in the SRBA and HRBA databases), the related AFBA burned area is taken into account for the compilation of burned area estimates at national and regional levels and at daily frequency during the full fire season. When an event appears in the SRBA or HRBA databases the AFBA estimate is replaced by the estimate derived from the SRBA or HRBA event, with priority to HRBA product as it is considered to have higher accuracy.

However the practical implementation of this approach is complex due to the difficulty to set unique correspondences between fire events from the three burned area products. It happens often that several AFBA polygons overlap with one unique HRBA polygon, due to a complex spatial pattern or to limitations in data availability. The relationship between AFBA and SRBA polygons is in general even more complex as one single fire event on the ground can correspond to several polygons with no spatial correspondence between the two set of polygons. The impact of this lack of coherence on burned area estimates is limited over large territories, e.g., at national or regional scale. However this issue has to be taken into account for assessment at the level of individual fire events.

In order to address such issue, the integration procedure includes a step of polygon clustering. The clustering procedure is aimed at identifying polygons that are likely to be related to the same fire event. The SRBA and HRBA polygons are grouped within clusters which are linked to the AFBA polygons. An analysis of interlinkages between polygon pairs is carried out for the AFBA–SRBA and AFBA–HRBA combinations. The clustering procedure subdivides the total set of polygons into subsets of polygons which are considered to be related to single fire events. This clustering procedure provides for more detailed intercomparison and analysis at individual fire event level.

14.4 Burned Area Assessment over Russian Federation for Year 2011

The three burned area mapping methods, AFBA, SRBA and HRBA, and the integrated assessment approach have been applied over the full territory of the Russian Federation to estimate the extent and impact of the fire season of year 2011.

From the AFBA product the estimate of total burned areas for year 2011 over the entire country is 10.27 million ha, including 5.06 million ha of burned forest areas. For the same year the SRBA method leads to an estimate of 10.41 and 4.38 million ha of total burn areas and burned forest areas respectively. When looking at the burn area estimates derived from the SRBA method during the last 7 years, it appears that the 2011 fire season was obviously of not exceptional magnitude in Russia (Figure 14.9).

From the FFMIS database of available Landsat-TM/ETM+ imagery acquired during year 2011, the HRBA product has resulted in 3,609 polygons with a total burned area of 5.94 million ha, including 4.00 million ha of burned forests. The burned area sizes of individual fire events show a wide range as presented by their distribution histogram (Figure 14.10). Being not comprehensive enough to provide an accurate estimate at country level, this data set can be used as reference for and evaluation of the accuracy of burned area products derived from MODIS data. This product is also critical for the integrated burned area assessment.

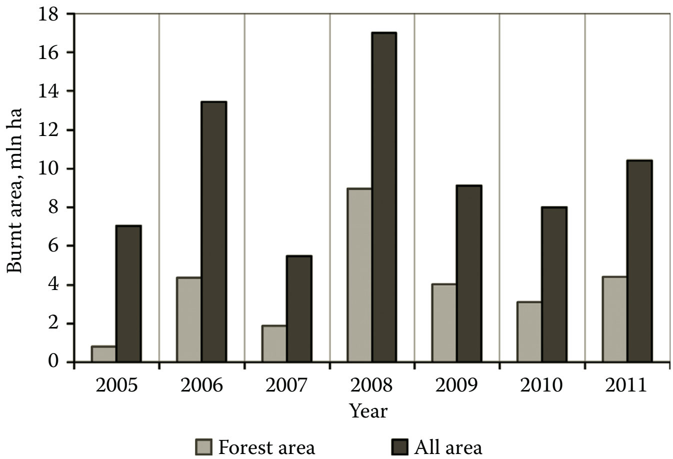

FIGURE 14.9
Annual estimates of burned areas (derived from the SRBA product) over the Russian Federation from 2005 to 2011.

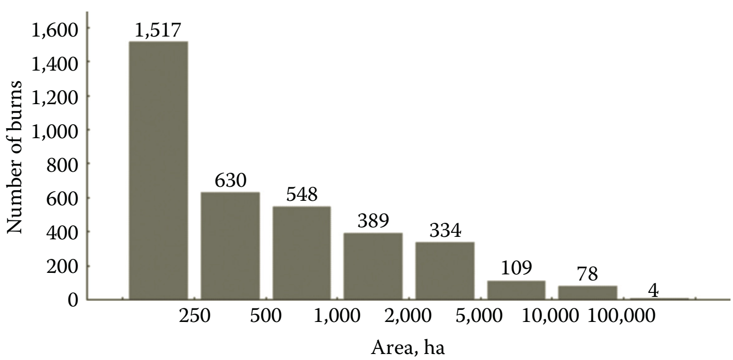

FIGURE 14.10
Burned area distribution of fire events from the HRBA product derived from Landsat-TM/ETM+ imagery.

The cross-comparison of Landsat-TM/ETM+ and MODIS hot spot–derived burned area products including both initial and corrected estimates (correction using Formula 14.1) demonstrates a bias reduction for corrected estimates in particular for small burned areas (<1,000 ha) burns (Figure 14.11).

The accuracy of forest burned area estimates derived from the AFBA product and corrected with Formula 14.1 has been assessed from the comparison to the HRBA product with the following results:

$$\text{RMSE} = \pm 2.43\% \text{ and bias} = -14.1\%$$

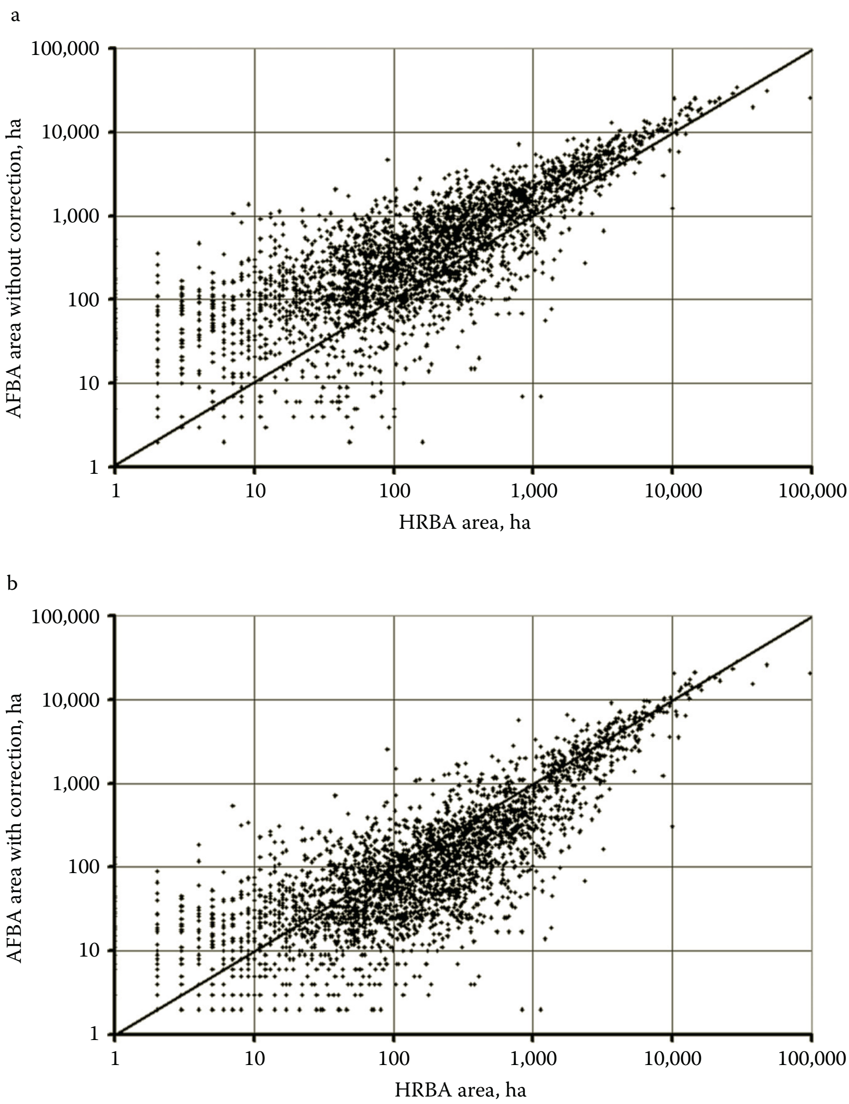

FIGURE 14.11
Correlation between burned areas from the AFBA product (MODIS hot spots) and burned areas from the HRBA product (Landsat-TM/ETM+): (a) before correction and (b) after correction for bias using Equation 14.1.

A similar assessment has been made for the SRBA product (Figure 14.12):

$$\text{RMSE} = \pm 1.52\% \text{ and bias} = -8.7\%$$

Figure 14.13 shows a decrease of RMSE as a function of the area size for small burns (<1,000 ha) considering either all wildfires together or only forest fires.

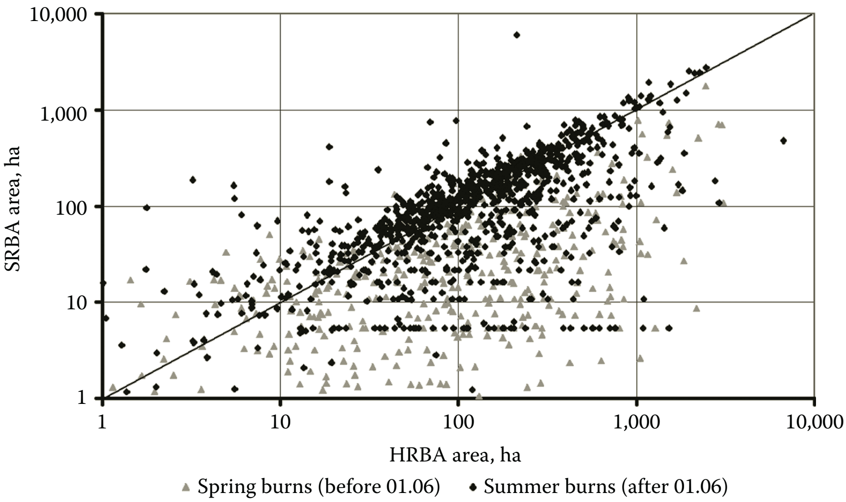

FIGURE 14.12
Correlation between burned areas from the SRBA product (MODIS surface reflectance change) and burned areas from the HRBA product (Landsat-TM/ETM+) with identification of spring and summer fires (before or after June 1).

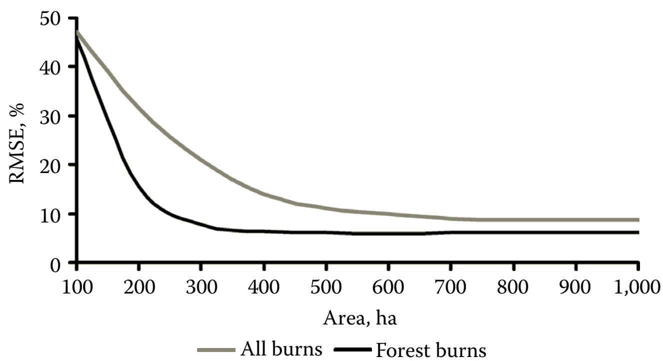

FIGURE 14.13
RMSE (root mean square error) of burned area estimates from the SRBA product in relation to burned area size for total burned areas and forest burned areas.

The combined use of all three burned area products into an integrated assessment leads to an estimate of 14.32 million ha of total burned area including 5.79 million ha in forest domain only. Table 14.1 shows the burned area estimates from the three burned area products and from the integrated assessment at the levels of entire country and federal districts of Russian Federation. Figure 14.14 shows spatial distribution of the burned areas of the year 2011 across the territory of Russia.

TABLE 14.1

Burned Area in Russia for the Year 2011 as Estimated Using MODIS and Landsat-TM/ETM+ Data with Three Different Methods and Integrated Assessment Scheme

Federal District	AFBA Product (ha)		SRBA Product (ha)		HRBA Product (ha)		Integrated Assessment (ha)	
	Total Area	Forest Burns	Total Area	Forest Burns	Total Area	Forest Burns	Total Area	Forest Burns
Central	190,923	11,957	837,272	11,321	36,215	6,066	921,400	24,845
Southern	519,866	3,726	855,424	3,930	9,745	2,639	1,053,002	3,702
Northwestern	163,879	96,794	267,839	142,798	155,947	112,242	247,852	138,478
Far Eastern	5,144,318	3,320,603	4,023,000	2,855,103	3,924,097	2,818,567	6,194,216	3,900,744
Siberian	3,231,180	1,335,362	2,660,764	1,109,667	1,356,684	817,199	3,794,757	1,375,317
Urals	622,398	281,640	808,306	250,709	445,511	242,796	1,002,686	333,100
Volga	177,963	7,204	707,892	6,893	8,435	1,414	767,978	9,211
North Caucasian	215,802	1,711	247,488	159	800	512	340,224	1,458
Russian Federation	10,266,329	5,058,997	10,407,985	4,380,580	5,937,433	4,001,436	14,322,117	5,786,855

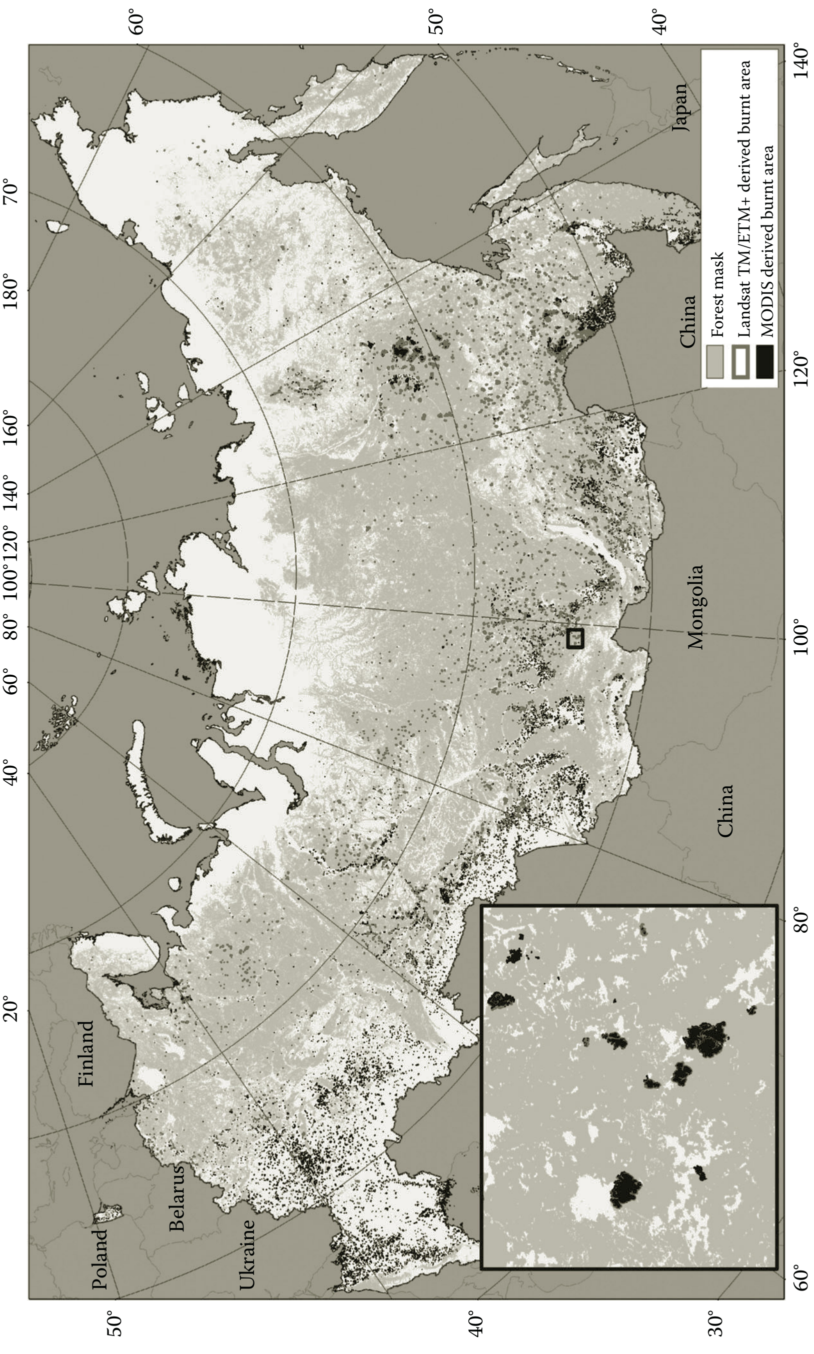

FIGURE 14.14
(See color insert.) Burned areas for the year 2011 over Russian Federation as depicted by the SRBA product (black areas) and the HRBA product (red polygons).

14.5 Conclusions

This chapter presents an approach for the mapping of burned forest area that combines two remote sensing data sources: MODIS and Landsat-TM/ETM+ satellite imagery. This approach is aimed to answer to two main users' requirements: rapidity of information delivery and accuracy of estimates. The approach includes three complementary burned area products at 1 km, 250 m, and 30 m spatial resolution, respectively.

The first burned area product (AFBA) is based on temperature anomalies detected from MODIS data at 1 km resolution. This product is generated with the most rapid but least accurate method. It allows providing burned area estimates several times a day with an acceptable level of accuracy. The second burned area product (SRBA) is based on the use of MODIS data-detected surface reflectance changes combined with radiation temperature anomalies. This method is less rapid (daily assessments are produced within 20–30 days delay) but leads to more accurate results at 250 m resolution. These two methods are fully automated and allow producing regular updated wall-to-wall burned assessments for the entire Russian Federation during a fire season.

The most spatially accurate burned area product (HRBA) is derived from Landsat-TM/ETM+ imagery. This product on its own does not allow providing a comprehensive burned area assessment at the country level but is considered as complementary to the MODIS data-derived estimates. However, this approach was applied operationally over the Russian Federation for the fire season of year 2011 and has resulted in the detailed mapping of 3,609 burned area events. The total burned areas derived from Landsat-TM/ETM+ imagery correspond to about 57% of total burned areas and to about 91% of total burned forest areas derived from the 250 m product for entire Russia during the year 2011.

The MODIS-derived products have different levels of RMSE (14.1% and 8.7% for AFBA and SRBA, respectively) with an underestimation of burned areas. Our integrated burned area assessment approach allows providing more comprehensive and accurate estimates.

About the Contributors

Sergey Bartalev is head of the Terrestrial Ecosystems Monitoring Laboratory at the Space Research Institute of the Russian Academy of Sciences, Moscow, Russia. He graduated from the space applications faculty of the Moscow State University of Geodesy and Cartography, Moscow, Russia. He received his PhD in remote sensing and a doctor of sciences in experimental physics.

His research interests are focused on the development of highly automated methods for land cover mapping and monitoring over large areas using time series of earth observation data. He has coauthored more than 80 peer-reviewed scientific publications.

Vyacheslav Egorov is a senior scientist at the Space Research Institute of the Russian Academy of Sciences, Moscow, Russia. His current research interests include the development of remote sensing techniques for forest mapping and change detection in boreal Eurasia. Vyacheslav Egorov graduated from the Moscow Institute of Physics and Technology, Moscow, Russia, and received his PhD in remote sensing from the Moscow State University of Geodesy and Cartography, Moscow, Russia. He has coauthored about 20 peer-reviewed publications in scientific journals.

Victor Efremov is a scientist at the Space Research Institute of the Russian Academy of Sciences, Moscow, Russia. He graduated from the Moscow Institute of Physics and Technology, Moscow, Russia, and his work is focused on the development of large data archives and user Web interfaces for various environmental monitoring systems based on remote sensing techniques. He has coauthored about 40 peer-reviewed publications in scientific journals.

Evgeny Flitman is a scientist at the Space Research Institute of the Russian Academy of Sciences. His primary professional activity is the development of software for the highly automated processing of persistent data streams. He is currently responsible for the development of an automatic data-processing and archiving system for monitoring forest fires. He has a masters degree in computing methods for civil engineering. He has coauthored about 70 peer-reviewed publications in scientific journals.

Evgeny Loupian graduated from the Moscow Institute of Physics and Technology, Moscow, Russia. He has a doctor of science diploma and works as a deputy director at the Space Research Institute of the Russian Academy of Science, supervising earth remote sensing research. He works at developing methods and techniques of automated satellite data processing. He participated in many projects concerning satellite data accumulation, processing, and distribution. He has coauthored more than 130 peer-reviewed publications in scientific journals.

Fedor Stytsenko is a PhD student at the Space Research Institute of the Russian Academy of Sciences, Moscow, Russia. He has a master of science degree from the Moscow State University of Geodesy and Cartography, Moscow, Russia. His current research is focused at continental-scale forest monitoring using optical remote sensing data and developing systems and methods for satellite data processing.

References

Arino, O., Plummer, S., and Defrenne, D., Fire disturbance: The ten years time series of the ATSR World Fire Atlas. *Proceedings of the MERIS-AATSR Symposium*, ESA publication SP-597, 2005.

Bartalev, S.A. et al., The vegetation mapping over Russia using MODIS spectroradiometer satellite data. *Contemporary Earth Remote Sensing from Space*, 8, 285, 2011. [in Russian]

Bartalev, S.A. et al., Multi-year circumpolar assessment the area burned in boreal ecosystems using SPOT-Vegetation. *International Journal of Remote Sensing*, 28, 1397, 2007.

Bartalev, S.A. et al., The forest fire satellite monitoring information system of Russian Federation's forest agency (actual status and development perspectives). *Contemporary Earth Remote Sensing from Space*, 5, 419, 2008. [in Russian]

Bartalev, S.A., et al., Automatised forest burned area delineations based on HRV and HRVIR satellite data. *Contemporary Earth Remote Sensing from Space*, 6, 335, 2009. [in Russian]

Eva, H.D. and Lambin, E.F., Remote sensing of biomass burning in tropical regions: sampling issues and multisensor approach. *Remote Sensing and Environment*, 64, 292, 1998.

Fraser, R.H., Li, Z., and Landry, R., SPOT-VEGETATION for characterising boreal forest fires. *International Journal of Remote Sensing*, 21, 3525, 2000a.

Fraser, R.H., Li, Z., and Cihlar, J., Hotspot and NDVI Differencing Synergy (HANDS): A new technique for burned area mapping over boreal forest. *Remote Sensing and Environment*, 74, 362, 2000b.

Giglio, L., et al., An enhanced contextual fire detection algorithm for MODIS. *Remote Sensing and Environment*, 87, 273, 2003.

Giglio, L., et al., Global estimation of burned area using MODIS active fire observations. *Atmospheric Chemistry and Physics*, 6, 957, 2006.

Grégoire, J.M., Tansey, K., and Silva, J.M.N., The GBA2000 initiative: Developing a global burned area database from SPOT-VEGETATION imagery. *International Journal of Remote Sensing*, 24, 1369, 2003.

Hall, D.K., Riggs, G.A., and Salomonson, V.V., Development of methods for mapping global snow cover using moderate resolution imaging spectroradiometer data. *Remote Sensing and Environment*, 54, 127, 1995.

Isaev, A.S., et al., Using remote sensing to assess Russian forest fire carbon emissions. *Climate Change*, 55, 235, 2002.

Justice, C., et al., *MODIS Fire Products Algorithm Technical Background Document. Version 2.3,* 2006. http://modis.gsfc.nasa.gov/data/atbd/atbd_mod14.pdf. Accessed on March 30, 2012.

Korovin, G.N., Analysis of the distribution of forest fires in Russia, in fire in ecosystems of boreal Eurasia. *Forestry Sciences*, 48, 112, 1996.

Li, Z., et al., A review of AVHRR-based fire active fire detection algorithm: Principles, limitations, and recommendations. In *Global and Regional Vegetation Fire Monitoring from Space, Planning and Coordinated International Effort*, SPB Academic Publishing, The Hague, The Netherlands, 199–225, 2001.

Loboda, T. and Csiszar, I., Estimating burned area from AVHRR and MODIS: Validation results and sources of error. *Contemporary Earth Remote Sensing from Space*, 2, 415, 2005.

Loupian, E.A., et al., Satellite monitoring of forest fires in Russia at federal and regional levels. *Mitigation and Adaptation Strategies for Global Change*, 11, 113, 2006.

Loupian, et al., Satellite service VEGA for vegetation monitoring. *Contemporary Earth Remote Sensing from Space*, 6, 190, 2011. [in Russian]

Roy, D.P., et al., The collection 5 MODIS burned area product: Global evaluation by comparison with the MODIS active fire product. *Remote Sensing and Environment,* 112, 3690, 2008.

Sukhinin, A.I., et al., Satellite-based mapping of fires in Russia: New products for fire management and carbon cycle studies. *Remote Sensing and Environment*, 94, 428, 2005.

Tansey, K., et al., A new, global, multi-annual (2000–2007) burned area product at 1 km resolution and daily intervals. *Geophysical Research Letters*, 35, L01401, 2008.

Toller, G.N., et al., *MODIS Level 1B Product User's Guide for Level 1B Version 6.1.0 (Terra) and Version 6.1.1 (Aqua)*, NASA Goddard Space Flight Center, 2006. http://mcst.gsfc.nasa.gov/uploads/files/M1054.pdf.

Tolpin, V.A., et al., Development of user interfaces for satellite data based environment monitoring systems (GEOSMIS system). *Contemporary Earth Remote Sensing from Space*, 8, 93, 2011. [in Russian]

Zhang, Y.H., et al., Monthly burned area and forest fire carbon emission estimates for the Russian Federation from SPOT VGT. *Remote Sensing and Environment*, 87, 1, 2003.

Zlatopolskyy, A.A., Image segmentation for objects with discontinued limits. *Automatic and Telemechanics,* 9, 109, 1985. [in Russian]

15

Global Forest Monitoring with Synthetic Aperture Radar (SAR) Data

Richard Lucas and Daniel Clewley
Aberystwyth University

Ake Rosenqvist
solo Earth Observation

Josef Kellndorfer and Wayne Walker
Woods Hole Research Center

Dirk Hoekman
Wageningen University

Masanobu Shimada
Japan Aerospace Exploration Agency

Humberto Navarro de Mesquita, Jr.
Brazilian Forest Service

CONTENTS

15.1 Introduction

Remote sensing data acquired by synthetic aperture radar (SAR) provide unique opportunities for forest characterization, mapping, and monitoring, largely because of sensitivity of the radar signal to vegetation physiognomic structure and the provision of observations that are largely independent of atmospheric (e.g., cloud and smoke haze) and solar illumination conditions. Spaceborne SAR have been operating at a near global level since the 1990s, and the wide range of frequencies, polarizations, and observation strategies provide numerous opportunities for retrieving information on the past and current state of forests and surrounding landscapes and changes associated with natural and anthropogenic change, including climatic fluctuation. The development of systems and algorithms for characterizing, mapping, and monitoring forests, however, has been informed by studies using data acquired by SAR onboard airborne and spaceborne systems (e.g., the Shuttle Imaging Radar) and through dedicated missions.

This chapter reviews the use of spaceborne SAR for forest monitoring at regional to global scales. Particular focus is on the use of single- and dual-polarization backscatter data acquired at X-, C-, and L-bands, as these are the most widely available to those charged with forest monitoring. However, examples of how polarimetric SAR (POLSAR) and inteferometric SAR (InSAR) data can be used to improve monitoring are considered. The chapter provides essential background information on SAR and an overview of how key change processes of deforestation, degradation, and regeneration/afforestation can be detected using these data. Case studies relating to SAR-based monitoring of tropical rainforests in the Brazilian Amazon and Borneo, tree–grass savannas in Australia, and boreal forests in Siberia are then presented. Advantages of SAR for forest monitoring, either singularly or in combination with other sensors, are conveyed. The future of SAR for forest monitoring is discussed, particularly as this type of data is now increasingly used in support of local, national, and regional to global forest monitoring frameworks.

15.2 Suitability of SAR for Forest Monitoring

15.2.1 Forest Structural Diversity and Radar Modes

A wide range of forest types exist globally, with distinct formations occupying large areas including tropical rainforests, boreal and temperate forests, and tree–grass savannas. In all biomes, forests can be broadly categorized into evergreen, semi-deciduous, or deciduous. Common leaf types include broad-leaf, needle-leaf, and palm-like. Canopy cover ranges from sparse to closed and primarily as a consequence of prevailing environmental conditions (e.g., precipitation, evapotranspiration, soil types). As well as cover, forests are often distinguished on the basis of height and the number of canopy layers which, when distinct, can range from single layer (with no understory) to multilayer. The plants themselves also vary in their moisture content, canopy form and orientation, density, and size of their foliar and woody components. The substrate underlying forests may range from dry to wet and be smooth or rough, depending on the soil and geology and levels of inundation. Forest structure in all regions is highly variable and depends on growth stage, management practices, and natural and human-induced events and processes.

These different characteristics of forests are primary determinants of the variability in the SAR response at different frequencies and polarizations and over time. Hence, an understanding of microwave interactions with different components of the vegetation and the underlying surface is essential if these data are to be used for monitoring. A recent overview of imaging radar principles is provided in Kellndorfer and McDonald (2009), but information specific to forest monitoring is conveyed in the following sections.

15.2.2 SAR Frequencies and Polarisations

Spaceborne SAR, which provide capacity for monitoring over large areas, operate at X- (~9.6 GHz, 3.1 cm), C- (~5.3 GHz, 5.7 cm), and L-bands (~1.275 GHz, 23.5 cm). Within closed-canopy and taller forests, the shorter X- and C-band waves interact primarily with the foliage and smaller branches in the upper layers of the canopy and allow discrimination of forest types primarily as a function of differences in their leaf and small branch dimensions, orientations, and densities (Mayaux et al. 2002). However, in more open forests (e.g., tree–grass savannas), interactions may occur with the ground and woody components of the vegetation (Lucas et al. 2004). In all forests, microwaves emitted at lower frequency (L- and P-bands) generally penetrate through the smaller elements of the canopy and interact with the larger woody branches and trunks and ground surface.

At all frequencies, single- and double-bounce scattering result in a large amount of reflected energy returning to the sensor in the same polarization as that transmitted (i.e., HH or VV, with H and V representing the horizontal and vertical polarizations, respectively). The strongest returns are often at HH polarization, where double-bounce scattering between the ground surface and vertical structures (e.g., plant stems) occur, enhanced when forests are inundated by water. Volume scattering leads to depolarization of the transmitted signal and is caused by multiple interactions with structures (e.g., branches, leaves) that have multiple angles of orientation. Returns are comparatively lower from the cross-polarized wave (i.e., HV or VH) and are typically minimal for bare areas, including water. However, the HV backscatter generally increases asymptotically with the amount of plant material in the canopy and has been related to the above ground biomass (AGB) of forests at lower frequencies.

15.2.3 Interferometry

Spaceborne X-, C-, and L-band interferometric data have been used to map forest extent, the distribution of plant components in the forest volume, and canopy height. With *single pass interferometry*, one antenna is used to emit and receive a wave (in a single polarization), while a second detects the same polarization component of the reflected wave. In other words, both antennas measure the backscatter in the same polarizations but, as they are separated in range direction over a certain baseline, this causes a very small time lapse between the reception of reflection. This can be associated with the angle of the observed scatterer while the total elapsed time corresponds with the distance of the scatterer. Consequently, the position and height of the so-called scattering phase center can be determined. In areas without vegetation, the height of the terrain can be determined, while in areas with high vegetation in a single-resolution cell, scatterers over a range of heights are present. This range of phases is expressed by a parameter called interferometric phase difference, and the total correlation (normalized similarity) between the two data is commonly referred to as coherence. Most current SAR systems allow *repeat pass interferometry*, which is based on the use of only one antenna where the second measurement is undertaken within a short time period (from hours to weeks) and from a slightly different position (thereby forming the baseline). Coherence is high (approaches 1) when the same interaction with objects on the ground occurs between two images and decreases as a result of temporal decorrelation (e.g., because of changes in environmental conditions including surface moisture and wind) and volume decorrelation (because of variable scattering within volumes, including forests, as a function of observation parameters). Interferometric coherence is typically lower over forests, although it depends upon the season of observation.

15.3 Development of SAR for Forest Monitoring

15.3.1 Sensors Available for Monitoring

The benefits of using SAR for forest monitoring were recognized by a number of early studies, commencing with the 1970 Brazilian RADAMBRASIL project, in which airborne X-band SAR data were acquired over the entire Brazilian Amazon Basin, and followed by those making use of the shuttle imaging radar (SIR-A/B, SIR-C) SAR missions and other airborne datasets (e.g., NASA's AIRSAR). The Japanese Earth Resources Satellite (JERS-1) SAR provided the first L-band observations globally over the years 1992 to 1998 while the Canadian RADARSAT SAR and SAR on board the European Remote Sensing (ERS-1 and -2) satellites provided C-band observations and interferometric capability. From the mid-2000s and onwards, Italy and Germany launched X-band satellite missions, the COSMO SkyMed constellation and TerraSAR-X. Fully polarimetric observations were provided by the advanced land observing satellite phased array L-band SAR (ALOS PALSAR) (L-band), RADARSAT-2 (C-band), and TerraSAR-X (X-band) instruments at a near global level. The 2000 Shuttle Radar Topographic Mission (SRTM) and the TanDEM-X mission from 2010 provided unique capability for generating digital surface models (DSMs) at global scales, allowing retrieval of canopy height in more densely vegetated areas and the topographic ground surface.

The practical use of SAR for forest monitoring has followed developments in the technology and observation capability. The RADAMBRASIL project was the first to provide a baseline of the extent of forest cover in the Brazilian Amazon without interference from cloud or smoke haze. Focusing on more local areas, the SIR-C missions (X-, C-, and L-bands) allowed researchers to identify the benefits of using different radar wavelengths and polarizations for detecting forest extent, characterizing areas cleared of forest, and retrieving forest biomass and structural attributes (Kellndorfer et al. 1998). The capacity of interferometric SAR for retrieving forest height across larger areas was demonstrated using SRTM (Kellndorfer et al. 2004). The JERS-1 mission provided the first consistent pan-tropical and pan-boreal observations, from which regional-scale mosaics of the boreal and tropical zones were generated as part of the global rain forest mapping (GRFM) and global boreal forest mapping (GBFM) projects (Rosenqvist et al. 2000). The long-wavelength L-band SAR data proved useful for the classification of forest/nonforest areas and identification of secondary growth (Sgrenzaroli et al. 2002), particularly when time-series data were used. The L-band HH data also facilitated temporal mapping of standing water below closed-canopy forests, and hence differentiation of floodplain and swamp forests, and better understanding of the seasonal dynamics of inundation across large river catchments such as the Amazon and Congo (Hess et al. 1995). The successor of the JERS-1 SAR, the ALOS PALSAR, provided the first global systematic observations at a global level between 2006 and 2011. The ALOS mission highlighted the potential of SAR for operational forest monitoring, with the HV data providing better detection of deforestation across many regions compared to HH data. As the data accumulated into a time series, the benefits of using these and also JERS-1 SAR data for identifying events or processes that might lead ultimately to expansion of the area deforested or degraded or tracking histories of land use became apparent. As well as changes in the backscattering coefficient, interferometric observations proved useful for detecting disturbances within the canopy and suggested capacity for mapping degraded forest or identifying specific events (e.g., selective logging). In the boreal regions in particular, the advantages of using coherence data derived from combinations of spaceborne C- and L-band SAR for forest characterization, mapping, and monitoring became apparent. The advantages of integrating data from multifrequency SAR, optical sensors, and light detection and ranging (LiDAR) were also recognized.

15.3.2 SAR Observation Strategies

The use of satellite data for forest monitoring is currently moving from local studies on a limited number of satellite scenes, to regional or national scales where whole countries are to be monitored on a regular basis. Many countries have or are establishing operational national forest monitoring systems to meet their national reporting obligations in support of international conventions, with a key driver being the UN Framework Convention on Climate Change (UNFCCC) Reduction of Emissions from Deforestation and Degradation (REDD+). However, national-scale monitoring requires the availability of satellite sensor data that are consistent over countries, in terms of both coverage (no gaps) and temporal frequency (all acquisitions within a limited time period). A major strength of remote sensing technology is that long-term, systematic, and repetitive observations can be provided over large areas, particularly as SAR is not limited by low sun angles or persistent cloud cover. However, many moderate (10–30 m) spatial resolution sensors have not acquired data uniformly and regularly across large areas but have, instead, focused on areas where specific requests have been submitted. Consequently, some areas have received systematic coverage over long periods of time while neighboring areas have been totally neglected. Many satellite missions have also followed gap-filling background mission objectives as and when operational resources permit. However, the data have often been acquired without consideration given to the impacts of temporal effects, and the heterogeneous archives are of limited use.

Optical missions, and notably Landsat, have generally been more successful than their microwave counterparts, particularly over countries that have their own ground receiving stations. However, where regions are associated with frequent cloud cover, obtaining a full national coverage on an annual basis remains a major challenge. While more or less continuous observations are available through coarser spatial resolution MODIS or AVHRR data, the significantly higher data rates associated with moderate or fine spatial resolution sensors require a higher degree of planning if regional fragmentation is to be avoided. Therefore, a systematic observation strategy is needed for moderate and also fine (<10 m) spatial resolution datasets in order to meet the requirements of a remote sensing–based national forest monitoring system. In particular, the following should be taken into consideration, as highlighted by Rosenqvist et al. (2003):

- Spatially and temporally consistent observations over large areas to avoid gaps in acquisitions and minimize backscatter variations caused by seasonal differences in surface conditions between passes
- Adequate repetition frequency to facilitate detection of temporal changes as a result of, for example, flooding or land use
- Appropriate timing such that long-term repetitive observations are taken over the same time frame each year and ideally targeted to seasons where backscatter conditions are more stable
- Consistency in sensor observation modes such that acquisitions are limited to a small number of "best trade-off" sensor modes, thereby maximizing data homogeneity and minimizing programming conflicts
- Long-term continuity such that observations can be continued from sensors that are preceding or launched in the future

The first radar-based systematic observation strategy dates back to experiences gained with the JERS-1 SAR which, during the last 3 years of its lifetime (1995–1998), was used to acquire data in a consistent manner over the entire tropical and boreal zones of the Earth (Rosenqvist et al. 2000). For the first time, the utility and feasibility of acquiring moderate spatial resolution data systematically and repetitively at continental scales was demonstrated. The global acquisition strategy concept was implemented, in full, for the ALOS satellite, with the PALSAR programmed to achieve at least one gap-free coverage of all land areas every 6 months (Rosenqvist et al. 2007), as illustrated in Figure 15.1.

The importance of systematic acquisition strategies is becoming increasingly recognized, and a number of near-future satellite missions are planning similar global observation plans. Of particular note was the joint effort made from 2012 to establish a coordinated multimission acquisition strategy by a number of national space agencies under the framework of the global forest observation initiative (GFOI) of the group on Earth observations (GEO), comprising moderate-to-fine (<10 m) spatial resolution optical and X-, C-, and L-band SAR.

15.3.3 Synergistic Use of SAR and Optical Data

The development of a forest monitoring program that integrates both SAR and optical data acquired across a range of frequencies is ideal and the benefits are being increasingly realized, with demonstration in a few cases

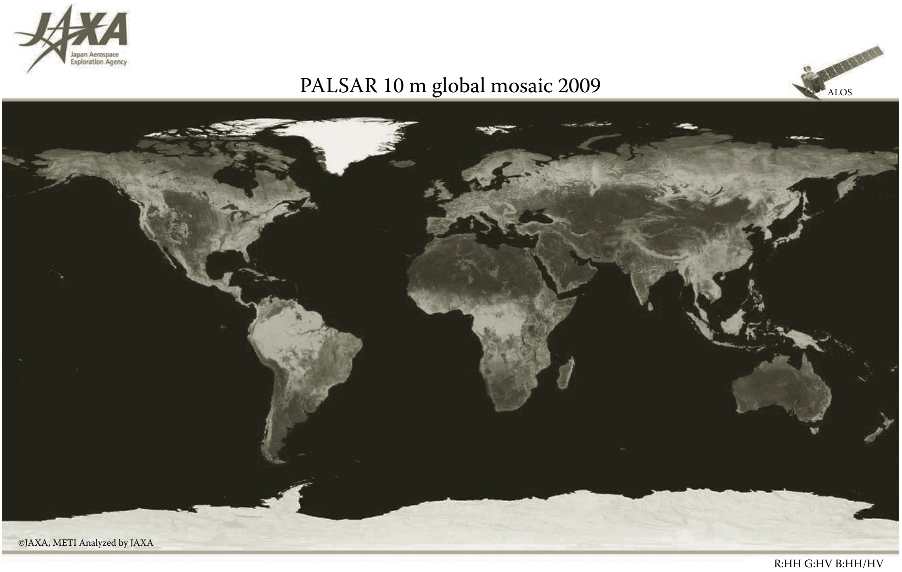

FIGURE 15.1
(See color insert.) Global ALOS PALSAR color composite mosaic at 10 m pixel spacing (R: HH, G: HV, B: HH/HV). 95% of the data—a total of approximately 70,000 scenes—were acquired within the time period June–October 2009. (Courtesy of JAXA EORC, Tsukuba, Japan.)

(e.g., Queensland, Australia). The benefits include the provision of complementary information on the foliage/canopy and woody components of vegetation, which can assist mapping of forest types (e.g., regrowth, mangroves) and retrieval of linked biophysical properties (e.g., canopy cover and AGB). SAR data can also be used to "in fill" gaps in time series of optical remote sensing data where cloud or haze cover prevents acquisition of the latter or the revisit frequency or timing of acquisition is suboptimal. ScanSAR data, in particular, have proven to be particularly useful for this purpose. Where the timing of SAR and optical data acquisitions is not coincident, more comprehensive time-series datasets detailing changes in forest cover can be generated. SAR data may also prove to be the workhorse of operational monitoring programs in the event of failure by one or more sensors (e.g., Landsat).

A multi-sensor and multi-scale approach to monitoring also allows better detection of hotspots of change (e.g., through observations of fire activity from, for example, MODIS) or areas that are vulnerable to future change. For example, fire activity detected by sensing in the middle or thermal infrared wavelengths from coarse spatial resolution sensors of high temporal frequency can be followed up by SAR observations of the area affected (Siegert and Hoffman 2000). Adverse changes in the long-term trends in measures of vegetation productivity (e.g., the normalized difference vegetation index [NDVI] or enhanced vegetation index [EVI]), as derived from coarse spatial resolution optical data, may indicate areas of regrowth or degradation involving accumulation or loss of plant material, which can potentially be characterized through time-series comparison of SAR data. In both cases, fine spatial resolution and programmable data, such as that provided by the Tandem-X mission or very high-resolution (VHR) optical sensors (e.g., Worldview, Quickbird), can then be used to associate observed changes with an actual or likely cause such that measures can be put in place to prevent further loss or degradation of forests. Long-term and regular wall-to-wall observations at a regional level are critical as approaches that sample the landscape often omit changes in forest cover because of their restricted extent (e.g., along road networks or the borders between lowlands and uplands). In all cases, the combination of optical and SAR data provides enhanced benefits for forest monitoring and also understanding the processes of change.

15.4 Processes of Forest Change

Changes in forest cover are typically associated with specific events (e.g., clearcutting), long-term degradation, natural succession, or human-induced regeneration following clearance or disturbance. In each case, SAR can play a role in mapping and monitoring change and also estimating the magnitude of changes in structure and AGB, as outlined in the following sections.

15.4.1 Deforestation

Deforestation is defined as a conversion of forest to nonforest. However, establishing the boundary between forests and nonforest or the magnitude of change that constitutes a deforestation event is often compromised by factors including the nature of forest loss in terms of structural components removed and the methods of clearing. Using SAR data, such definitions are compromised by prevailing climatic (e.g., rainfall, freeze–thaw cycles) and background conditions (e.g., surface roughness, soil water-holding capacity).

Deforestation is ordinarily associated with complete removal of woody vegetation and hence a change in the dominance of volume and double-bounce scattering to surface scattering. However, in some cases, cut stumps, fallen woody material, and individual trees (e.g., palms, nonproductive timbers) are often remaining following clearance events. In the tropics and at L-band, an increase in the backscattering coefficient at HH polarization is typically observed because of double-bounce interactions with woody debris (slash; Almeida-Filho et al. 2009), which can be greater than that of the original forest, as shown in the example from Riau Province in Indonesia (Figure 15.2a). However, this is typically followed by a rapid decline because of loss of woody

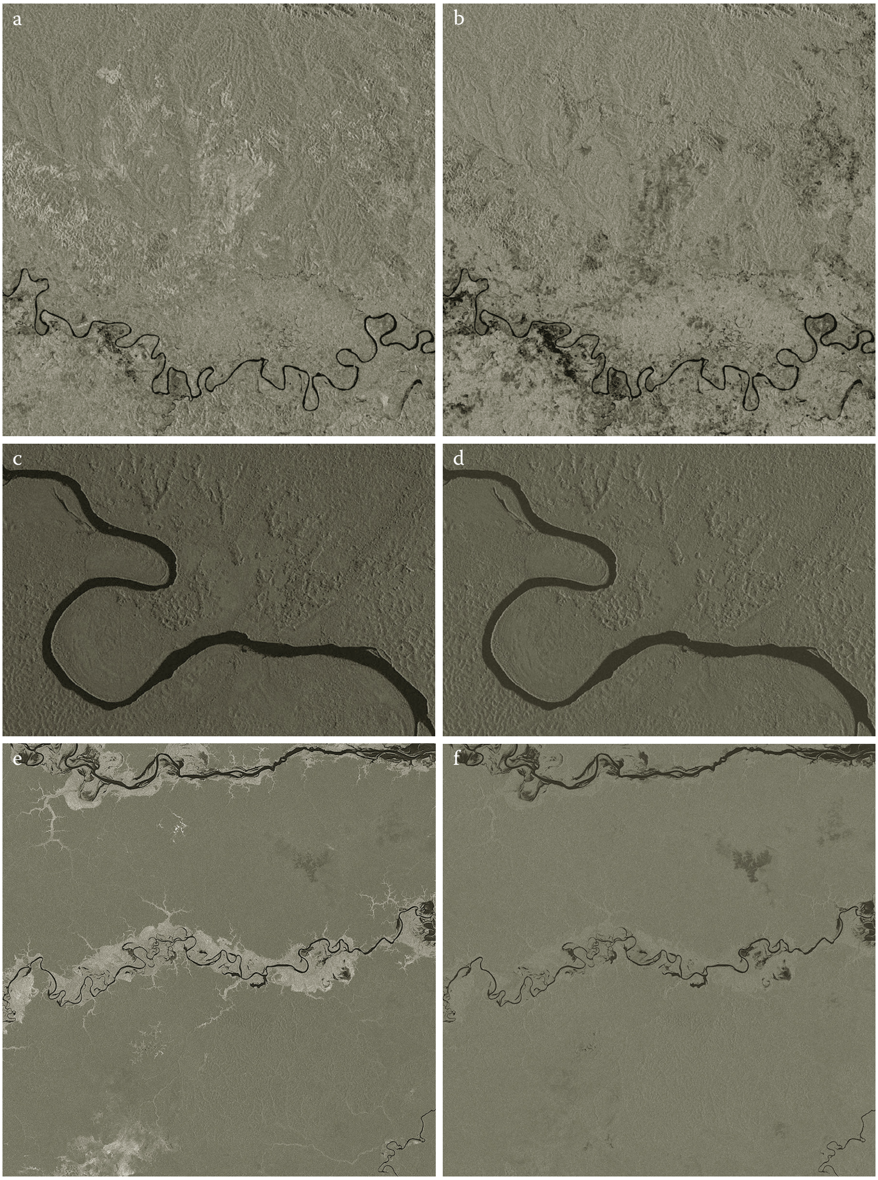

FIGURE 15.2
For a site in Riau Province, Indonesia, ALOS PALSAR image highlighting the difference between forest and nonforest at (a) HH polarization and (b) HV polarization. For a tropical rainforest site in Guyana, open gold mining is less evident within Cosmo-SkyMed X-band (c) HH polarization data compared to (d) **(See color insert.)** a composite of HH data from two dates (September 12 and 15, 2011) and coherence (in RGB respectively; blue areas indicate deforested areas). Due to double-bounce scattering between tree stems and the water surface at L-band, inundated forest in the Central Amazon Basin is clearly visible (bright) at (e) HH polarization, while barely visible at (f) HV polarization.

debris such that deforested areas often become indistinguishable for a short period because of similarity in backscatter with adjacent forest. Over time, however, these become more separable, exhibiting a lower backscatter than primary forest because of the dominance of specular scattering. In some cases, woody material can be piled into rows, which leads to a high backscatter at HH polarization. Trees can also be left standing and exhibit a high return at L-band HH but a lower return if observed using, for example, C-band SAR or optical data (Lucas et al. 2008). Areas of open ground may also exhibit a similar backscatter as areas with dead standing trees. For detecting deforested areas, greater contrast with undisturbed forests is generally obtained at L-band at HV polarization (Figure 15.2b). However, the distinction between forest and nonforest is often compromised using higher frequency (C-band/X-band) SAR single-polarization data because of similarities in backscatter with herbaceous vegetation (e.g., pastures). Differences are greater where interferometric coherence data are used, as illustrated in the X-band example in Figure 15.2c and d, allowing detection of the deforested area (appearing blue in Figure 15.2d). The environmental conditions prevailing at the time of the SAR image acquisition also have implications for mapping and monitoring the extent of forest cover. For example, a reduction in SAR backscatter may occur as a consequence of thawing or snowmelt, reductions in precipitation, or lowering/raising of the water level beneath a forest canopy. In the latter case, the signature can be similar to recently cleared forest, and hence misinterpretations may occur when mapping deforested areas (Figure 15.2e and f).

Methods for defining the forest/nonforest boundary have ranged from simple thresholding to more complex classifications, but, in each case, compromises have been necessary or errors are introduced for the reasons mentioned above. However, the decision as to what constitutes the boundary has significant implications for countries reporting on the extent of forest cover and hence the detection of change. An alternative option is to retrieve biophysical attributes of forests (e.g., area, height, and cover) that are used in standard definitions of forest cover and can be more easily interpreted, although this has rarely been undertaken to date.

15.4.2 Forest Degradation and Natural Disturbances

Forest degradation typically involves the removal of individuals or groups of trees through processes such as selective logging and fuel wood collection as well as dieback as a consequence of, for example, burning or drought. Typically, degradation results in a loss of trees and hence canopy material, with a corresponding reduction in backscattering coefficient and a change in texture typically evident within the SAR image depending on frequency and polarization.

Many studies have highlighted how forest degradation can be observed from SAR data. One example is in the peat swamp forests of Indonesia where drainage of the central dome contributed to underground peat fires, which eventually led to the collapse of the forest. This sequence of events was captured in a time series of JERS-1 SAR data acquired between 1995 and 1998 (Figure 15.3). Until 1996, the dome was still hydrologically intact, but the construction of a very wide canal through the dome was visible in the JERS-1 SAR image of 1997. In the third image of the sequence (September 1997), the canal was filled with water leading to specular scattering away from the sensor and hence its black appearance in the image. A small but bright area is also evident, which then grew in area, becoming brighter until the collapse of the forest, as observed in January 1998. For many peat swamp areas in Borneo and Sumatra, large series of historical JERS-1 images collected during the period 1992–1998 (as many as 30 scenes) and ALOS PALSAR data from 2007 to 2010 show evidence of degradation of the peat swamp forests. The sequence illustrated highlights the benefits of using time series of SAR data from L-band, although data from other sensors can also indicate degradation.

From single-date SAR imagery, selective logging is often difficult to discern because of the relatively coarse spatial resolution, although multitemporal datasets can be used to better identify such areas. SAR coherence measurements can also indicate disturbance. As examples, interferometric ERS-2 SAR data have been used to detect losses of canopy in Kalimantan following large wildfires, while ALOS PALSAR coherence data have proved useful for detecting the impacts of severe fires in Victorian forests in Australia in 2009. These data also have the potential for detecting natural disturbances associated with, for example, downdrafts and lightning strikes as well as long-term declines in the condition of forests as a consequence of drought or flooding.

15.4.3 Secondary Forests and Woody Thickening

Secondary forests often establish following deforestation or degradation while in some intact forests, thickening of the vegetation may occur as a consequence of rainforest expansion or lack of burning over long time periods. A limitation of using SAR data, particularly in tropical regions, is that the rapid increase in woody material renders them indistinguishable from primary forest within a few years. Therefore, most information relating to different stages of regrowth is gathered in the early years of regrowth.

Where forests regenerate on land used previously for agriculture or clear felled of trees, these can be identified through time-series comparison of SAR data, although the point at which regrowing woody vegetation can be considered to be forest can be contentious. Temporal datasets can, however, be used to track the progression of regrowth as the SAR backscatter typically increases over time up to the level of saturation. As an example, the recovery of mangroves in Perak, Malaysia, that had been cleared in rotation can be readily detected using time series of JERS-1 SAR and ALOS PALSAR data through changes in backscattering coefficient. Time-series comparisons of remote sensing data classifications assume that forests of the same age are

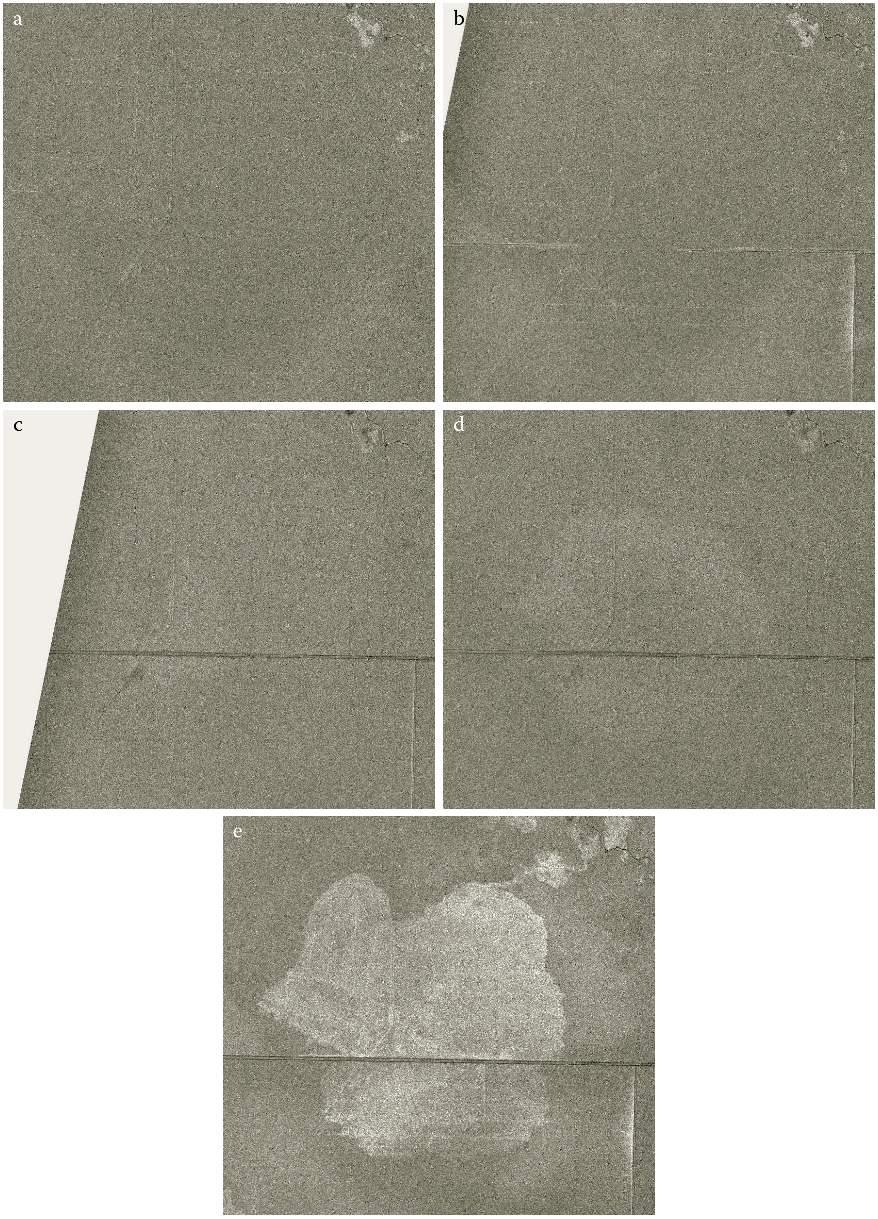

FIGURE 15.3
The collapse of a forest on top of a peat dome in Central Kalimantan, Indonesia, as observed using time series of JERS-1 SAR data acquired on (a) July 12, 1995, (b) March 19, 1997, (c) September 11, 1997, (d) October 25, 1997, and (e) January 21, 1998. The image width is ~21 km.

similar in terms of their structure, species composition, and biomass. SAR data can, however, be used to differentiate forests that are of similar age but may differ in terms of their structure or accumulated AGB.

The use of multifrequency SAR and optical data provides unique opportunities to map the extent of regrowth and differentiate growth stages based on structural development rather than age. At C-band, early stages of regrowth are often indistinguishable from herbaceous vegetation while at L-band and particularly at P-band, these may be unable to be distinguished from nonforested areas as the stem size and density may be insufficient to evoke a response. Forests at more advanced stages of growth are, however, able to be detected. Hence, the use of X- and/or C-band or optical data to establish the presence of plant material and lower frequency L- and P-band SAR to determine whether woody components exist and their relative sizes are useful for determining the nature of regrowth as a function of its structural development. Applying thresholds to SAR data to discriminate regrowth forests from nonforest is often problematic because of confusion with other land and water surfaces and hence the application of thresholds to layers representing retrieved biophysical attributes (e.g., AGB retrieved from SAR data) may be more appropriate.

15.5 Forest Monitoring

15.5.1 Overview

Using SAR data, a large amount of information on the extent and nature of deforestation and degradation associated with human activities, natural disturbances through specific events and long-term processes, and the patterns and dynamics of regrowth can be quantified. Such knowledge can be used to inform subsequent use of the land, in planning for conservation and sustainable management of the existing forest area, and for restoring forests on land that had been previously cleared or degraded. In many cases, forested landscapes have been classified into thematic categories (forest, nonforest, regrowth stages, logged forest), with thresholds or specific algorithms used. Forests can, however, be described on the basis of retrieved biophysical attributes (e.g., height from interferometric SAR or AGB obtained from lower frequency SAR), with continuous surfaces produced which are subsequently subdivided according to predefined intervals. Nevertheless, complications in the description, mapping, and monitoring of change have arisen from variations in environmental conditions (e.g., surface moisture). The following sections provide several case studies from boreal and tropical forests as well as wooded savannas in which SAR data have been used for monitoring forests at local to regional levels and demonstrate how some of the issues presented above have been addressed.

15.5.2 Xingu Watershed, Mato Grosso, Brazil

The Xingu watershed headwaters in southeastern Brazil is representative of many areas along the Amazon's "arc of deforestation." The native vegetation within the 387,000 km^2 of the headwaters includes tall evergreen (25–45 m) and transitional semideciduous (10–30 m) and riparian forests as well as savannas, with these encompassing cerrado woodland, grassland mosaics, thickets, and gallery forest. In the late 2000s, the headwaters contained more area in dense humid forest (~221,000 km^2) than 90% of the world's tropical nations. However, annual deforestation in the forest biome from 2000 to 2007 ranged between 649 km and 3,170 km^2, with an average annual rate over the 7-year period of 1951 km^2. This represents between 5% and 13% of all deforestation in the Brazilian Amazon (Stickler et al. 2008).

Using a mosaic of ALOS PALSAR data generated using spatially and temporally consistent images acquired during the period June to August 2007 (Figure 15.4a), areas of forest and nonforest (Figure 15.4b) were differentiated by applying a random forest algorithm to objects generated using eCognition and aggregating classes at several levels (Walker et al. 2010). This resulted in an accuracy of 92.4% when ancillary spatial/topographic predictor variables were included. A similar approach applied to a Landsat sensor mosaic (Figure 15.4c), comprised of data acquired over the same timeframe, resulted in an accuracy of 94.8%. The overall agreement between the PALSAR and Landsat-based forest cover products varied from 89.7% (1 pixel window) to 93.8% (11 pixel window), with minor discrepancies in some class boundaries (e.g., in the agreement of forests/field edges) being the primary source of spatial dissimilarity between the maps.

The observation strategy developed for the ALOS PALSAR allowed the generation of both dual and single polarimetric data mosaics from quasi-identical periods between 2007 and 2009. Change detected through comparisons of backscatter included clearcutting, logging, and wildfires. For the detection of change, the use of objects rather than pixels was preferred, as management activities or natural degradation typically occurred in areas larger than single pixels. Furthermore, the reduction in image speckle associated with averaging pixels within objects increased signal stability. Change gradients, based on regression tree approaches (e.g., random forest or support vector machines), were preferred over simple comparisons of forest cover maps at several time steps, because of reductions in errors.

A composite of HV data acquired in 2007, 2008, and 2009 over the Xingu watershed is shown in Figure 15.5. Forests clearcuts with slash removed between the 2007 and 2008 acquisitions appear in bright red because of significantly lower backscatter from clearcut areas (darker green and blue tones due after logging). Areas with the same treatment imposed between the 2008 and 2009 acquisitions appear in bright yellow. Other land covers include lower biomass cerrado with no significant change (medium gray), grassland, and bare soil (dark gray to black). Agricultural fields are generally darker,

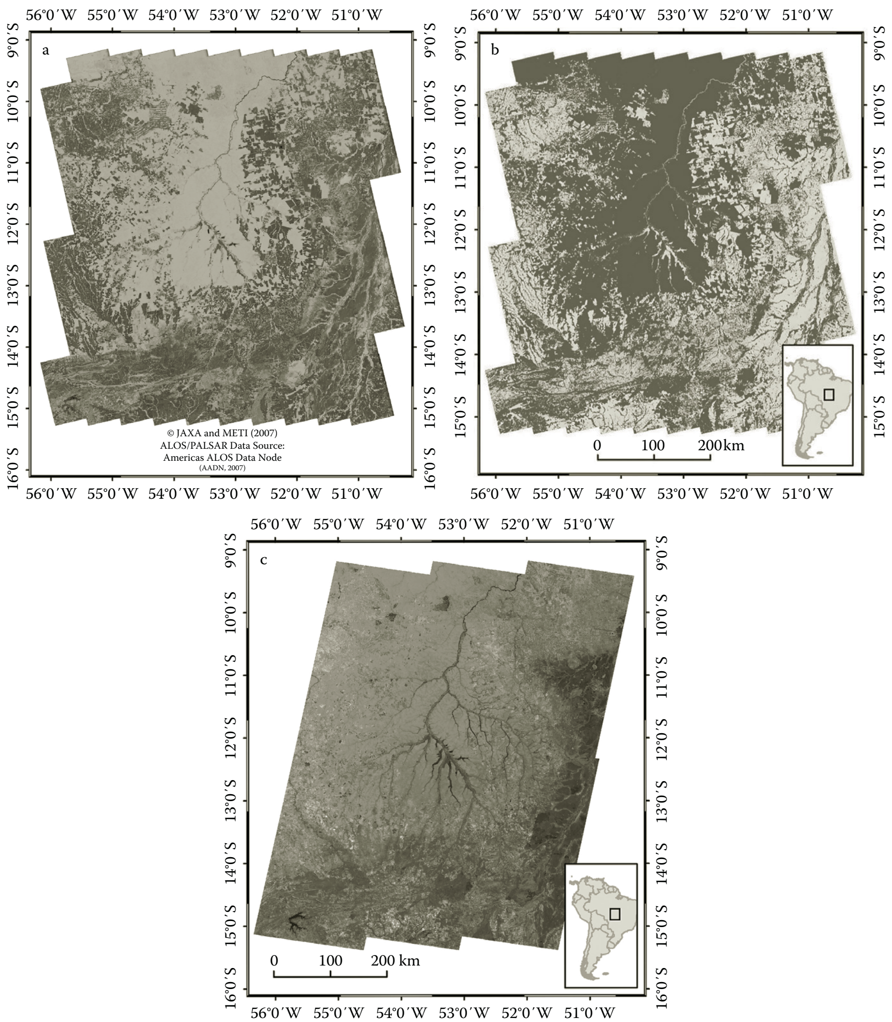

FIGURE 15.4
(See color insert.) Satellite image mosaics produced for the Xingu River headwaters region. (a) ALOS PALSAR mosaic consisting of 116 individual Level 1.1 (single-look complex) fine beam, dual-polarimetric scenes (R/G/B = polarizations HH/HV/HH-HV difference). (b) Map of forest (green) and nonforest (beige) generated with an overall classification accuracy of 92.4% ± 1.8%. (c) Landsat 5 mosaic consisting of 12 individual Level 1G (Geocover) scenes (R/G/B = bands 5/4/3).

with the variability in backscatter associated with changes in crop phenology and also surface (soil and vegetation) moisture. While algorithms for change detection can be based on general principals of change, several ambiguities need to be taken into account when mapping change. In particular, moisture changes from rain events can enhance the backscatter signal but are

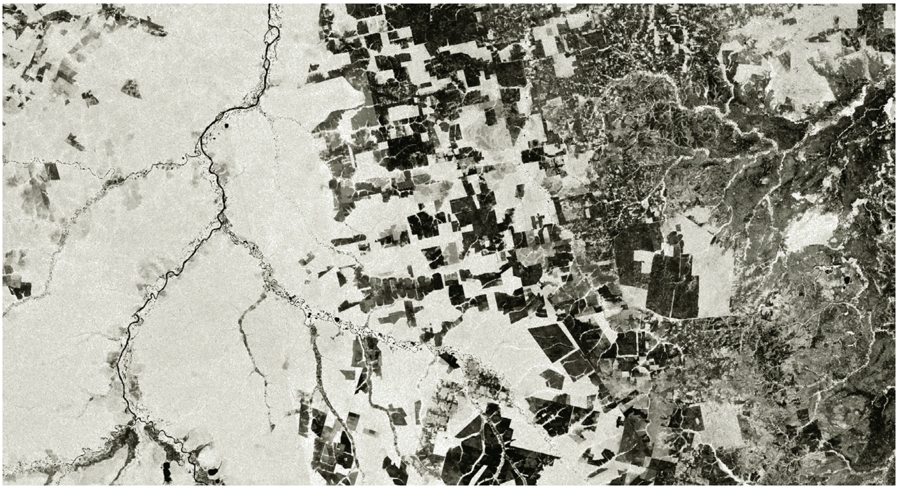

FIGURE 15.5
(See color insert.) Multitemporal ALOS PALSAR L-band HV image generated from data acquired in 2007 (red), 2008 (green), and 2009 (blue) for a part of the Xingu watershed. Closed forest (white) is interspersed with fire scars (red tones) along the main stem of the Xingu River and tributaries (black).

often readily identified at a swath scale and bias corrections can sometimes be applied in mosaic generation. In general, backscatter levels of standing (primary) forest are around –7 to –9 dB in HH and –13 to –15 dB in HV, and losses in AGB associated with logging, clearcutting, or fire reduce the ALOS PALSAR backscatter by 5–7 dB. Smaller changes are mostly related to agricultural activities and changes in both phenology and surface moisture.

15.5.3 Detecting Forest Degradation in Borneo

Borneo is the third largest island in the world and covers an area of approximately 750,000 km^2. Almost three quarters of the island is part of Indonesia (Kalimantan) while Sarawak and Sabah are territories of Malaysia, and the Sultanate of Brunei Darussalam occupies a small area. Until the 1950s, Borneo was almost entirely covered by tropical evergreen broadleaved forest, with other major natural vegetation covers including peat swamp forests along the coastal and subcoastal lowlands, freshwater swamps along the inland rivers, and mangrove forests on the coastal plains. However, intensive logging of predominantly commercial dipterocarp species and conversion to cropland, oil palm, and timber plantations have reduced forest cover significantly.

The establishment of baseline maps of forest cover and type against which to quantify and determine the nature and impact of change is essential. Using ALOS PALSAR fine beam single (FBS) and dual (FBD) polarization (path) image pairs acquired in 2007, a map of forest and land cover types was generated (18 classes in total). These maps have been used subsequently to assist government agencies in their spatial planning and reporting on the status of the environment, thereby allowing compliance with international environmental treaties (Hoekman et al. 2010). Furthermore, maps were generated annually using data acquired in 2008 and 2009, with these highlighting areas of forest degradation through selective logging (Figure 15.6).

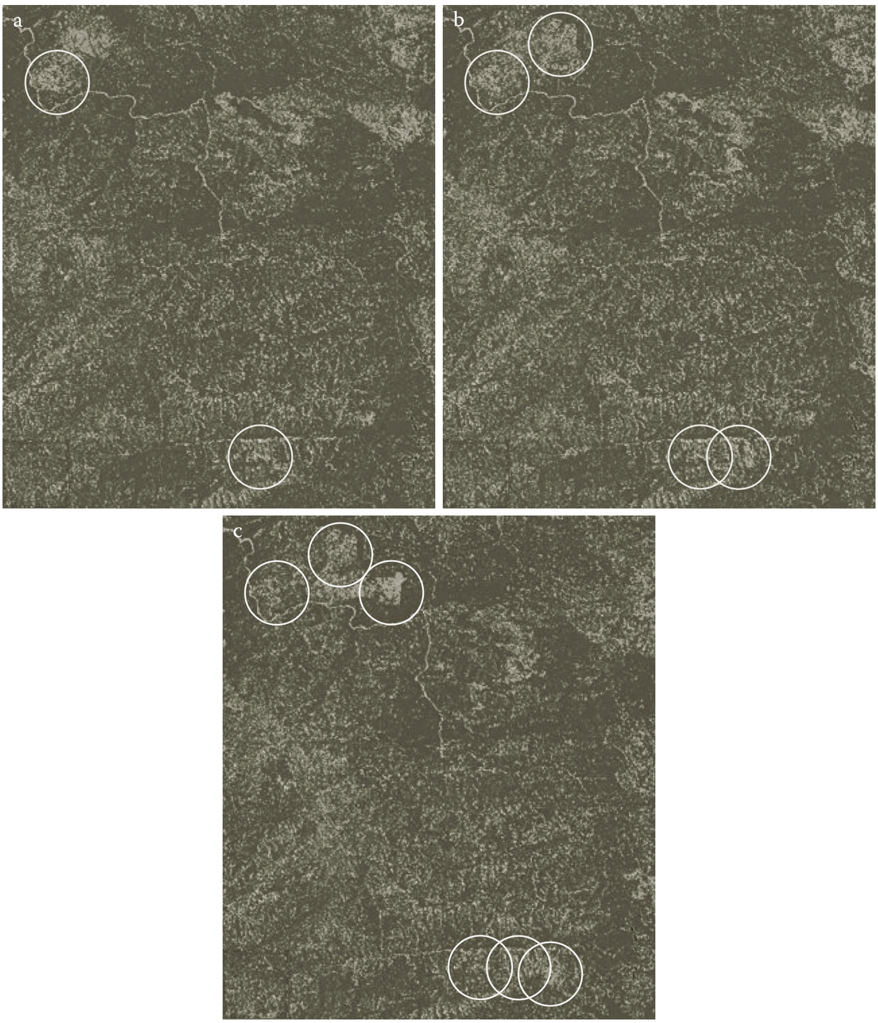

FIGURE 15.6
(See color insert.) Forest degradation in Sarawak through selective logging observed through comparison of forest maps generated using ALOS PALSAR data for the years (a–c) 2007 through to 2009.

15.5.4 Rapid Detection of Deforestation by ScanSAR

Using optical imagery, deforestation in the Brazilian Amazon is monitored and reported on an annual basis by the Brazilian Institute of Space Research (INPE). The majority of data is acquired during the dry season (July to October), although smoke haze and cloud reduce acquisition rates as this season progresses and during the wet season. While INPE provides deforestation alerts every 15 days, the Brazilian Institute for Environment and Natural Renewable Resources (IBAMA) is charged with implementing measures that prevent deforestation before it occurs. For this purpose, the Japan Aerospace Exploration Agency (JAXA) operated the ScanSAR routinely over Brazil every 3 days and provided the processed ScanSAR images to the IBAMA within 5 days from the acquisition date. Provided with information on deforestation events from IBAMA's Remote Sensing Centre, environmental law enforcement agents visit affected sites through ground or helicopter transportation. The imagery also assists the agents to define the logistics and strategies for subsequent field actions. While optical imagery is used, the wide-swath ScanSAR mode of the ALOS PALSAR has allowed detection of early deforestation. Each area identified as indicating a change is delineated within the image and the area is classified as being in the initial processes of deforestation or is a consequence of ongoing clearcutting of the forest. The information is assembled into a deforestation indication document enabling the law enforcement agents to respond rapidly to deforestation events, with particular focus on halting those that are illegal.

15.5.5 Change Detection in Boreal Forests

Boreal forests are extensive throughout the northern hemisphere and are located primarily in Siberia and North America. The SIBERIA project aimed to generate baseline maps of boreal forest cover across Siberia by using a combination of ERS-1 and ERS-2 SAR tandem coherence data and JERS-1 SAR backscatter data for 1997 to 1998. Mapping of forest cover was informed by relationships established between growing stock volume and both C-band coherence and L-band backscatter. The classification was undertaken using a maximum likelihood algorithm based on class statistics generated from training data.

Within the boreal zone, the ability to detect change depends upon the timing of observation. During the winter months, extensive snow cover and frozen conditions limit detection of forest cover using backscatter data. However, using interferometric pairs of ALOS PALSAR data, Thiel et al. (2009) established that temporal decorrelation was low during the winter months, and areas of forest and nonforest could be separated using a combination of winter-coherence data and PALSAR summer backscattered intensities. Operational delineation of forest cover was suggested, with accuracies exceeding 90% when an object-based classification was applied.

15.5.6 Quantifying Regrowth Dynamics in Amazonia and Australia

Australia supports a diversity of vegetation, with the greatest expanse associated with sparse to open tree–grass savannas. Temperature, sub-tropical, and tropical closed forests occur towards the coast and often at higher elevations. Within Queensland, Australia, vegetation monitoring is undertaken through the Statewide Landcover And Trees Study (SLATS) (Danaher et al. 2010) and primarily using time series of Landsat sensor data. The extent of woody vegetation is mapped on an annual basis using Landsat-derived foliage projective cover (FPC). The type and ecological importance of vegetation cleared is determined by intersecting mapped areas of deforestation with regional ecosystem (RE) mapping of vegetation types. Through this approach, changes in vegetation cover are tracked and ameliorative measures taken where appropriate.

While SAR data have not yet been used for operational monitoring in Queensland, potential exists for refining maps of woody vegetation and forest growth stage, thereby increasing the reliability of estimates of deforestation and regenerating forest areas. For example, confusion between herbaceous and woody vegetation occurring within Landsat sensor data is largely overcome by integrating ALOS PALSAR data because of the lack of interaction with the former although confusion with rough ground can occur, particularly with increasing amounts of surface moisture. Integration of the ALOS PALSAR with Landsat FPC data also allows the detection of the early stages of woody regrowth, which typically exhibit an FPC equivalent to forest (i.e., >12%, equivalent to a canopy cover of 20%) but an L-band backscatter more characteristic of nonforest (Lucas et al. 2006). Using such an approach, the dynamics of regrowth can be tracked, including the progression of regrowth through different stages.

15.5.7 Wider Use and Future Sensors

The studies outlined above have highlighted the benefits of using SAR data for monitoring deforestation, degradation, regrowth dynamics, and natural disturbances. In each case, the benefits for better understanding the cycling of carbon through landscapes, conserving biodiversity, and contributing to a range of national policy and international conventions are evident. However, in many cases, such datasets have not been effectively exploited nor recognized.

In the future, a number of SARs are planned, which are anticipated to provide significant advances in forest characterization, mapping, and monitoring at a global scale. These include the European Space Agency (ESA) Sentinel satellites, which are anticipated to provide interferometric and polarimetric observations at C-band (two satellites). The ALOS-2 and the Argentinian SAOCOM satellites are expected to provide L-band SAR observations while the ESA BIOMASS mission will be the first to provide P-band observations, specifically for the retrieval of forest biomass. The NASA DESDynI mission is also intended to provide a dedicated L-band SAR. The challenge will be the full integration of data from these sensors into forest monitoring systems and the use of data acquired in different modes and following different acquisition strategies.

15.6 Conclusions

While optical remote sensing data are the workhorse of many forest monitoring systems, SAR are able to acquire data regardless of clouds and haze, and are increasingly providing opportunities to uniquely detect deforestation activity as well as degradation and regeneration in a consistent and repetitive manner. These data can also inform on the conditions imposed through clearance operations or during subsequent use of the land.

The benefits of providing routine and consistent observations have been demonstrated through the JERS-1 SAR and ALOS PALSAR and while the archives only span over limited number of years, comparison of these data has allowed long-term trends in the amount and type of woody vegetation to be quantified in some cases.

While the relative benefits of SAR and optical data have been debated in the remote sensing community for some time, the integration of these datasets provides the greatest potential for monitoring systems. In particular, SAR data can fill in gaps where cloud cover or smoke haze prevents observations from optical sensor data (for periods covering several years) or can be integrated to provide better mapping of, for example, regeneration stages.

The increasing diversity of observation modes is expected to enhance the use of SAR into the future. The continued and future provision of global single, dual, and fully polarimetric data at X-, C-, and L-bands and interferometric capability together with a greater understanding of the information content of these data is anticipated to lead to increased use of SAR in many forest monitoring activities across a range of biomes and scales. The key challenge is to optimize the development and use of these data such that they ultimately contribute to not only halting the relentless loss of forest but also restoration through better understanding of the dynamics of the forest ecosystems in response to human activities.

About the Contributors

Richard M. Lucas obtained his PhD in 1989 from the University of Bristol, Bristol, United Kingdom. He currently leads the Earth Observation Group at Aberystwyth University, Aberystwyth, United Kingdom, where his research focuses on understanding change in terrestrial ecosystems through integration of ground, airborne, and spaceborne remote sensing data. Following a research position at Swansea University, Swansea, United Kingdom, focusing on mapping and understanding regrowth dynamics in Amazonia and Central Africa, he joined the University of New South Wales, Sydney, Australia (1998), where he initiated the long-term Injune Landscape Collaborative Project in central Queensland, which is aimed at understanding the implications of natural and human-induced change on woodland dynamics. He has been actively involved with the Japan Aerospace Exploration Agency (JAXA) Kyoto & Carbon Initiative, with research focusing on forest (including mangrove) characterization, mapping, and monitoring in the tropics and subtropics.

Ake Rosenqvist received his Dr Eng degree in microwave remote sensing from the University of Tokyo, Tokyo, Japan, in 1997. He joined the Swedish Space Corporation in 1990, where he was engaged in the French/Swedish SPOT program. He was invited to the National Space Development Agency of Japan, Tokyo, in 1993, where he became involved in the development of the JERS-1 application program and the establishment of the Japanese Earth Resources Satellite (JERS-1) SAR Global Forest Mapping project. He spent 6 years at the European Commission Joint Research Centre, Ispra, Italy, and another 5 years as a senior scientist at the Japan Aerospace Exploration Agency (JAXA), where he developed the concept of systematic data observations, which was adopted by JAXA and implemented for the advanced land-observing satellite (ALOS) mission. He founded solo Earth Observation (soloEO), Tokyo, in 2009, and is currently involved in the group on Earth observations (GEO) forest carbon tracking task, coordination of the Kyoto and Carbon (K&C) Initiative, and supporting the development of systematic acquisition strategies for the ALOS-2 and Argentinean SAOCOM-1 missions. Rosenqvist was awarded the International Society for Photogrammetry and Remote Sensing (ISPRS) President's Honorary Citation in 2000.

Josef M. Kellndorfer received his PhD in geosciences from the Ludwig–Maximilians University in Munich, Germany. His research focuses on the monitoring and assessment of terrestrial and aquatic ecosystems, and the dissemination of earth observation findings to policy makers through education and capacity building. Using geographic information systems, remote sensing, and modeling, he studies land use, land cover, and climate change on a regional and global scale. His projects include carbon and biomass mapping of the United States and mapping forest cover across the tropical forested regions of Latin America, Africa, and Asia through the generation of consistent data sets of high-resolution, cloud-free radar imagery. Before joining the Woods Hole Research Center, Falmouth, Massachusetts, he was a research scientist with the radiation laboratory in the Department of Electrical Engineering and Computer Science at the University of Michigan, Ann Arbor, Michigan.

Dirk H. Hoekman received his PhD degree from Wageningen University, Wageningen, The Netherlands, in 1990. He is employed at Wageningen University since 1981 where he currently holds the position of Associate Professor in remote sensing with main interests in the physical aspects of remote sensing, microwave remote sensing, and applications of remote sensing in forestry, agriculture (agro), hydrology, climate studies, and environmental change. He was scientific coordinator for the European Space Agency/Brazilian Institute of Space Research (ESA/INPE) Amazonian expedition (1986); for tropical rain forest sites in Colombia and Guyana (1992–1993); co-coordinating investigator for tropical rain forest sites in Indonesia, including NASA's Pacific Rim (PACRIM)-2 campaign (2000), and ESA's INDREX-1 and -2 campaigns (1996, 2004). He is currently coordinating research programs to support the realization of operational wide-area radar monitoring systems for sustainable forest management and the United Nations Reduction of Emissions from Deforestation and Degradation (UN REDD), and exploring the scientific use of advanced land-observing satellite phased array L-band synthetic aperture radar (ALOS PALSAR) for tropical peat swamp forest hydrology and forest cover change monitoring in Indonesia and the Amazon in the framework of the Japan Aerospace Exploration Agency (JAXA) Kyoto & Carbon Initiative.

Masanobu Shimada (M'97–SM'04–F'11) received his PhD degree in electrical engineering from the University of Tokyo, Tokyo, Japan, in 1999. Since 1979, he has been with the National Space Development Agency of Japan (NASDA), Tokyo, which is currently the Japan Aerospace Exploration Agency (JAXA). He has been assigned duties at the Earth Observation Research Center, where he serves as the advanced land-observing satellite (ALOS) science manager, is responsible for ALOS calibration/validation activities, global forest mapping, and SAR interferometry projects since 1995, and is currently a principal researcher. With JAXA, he designed a NASDA scatterometer. From 1985 to 1995, he developed data-processing subsystems for optical and SAR data (i.e., MOS-1, SPOT, and JERS-1) at the Earth Observation Center. He was a visiting scientist at the Jet Propulsion Laboratory, Los Angeles, California, in 1990.

Daniel Clewley received his BSc (Physics), MSc (remote sensing and GIS), and PhD from Aberystwyth University, Aberystwyth, United Kingdom, in 2006, 2007, and 2011, respectively. His work had focused on modeling and inversion of microwave interactions in tree–grass systems and mapping of regrowth stages in Queensland, Australia, using combinations of SAR and optical data. He is currently based at the University of Southern California, Los Angeles, California.

Wayne S. Walker received a PhD in remote sensing from the University of Michigan's School of Natural Resources and Environment, Ann Arbor, Michigan. He is an ecologist and remote sensing specialist interested in applications of satellite imagery to the assessment and monitoring of temperate and tropical forests at regional to global scales. His research focuses on measuring and mapping forest structural attributes, land cover/land use change, and terrestrial carbon stocks in support of habitat management, ecosystem conservation, and carbon cycle science. He is committed to building institutional capacity in the tools and techniques used to measure and monitor forests, working in collaboration with governments, NGOs, and indigenous communities across the tropics.

Humberto Navarro de Mesquita Jr. received his MSc in ecology at the University of São Paulo (USP), São Paulo, Brazil, and a PhD from the São Paulo Landscape Ecology Laboratory in conjunction with the Department of Geography, University of Edinburgh, Edinburgh, United Kingdom. From 2000 to 2002, he was involved in the GRFM and GBFM initiatives and has extensive involvement with the Japan Aerospace Exploration Agency (JAXA) Kyoto and Carbon (K&C) Initiative. He was head of the Remote Sensing Centre (CSR) of the Brazilian Institute of Environment and Natural Renewable Resources (IBAMA) until June 2010.

References

Almeida-Filho, R. et al., Using dual polarized ALOS PALSAR data for detecting new fronts of deforestation in the Brazilian Amazônia. *International Journal Of Remote Sensing*, 30, 3735–3743, 2009.

Danaher, T., Scarth, P., Armston, J., Collett, L., Kitchen, J. and Gillingham, S., Remote Sensing of Tree-Grass Systems: the Eastern Australian Woodlands. In: *Ecosystem Function in Savannas: Measurement and Modeling at Landscape to Global Scales* (Eds., Michael J. Hill and Niall P. Hanan), CRC Press, Boca Raton, Florida, US, 175–194, 2010.

Hess, L.L. et al., Delineation of inundated area and vegetation along the Amazon floodplain with the SIR-C synthetic aperture radar. *IEEE Transactions on Geoscience and Remote Sensing*, 33, 896–904, 1995.

Hoekman, D.H., M.A.M. Vissers, and N.J. Wielaard, PALSAR wide-area mapping methodology and map validation of Borneo. *IEEE Journal of Selected Topics in Applied Earth Observations and Remote Sensing (J-STARS)*, 3(4), 605–617, 2010.

Kellndorfer, J. and MacDonald, K., Microwave remote sensors. in T. Warner, M.D. Nellis, and G.M. Foody (Eds.), *The SAGE Handbook of Remote Sensing* (586 pages), Sage, London, 13, 179–198, 2009.

Kellndorfer, J.M. et al., Toward consistent regional-to-global-scale vegetation characterization using orbital SAR systems. *IEEE Transactions on Geoscience and Remote Sensing*, 36, 1396–1411, 1998.

Kellndorfer, J.M. et al., Vegetation height estimation from Shuttle Radar Topography Mission and National Elevation Datasets. *Remote Sensing of Environment*, 93, 339–358, 2004.

Lucas, R.M., Moghaddam, M., and Cronin, N., Microwave scattering from mixed species woodlands, central Queensland, Australia. *IEEE Transactions on Geoscience and Remote Sensing*, 42(10), 2142–2159, 2004.

Lucas, R.M. et al., Integration of radar and Landsat-derived foliage projected cover for woody regrowth mapping, Queensland, Australia. *Remote Sensing of Environment*, 100, 407–425, 2006.

Lucas, R.M. et al., Assessing human impacts on Australian forests through integration of airborne/spaceborne remote sensing data. in R. Lafortezza, J. Chen, G. Sanesi, and T.R. Crow (Eds.). *Patterns and Processes in Forest Landscapes: Multiple Uses and Sustainable Management*. Springer, Dordrecht, pp. 213–240, 2008.

Mayaux, P. et al., Large scale vegetation maps derived from the combined L-band GRFM and C-band CAMP wide area radar mosaics of Central Africa. *International Journal of Remote Sensing*, 23, 1261–1282, 2002.

Rosenqvist A., Milne, A.K., and Zimmermann, R., Systematic data acquisitions: A pre-requisite for meaningful biophysical parameter retrieval? *IEEE Transactions on Geoscience and Remote Sensing* and *Communication*, 41(7), 1709–1711, 2003.

Rosenqvist, A., Shimada, M., and Watanabe, M., ALOS PALSAR: A pathfinder mission for global-scale monitoring of the environment. *IEEE Transactions on Geoscience and Remote Sensing*, 45(11), 3307–3316, 2007.

Rosenqvist, A. et al., The global rain forest mapping project: A review, *International Journal of Remote Sensing*, 21, 1375–1387, 2000.

Sgrenzaroli, M. et al. Tropical forest cover monitoring: estimates from the GRFM JERS-1 radar mosaics using wavelets zooming techniques and validation. *International Journal of Remote Sensing*, 23, 1329–1355, 2002.

Siegert, F. and Hoffmann, A.A., The 1998 forest fires in East Kalimantan (Indonesia): A quantitative evaluation using high resolution, multi-temporal ERS-2 SAR images and NOAA-AVHRR hotspot data. *Remote Sensing of Environment*, 72, 64–77, 2000.

Stickler, C.M. et al., The opportunity costs of reducing carbon emissions in an Amazonian agroindustrial region: The Xingu River headwaters. in Berlin Conference on the Human Dimensions of Global Environmental Change. Berlin, Germany, 2008.

Thiel, C., Thiel, C., and Schmullius, C., Operational large-area forest monitoring in Siberia using ALOS PALSAR summer intensities and winter coherence. *IEEE Transactions Geoscience and Remote Sensing*, 47(12), 3993–4000, 2009.

Walker, W.S., Large-area classification and mapping of forest and land cover in the Brazilian Amazon: A comparative analysis of ALOS/PALSAR and Landsat data sources. *IEEE Journal of Selected Topics in Applied Earth Observations and Remote Sensing*, 3, 594–604, 2010.

16

Future Perspectives (Way Forward)

Alan Belward and Frédéric Achard
Joint Research Centre of the European Commission

Matthew C. Hansen
University of Maryland

Olivier Arino
European Space Agency

CONTENTS

16.1 Introduction

Satellites in polar orbits, like Landsat, image the entire planet's surface every day or every couple of weeks, depending on the swath of the satellite overpass; images with detailed spatial measurements (1–30 m) are usually only available once or twice a month—for example Landsat 5 and 7 (image every 16 days at 30 m resolution)—while coarser resolution imagery (e.g., the MODIS sensor on Terra at 250 m or the SPOT satellites' Vegetation sensor at 1 km) are provided nearly daily. Because the information is captured digitally, computers can be used to process, store, analyze, and distribute the data in a systematic manner. And because the same sensor on the same platform is gathering images for all points on the planet's surface, these measurements are globally consistent and independent—a synoptic record of earth observations ready-made for monitoring, reporting, and verification systems linked to multilateral environmental agreements as well as individual government policies.

Forty years ago, the United States of America was the only source of earth observation imagery—today there are more than 25 space-faring nations

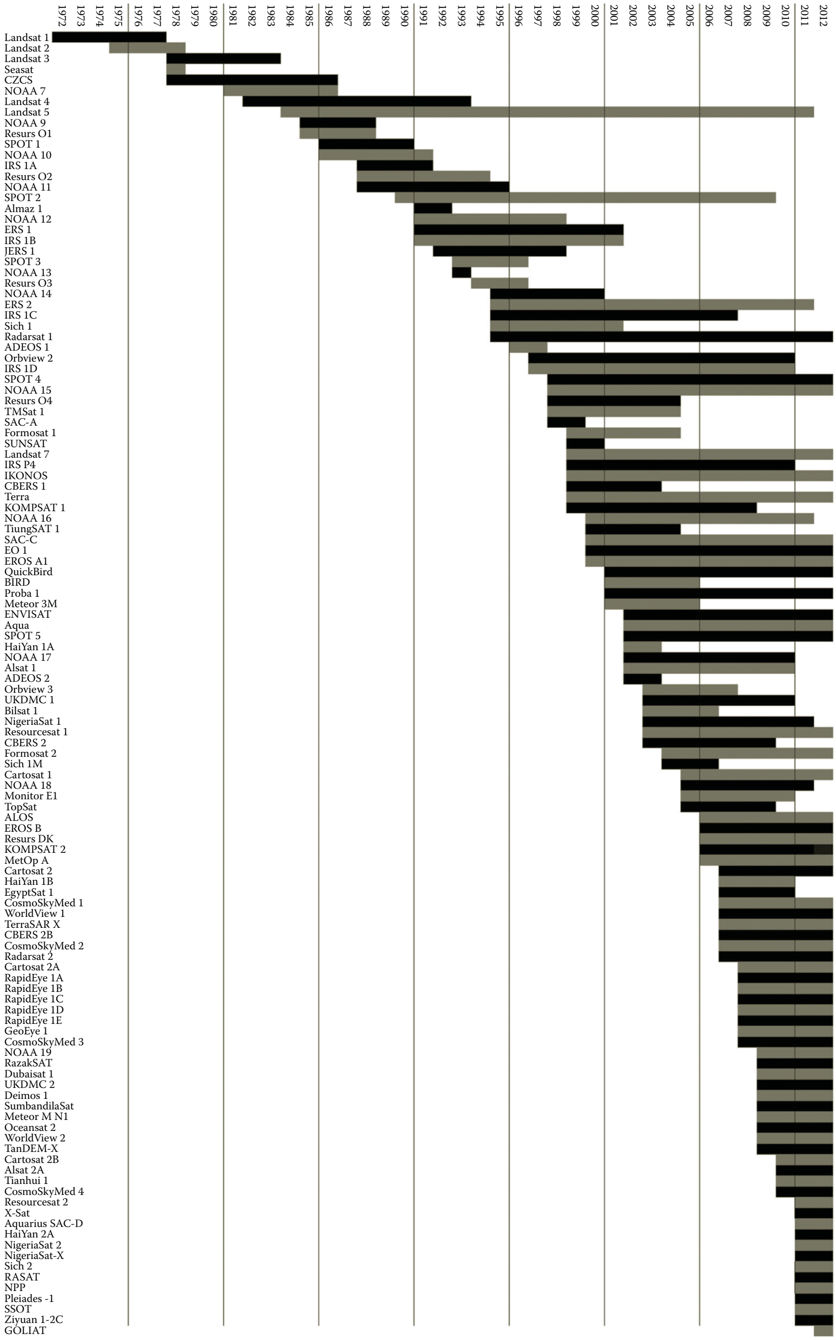

FIGURE 16.1
Polar orbiting satellites with imaging capability launched since 1972. The horizontal bars show period of operation.

flying imaging systems. In 1972, Landsat 1 was the only civilian satellite capable of imaging Earth at a level of spatial detail appropriate for measuring any sort of quantitative changes in forests; today there are more than 60 satellites flying that can provide suitable imagery (or at least they could, *if* they had a suitable data acquisition, archiving, processing, access, and distribution policy). Figure 16.1 lists the polar orbiting imaging satellites, in chronological order according to launch date and shows period of operation. Earth observations from space are becoming more widely employed and increasingly sophisticated. The latest systems launched, such as the Franco–Italian Pleiades system (the first of which was launched December 17, 2011), combine very high spatial resolution (70 cm) with a highly maneuverable platform, capable of providing an image of any point on the surface (cloud cover permitting) within a 24 h period. Concurrent to these technological advances is an increasing appropriation of the land surface in the production of food, fiber, and fuel at the global scale. Forests in particular are under increasing pressure from humankind. Earth observations are critical in assessing and balancing the immediate economic drivers of forest change with the equally important, but less appreciated ecosystem services forests provide.

The previous chapters of this compilation show that recent developments in regional to global monitoring of forests from earth observations have profited immensely from changes made to data policies and access (Woodcock et al. 2008). We now have an unbroken record of global observations stretching back over four decades, all freely available. This chapter provides some perspectives on future earth observation technology for monitoring forests at the global scale.

16.2 Future Earth Observation Technology

Monitoring forest areas over anything greater than local or regional scales would be a major challenge without the use of satellite imagery, in particular for large and remote regions. Satellite remote sensing combined with a set of ground measurements for verification plays a key role in determining rates of forest cover loss and gain. Technical capabilities and statistical tools have advanced since the early 1990s, and operational forest monitoring systems at the national level are now a feasible goal for most countries of the world.

The use of medium spatial resolution satellite imagery for historical assessment of deforestation has been boosted by changes to the policy determining access and distribution of data from the U.S. Landsat archive. In December 2008, the U.S. government released the entire Landsat archive at no charge (Woodcock et al. 2008). This open access data policy means that anyone interested in global forest monitoring now has access to an archive of data spanning four decades. Current plans for the Landsat Data Continuity

Mission (LDCM), with a launch scheduled for early 2013, and the European Sentinel-2 mission (Martimort et al. 2007), with a launch date of mid-2014, will both adopt global data acquisition strategies and will both (at least at the time of writing) provide free and open access to acquired imagery.

LDCM, to be christened Landsat 8 upon reaching orbit, will have a swath width of 185 km and feature a 15 m spatial resolution panchromatic band, nine 30 m multispectral bands (six of which will correspond to heritage Landsat bandwidths), and two 120 m thermal bands. The 16-day revisit rate will match that of past Landsat sensors but with an increased acquisition rate of at least 400 images per 24 h period. The open and free data policy will continue.

The Sentinel-2 satellite will have a swath width of 290 km and carry onboard a multispectral sensor having four bands with a spatial resolution of 10 m, five bands at 20 m, and three bands at 60 m. The Sentinel-2 mission comprises two identical satellites (the second has a tentative launch date for 2015) in identical orbits, but spaced 180° apart. This mission configuration gives a revisit time of 10 days for one satellite and 5 days when both satellites are operational. The Sentinel-2 mission will include a systematic acquisition plan of satellite imagery over all terrestrial land areas of the world between –56° and +83° latitude. The envisaged data policy will allow full and open access to Sentinel-2 data, aiming for maximum availability of earth observation data in support of environmental and climate change policy implementation.

In the near future, the practical utility of radar data is also expected to be enhanced from better data access, processing, and scientific advances. In particular, future space missions will provide complementary Synthetic Aperture Radar (SAR) imagery systems for the monitoring of forest area and biomass. The Sentinel-1 mission (Attema et al. 2007) is a pair of two C-band SAR sensors, the first is planned for launch in 2013 to be followed by a second satellite a few years later. This system is designed to provide biweekly global coverage of radar data at a fine spatial resolution (10 m × 10 m) with a revisit time of 6 days (a swath width of 240 km).

The finer spatial resolution of data from the Sentinel satellites (from 10 m × 10 m) can be expected to allow for more precise forest area estimates and canopy cover assessments, and therefore more reliable statistical information on forest area change, in particular for estimating forest degradation and forest regrowth.

16.3 Perspectives

The basic fact is that natural resources, such as natural forests, are becoming increasingly scarce. There is considerably more pressure on our natural resource base, and establishing a balanced use of forest resources is required. Do you use a forest as a carbon sink? Do you use it as a protected area for biodiversity? Or do you use it for fuel wood or agroindustrial development? To make sensible decisions on the trade-offs between different uses, information on where different forest resources are, what condition they are in, and how they are changing is required. In the framework of the UNFCCC REDD+ activities, the extension of the analysis of tropical deforestation to degradation and forest regrowth will be a crucial requirement (Asner et al. 2009). There are also strong incentives to reduce uncertainty in the estimation of carbon fluxes arising from deforestation by using better data on forest aboveground biomass or carbon stocks (Saatchi et al. 2011, Baccini et al. 2012) in combination with improved satellite-derived estimates of deforestation (Harris et al. 2012).

Mature forest monitoring methods need to be ported to operational settings. Monitoring systems such as Brazil's PRODES deforestation mapping program need to be replicated in other countries where results can be directly incorporated into policy and governance settings. Effective technology transfer of mature, proven methods to developing world institutions needs to be advocated and implemented. This can be envisaged as a leapfrog technology where agencies with little or no past technical capacity may advance in one step to the state of the art.

Researchers will be responsible for developing new capabilities by testing new data sets, processing methods, and thematic outputs. Future satellite image technology, including radar and optical imagery at finer spatial resolutions (10 m finer) and higher temporal frequencies, will require both improved scientific approaches, but also advanced processing systems, including cloud-computing environments (Nemani 2011). The ongoing methodological advances will narrow the gap between the demand for more accurate estimation of the global carbon budget and the limitations of current monitoring approaches.

The adoption of progressive data policies, such as those of NASA, USGS, ESA, and INPE, should be promoted. International coordination between space agencies and implementing institutions (e.g., through the Committee on Earth Observation Satellites—CEOS—or the Group on Earth Observations—GEO) is key to this prospect. Such international cooperation will ensure repeated coverage of the world's forests with varying observation types, all with easy access at low or no cost (GEO 2010). Progress will be measured by how quickly the methods reported here are made obsolete.

About the Contributors

Alan S. Belward works for the European Commission at the Joint Research Centre, where he heads the Land Resource Management Unit. Belward received a BSc degree in Plant Biology from the University of Newcastle upon

Tyne, United Kingdom, in 1981, and MPhil and PhD degrees in remote sensing studies of vegetation, both from Cranfield University's (Bedfordshire, United Kingdom) School of Agriculture Food and Environment in 1986 and 1993, respectively. In the 1990s, he cochaired the International Geosphere Biosphere Programme's Land Cover Working Group and chaired the Committee for Earth Observing Satellites (CEOS) Working Group on Calibration and Validation. From 2002 to 2006, he chaired the Global Climate Observing System's (GCOS) Terrestrial Panel, and in 2009 he was appointed to the GCOS Steering Committee. He is a member of the NASA and USGS Landsat Data Continuity Mission Science Team and the European Space Agency's Sentinel-2 Mission Advisory Group and is also a visiting lecturer at the Technical University of Vienna, Vienna, Austria, where he teaches environmental technologies and international affairs.

Olivier Arino received his PhD degree in physics specializing in remote sensing of surface albedo from the Institut National Polytechnique, Toulouse, France. He performed his research at the Laboratoire d'Etudes et de Recherche en Teledetection Spatiale, Toulouse, France. After two years of postdoctoral fellowship for the International Geosphere Biosphere Program and the European Commission, he joined the European Space Agency in 1991. Since 1999, as head of the projects section in the science applications and future technologies department of the Earth Observation Programme Directorate, he has managed the data user programme in close collaboration with user communities (e.g., 400+ user organizations involved). He was nominated senior advisor in the Earth Observation Programme Directorate in 2008 by a board of ESA directors. He has coauthored more than 20 peer-reviewed scientific papers in the fields of albedo, fire, vegetation, land cover, and sea surface temperature.

References

Asner, G.P. et al., A contemporary assessment of change in humid tropical forests. *Conservation Biology*, 23, 1386, 2009.

Attema, E. et al., Sentinel-1 the radar mission for GMES operational land and sea services. *European Space Agency Bulletin*, 131, 11, 2007.

Baccini, A. et al., Estimated carbon dioxide emissions from tropical deforestation improved by carbon-density maps. *Nature Climate Change*, 2, 182, 2012.

GEO, *Report on the Concept Phase for developing a Global Forest Observations Initiative*. The Group on Earth Observations, Geneva, Switzerland. 2010.

Harris, N.L. et al., Baseline map of carbon emissions from deforestation in tropical regions. *Science,* 336, 1573, 2012.

Martimort, P. et al., Sentinel-2 the optical high-resolution mission for GMES operational services. *European Space Agency Bulletin*, 131, 19, 2007.
Nemani, R. et al., Collaborative supercomputing for global change science. *EOS Transactions*, 92, 109, 2011.
Saatchi, S.S. et al., Benchmark map of forest carbon stocks in tropical regions across three continents. *Proceedings of National Academy of Science USA*, 108, 9899, 2011.
Woodcock, C.E., et al., Free access to Landsat imagery. *Science*, 320, 1011, 2008.

Index

M

N

S

T

U